THE EFFECTS OF ACID CONTACT TIME AND ROCK SURFACES ON ACID FRACTURE CONDUCTIVITY

A Thesis

by

MARIA GEORGINA MELENDEZ CASTILLO

Submitted to the Office of Graduate Studies of
Texas A&M University
in partial fulfillment of the requirements for the degree of

MASTER OF SCIENCE

August 2007

Major Subject: Petroleum Engineering

THE EFFECTS OF ACID CONTACT TIME AND ROCK SURFACES ON ACID FRACTURE CONDUCTIVITY

A Thesis

by

MARIA GEORGINA MELENDEZ CASTILLO

Submitted to the Office of Graduate Studies of
Texas A&M University
in partial fulfillment of the requirements for the degree of

MASTER OF SCIENCE

Approved by:

Chair of Committee, Ding Zhu
Committee Members, A. Daniel Hill
Wayne Ahr
Head of Department, Stephen A. Holditch

August 2007

Major Subject: Petroleum Engineering

ABSTRACT

The Effects of Acid Contact Time and
Rock Surfaces on Acid Fracture Conductivity. (August 2007)
Maria Georgina Melendez Castillo, B.S., La Universidad del Zulia
Chair of Advisory Committee: Dr. Ding Zhu

The conductivity created in acid fracturing is a competition between two phenomena: etching of the rock surface and weakening of the rock. This study presents experimental results of acid fracturing conductivity experiments with polymer gelled acid, while varying contact time and rock type. The experiments were conducted in a laboratory facility properly scaled from field to laboratory conditions to account for the hydrodynamic effects that take place in the field. The rocks of study were Indiana limestone, San Andres dolomite and Texas Cream chalk.

Our results illustrate that acid fracturing conductivity is governed by the etching pattern of the rock surface and influenced by the hardness of the rock. If channels are created, the fracture is more likely to retain conductivity after closure. The hardness of the rock is the dominating factor to determine the conductivity response when no channeling is present. Among the rocks tested, Texas Cream chalk had the lowest hardness measurement before and after acidizing and the fracture closed at a much lower stress compared with limestone and dolomite. Dolomite had the highest conductivity under all closure stresses even without a channeling pattern. Additionally, it was observed that a higher reduction in rock strength at the contact points for dolomite yielded lower conductivity after closure. The effects of hardness variation on conductivity are higher in dolomite than in limestone and chalk. It is apparent that longer contact times do not always provide higher conductivity after closure.

DEDICATION

To my parents, brother and sisters, for their unlimited support and encouragement throughout this work.

ACKNOWLEDGMENTS

I would like to express my sincere gratitude to my advisors Dr. Ding Zhu and Dr. A. Daniel Hill for giving me the opportunity to be a part of this project, for their encouragement to learn and to provide meaningful results. Their knowledge and suggestions were fundamental throughout this work. Thanks for your patience.

Thanks to the acid team: Maysam Pournik, Camilo Malagon, and Luis Antelo; without your help, support, and good attitude throughout all the experiments, this work would not have been possible. Thank you to my friends Fellipe Magalhaes and Toby Rice. You made a difference.

Thanks to Dr. Wayne Ahr for serving on my committee. Finally, thanks to the Crisman Institute at the Department of Petroleum Engineering at Texas A&M University for funding this study.

TABLE OF CONTENTS

Page

LIST OF FIGURES

FIGURE Page

LIST OF TABLES

CHAPTER I

INTRODUCTION

1.1. Acid Fracturing and Created Conductivity

Acid fracturing is a stimulation technique in which a fluid is injected in a carbonate formation at pressures above the fracturing pressures to create a fracture. After the fracture is created, acid is injected and as it contacts the fracture walls, it reacts with the rock face, creating uneven surfaces which should result in a conductive pathway when the fracture is closed.

The success of an acid fracturing treatment depends on the created conductivity being retained under closure stress. Conductivity is mainly a competition between two phenomena: the etching of the rock surface and the hardness variation caused by the acid. Under closure stress, in addition to uneven etching, fracture conductivity also depends on the strength of the rock to retain mechanical integrity.

The resulting conductivity is influenced by the amount of rock dissolved and the pattern in which the rock is dissolved[1]. Uniform etching does not provide a conductive pathway after fracture closure. However, due to the various minerals in carbonate reservoirs, differential etching is usually the result of the difference in reaction rates of the variety of minerals, and the influence of the injection rate. Fast reaction rates usually create a channeling pattern since more rock is dissolved than in minerals with slower reaction rates. In addition, injection rate also influences the etching pattern.

When fracturing pressure is withdrawn and the surrounding stress is applied to the fracture, stress usually causes crushing of the rock surfaces. If the rock lacks the strength to resist deformation, conductivity is greatly reduced. The strength of these asperities is commonly represented by the rock embedment strength (S_{RE}).

This Thesis follows the style of *SPE Journal.*

Several acid systems are used to properly create conductive fractures. While the most common one is straight hydrochloric acid at different concentrations (generally 15% and 28%), viscosified acid systems provide a better control of acid leaf-off into the formation, which increases the distance to which live acid penetrates. Among the viscosified acid systems, gelled acid is a popular system which combines hydrochloric acid with a gelling agent to increase its viscosity.

Finally, the reactions of limestone and dolomite with hydrochloric acid are:

Limestone: $CaCO_3+2HCl \longrightarrow CaCl_2+CO_2+H_2O$

Dolomite: $CaMg(CO_3)_2+4HCl \longrightarrow CaCl_2+MgCl_2+CO_2+2H_2O$

1.2. Literature Review

A few previous studies of acid fracture conductivity have considered the role of rock strength in the conductivity retained with elevated closure strength. The original correlation of acid fracture conductivity, presented by Nierode-Kruk[2], is based in experimental results relating the conductivity to the amount of the rock dissolved during acid injection, with the hardness of the rock in terms of embedment strength correlated with the conductivity.

Equations 1.1 to 1.4 show the correlation developed by Nierode-Kruk, where wk_f is fracture conductivity (md-in), σ_c is closure stress (psi), and S_{RE} is rock embedment strength (psi). In equation 1.3, the constant 13.9 is the corrected value from the original equation which presents a typographical error[3] as 19.9. Equation 1.2 presents the Dissolved Rock Equivalent Conductivity *(DREC),* which is ideal fracture conductivity dependent on a fracture of ideal width.

$$wk_f = C_1 \exp^{(-C_2\sigma_s)} \tag{1.1}$$

$$C_1 = 0.265(DREC)^{0.822} \tag{1.2}$$

$$C_2 x10^3 = 13.9 - 1.3\ln(S_{RE}),\ for: 0 < S_{RE} < 20{,}000\,psi \tag{1.3}$$

$$C_2 x10^3 = 3.8 - 0.28\ln(S_{RE}),\ for: 20{,}000\,psi < S_{RE} < 500{,}000\,psi \tag{1.4}$$

Equations 1.5 and 1.6 present the *DREC* and the ideal width calculation as described by Kunak[4]. The ideal width of the fracture is calculated based on the assumption that the amount of rock dissolved is assumed to be uniform and leaving an open channel of constant width, w_i (ideal width). The volume of rock dissolved was estimated from the profilometer device used to scan the surfaces of the rocks and from which the information could be easily obtained.

$$DREC = \frac{w_i^3 x 10^{11}}{30} \tag{1.5}$$

$$w_i = \frac{volume - of - rock - dissolved}{Lh} \tag{1.6}$$

Analyzing Equations 1.1 to 1.4, conductivity is dependent on two coefficients (C_1, C_2), besides the closure stress represented by σ_c. The first coefficient, C_1, accounts for the amount of rock dissolved through the dissolved rock equivalent conductivity (*DREC*). The amount of rock dissolved increases with contact time; thus this relationship suggests that conductivity increases with contact time. The second coefficient, C_2, accounts for the effect of the strength of the rock (S_{RE}). However, there are only two very broad categories considering very soft rocks or hard rocks. There is no consideration for the hardness variation caused by the acid, in consequence it limits the understanding on the influence that it has on acid fracture conductivity.

Further experimental work evaluated the creation of acid fracture conductivity and the influence of contact time and strength reduction. Beg *et al*.[5] concluded from their study that increasing contact time may not always increase the fracture conductivity, as suggested by the Nierode-Kruk correlation. Additionally, Gong *et al*.[6,7] conducted laboratory experiments of acid fracture conductivity in which they identified a relationship between fracture conductivity, surface roughness, and rock embedment strength. Based on their findings they developed a fracture deformation model to predict fracture conductivity with proper surface roughness, rock embedment strength, and fracture closure inputs. The shortcoming of Beg's and Gong's work was the use of a laboratory facility which lacked the scaling parameters to properly represent an acid fracturing treatment performed in the field.

Fracture conductivity measurements have also been performed by Navarrete *et al.*[8] in a lab carefully scaled to represent field conditions. Even though formation hardness tests were not performed on the core samples, from their results the authors observed that more etched volume did not always result in higher conductivities. More recently, Abass *et al.*[9] have performed experimental studies to investigate the effect of creeping on acid fracture conductivity. They recognized that acid weakens the contact points, causing creeping. From their findings, they suggested that the presence of strong contact points that transfer the creeping force would be more likely to retain conductivity under high closure stresses than weaker points. In the same vein, Nasr-El-Din *et al.*[10] have studied the effect of strength reduction from acid on production, suggesting that the effects of strength reduction are more significant on limestone than on dolomite. It is clear that acid has an effect on the created acid fracture conductivity, but a detailed study considering hardness variation has not been performed under which the effect can be carefully quantified.

1.3. Problem Description

The fracture conductivity as a result of an acid fracture job is one of the measures upon which engineers base their decision when selecting a particular stimulation treatment. Conductivity depends on treatment variables such as acid contact time, injection rate, temperature, and acid system, along with the particular properties of the formation of study. If conductivity is not correctly predicted, it may lead to inappropriate evaluation of treatment design. Therefore, acid fracture conductivity is a key aspect which requires a thorough understanding of the influence that treatment variables have on resulting conductivity.

Nowadays, conductivity prediction is mainly done by applying the existing correlation developed by Nierode-Kruk. The correlation requires hardness measurements, closure stress, and amount of rock dissolved as input parameters. Additionally, hardness variation studies for different rock types are few, and its effect on the resulting acid fracture conductivity is not well understood. Hence, there is a limited understanding on the influence of hardness variation and etching pattern on acid fracture conductivity.

Additionally, when experimental data is compared with the predicted results using the correlation, the conductivity values are not in agreement. Thus, a new correlation is needed that can properly predict acid fracture conductivity.

Previous work has aimed to fulfill the need of conductivity prediction improvement. However, a new correlation easily applicable to industry has not yet been achieved. Recent modeling work in development considers specific rock properties and treatment conditions, which require a thorough understanding of the influence that treatment variables have on acid fracture conductivity.

1.4. Objectives of Research

This research identified the effects of hardness variation and surface etching on the conductivity created from an acid fracturing treatment, based on experimental work performed in a carefully scaled facility[11] using modern acid systems. We used a profilometer device[12, 13] to characterize the surface profile. We also studied the effect of acid contact time and rock type on the created conductivity.

This study had two major objectives:

1. To conduct acid fracturing conductivity tests with core samples of limestone, dolomite, and chalk with a gelled acid system, while varying contact time between 10 and 30 minutes, in a laboratory properly scaled to represent field conditions.

2. To analyze the hardness measurements for each rock sample and relate the etching pattern to illustrate the effect on the resulting acid fracture conductivity. This project targeted a detailed analysis of the effect of hardness variation, formation type, and contact time on acid fracture conductivity.

This study provides a better understanding of treatment variables and its effect on fracture conductivity, which aids in the design of acid fracturing jobs and serve as valuable information to consider for future work.

CHAPTER II

EXPERIMENTAL SET UP, PROCEDURES, AND CONDITIONS

2.1. Experimental Set Up

The laboratory set up for acid fracturing experiments was previously designed[9] with a goal to perform etching of the faces of a rock sample placed together simulating a hydraulic fracture under specific experimental conditions. The laboratory used in this study provides appropriate scaling to represent the field conditions experimentally.

The test cell is made of Hastelloy material, corrosion resistant, with a cylindrical internal structure able to accommodate core samples 7 in. long, 1.7 in. high, and 3 in. in thickness. The test cell is a modified API RP-61 conductivity cell[14]. Fig. 2.1 shows the test cell and a typical core sample specifying its dimensions.

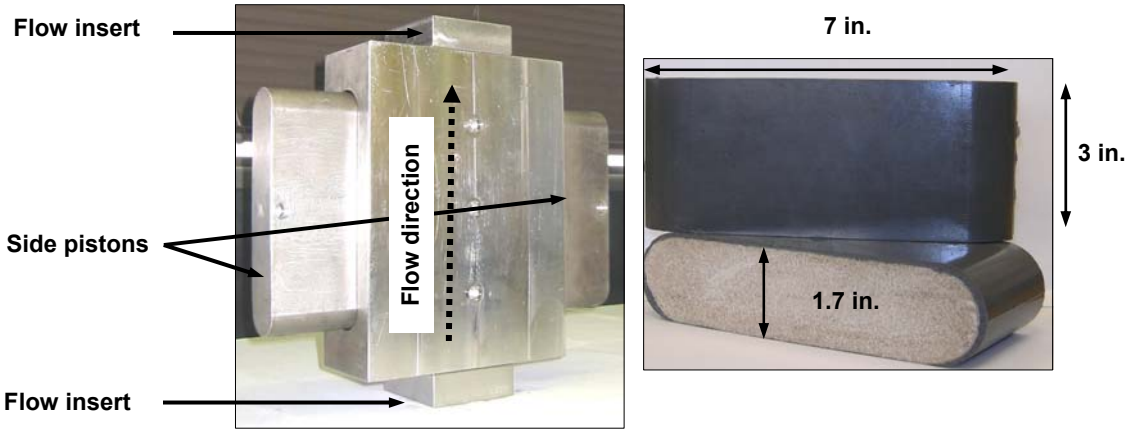

Fig. 2.1- Test cell and core samples used in this study

The core samples used in this study have a rectangular shape with rounded edges to provide the best fit of the core inside the cell. The cores are covered with a sealant material to provide a perfect fit inside the cell. Side pistons with o-rings on its edges are

used to keep the cores in place, and connectors in the bottom and upper surface of the cell attach the cell to the flow lines. Additionally, shims are used to achieve the desired fracture width setting before assembling the flow inserts at both ends. For all the tests a fracture width setting of 0.12 in. was used.

The schematic of the experimental apparatus for the acid etching procedure is shown in Fig. 2.2. We can observe from Fig. 2.2 that the test cell is placed in a vertical position in order to avoid gravity effects. There are two containers in the inlet of the flow line; one provides brine during pre-flush and post flush, and the other container is for acid injection. Injection rates can be as high as 1 lt/min and the flow can be controlled to be injected from 10-100% of its capacity. Ceramic heaters are used to heat the fluids until the desired experimental conditions. Temperatures up to 300°F are feasible in our set up.

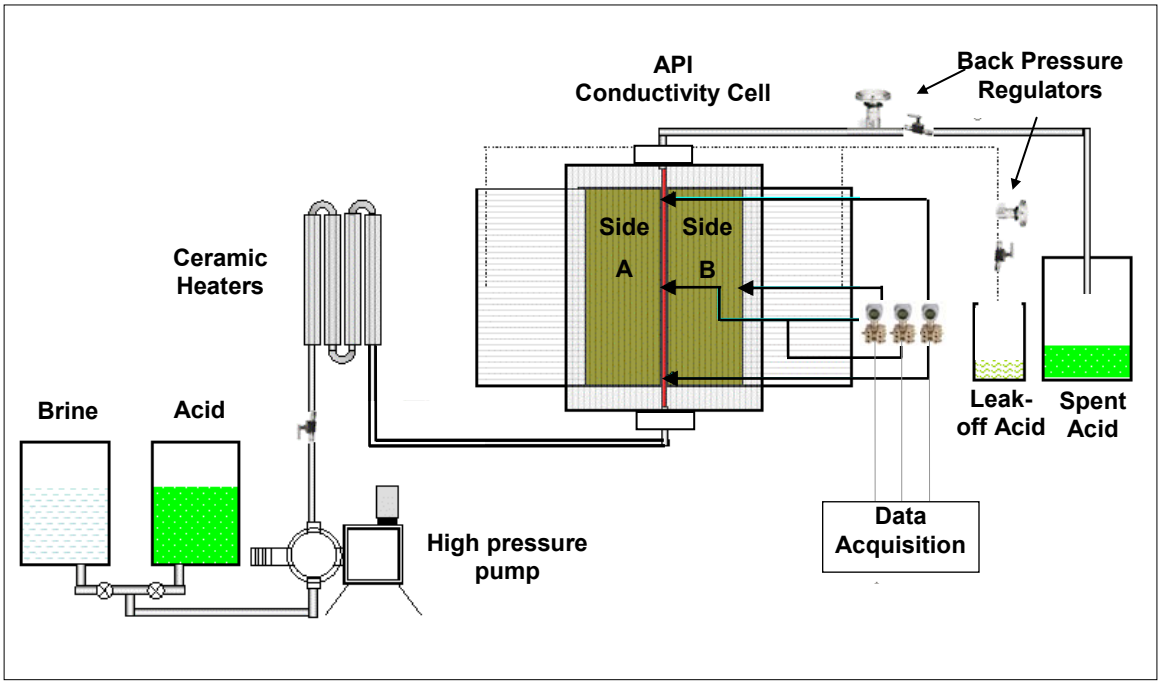

Fig. 2.2- Schematic of Acid etching laboratory set up (After Zou[10])

The cell pressure is kept constant at 1,000 psi controlled with the use of a backpressure regulator, with the goal of maintaining the CO_2 generated from the acid reaction in solution. The leakoff fluid is controlled through the use of a backpressure regulator in the leakoff line. A fracture differential between the leakoff port and the cell pressure was maintained constant at approximately 0.5 psi for all experiments.

Three different pressure transducers are used to monitor the experimental conditions throughout each test. One pressure transducer is used to monitor the pressure drop across the fracture, which allows us to evaluate if the fracture is open during acid injection. Another pressure transducer is used to monitor the cell pressure, and the third pressure transducer measures the pressure drop across the leakoff line.

Conductivity is measured by flowing nitrogen through the closed acidized fracture, and measuring the pressure drop across the fracture under different closure stresses. The conductivity apparatus is made up by two main components, a conductivity cell and a load frame. In Fig. 2.3 a schematic of the conductivity set up is shown.

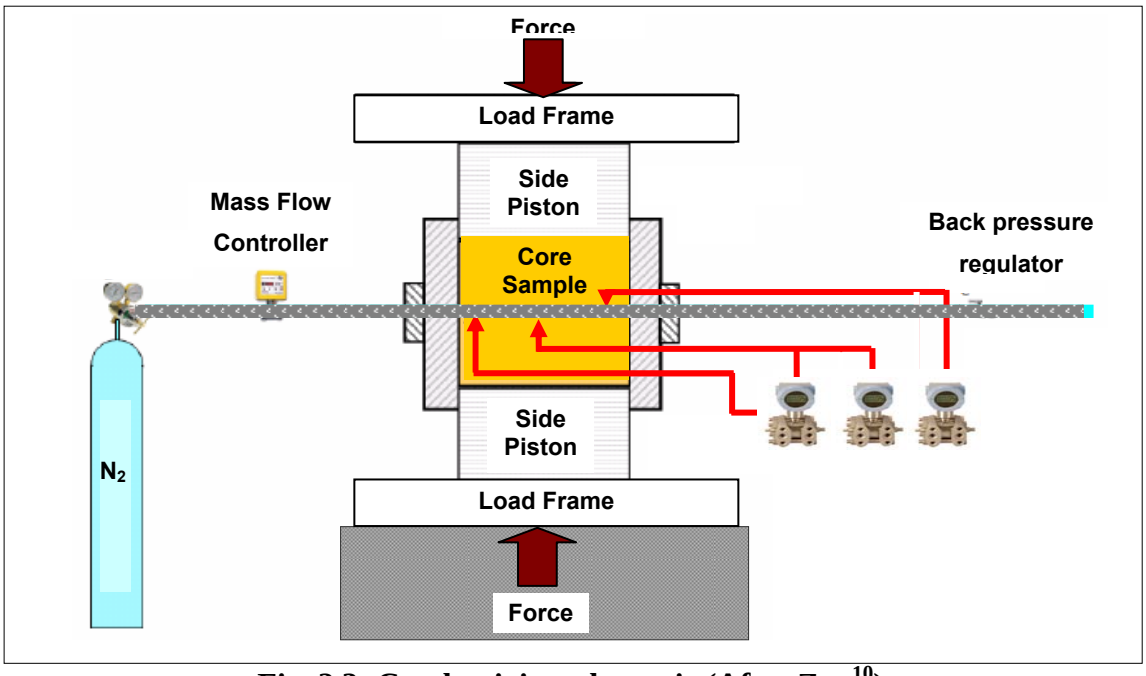

Fig. 2.3- Conductivity schematic (After Zou[10])

The conductivity cell has the same dimensions as the acidizing cell, but is made of stainless steel instead of Hastelloy material. The cell is placed horizontally in the load frame. The load frame is a compression tester that can apply up to 25,000 psi closure stress on the fracture faces, and has a ram area of 125 in^2. Since the core samples have a ram area of 12.47 in^2, an equivalent of 10 times the force applied to the load frame is actually being applied to the core samples[11]. Closure stresses from 0 psi in increases of 1,000 psi are applied to measure the pressure drop across the fracture face which is recorded under five different flowrates under each closure stress. The recorded pressure drop values are evaluated, and by using the Forcheimer's equation conductivity is calculated. A nitrogen mass flow regulator is used to control the nitrogen flow through the fracture and to vary the flowrates for which the data is recorded.

2.2. Experimental Procedure

The experimental procedure follows six consecutive steps (Fig. 2.4), the description of each step is explained below.

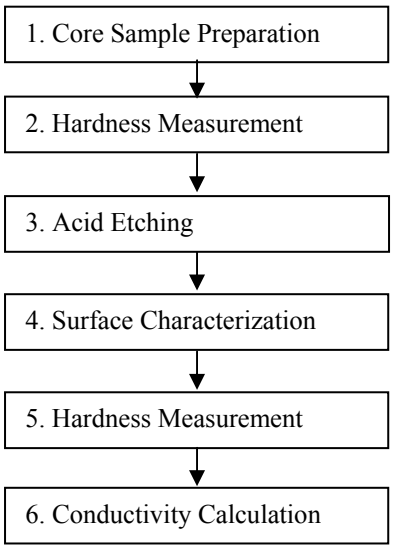

Fig. 2.4- Experimental process for acid fracturing conductivity

2.2.1. Core Sample Preparation

- Quantify the number of rocks necessary to conduct the tests. Since we conducted fifteen experiments, five of each rock type, we had all the rock samples available and cut to the required dimensions: rectangular blocks with round borders with a length of 7 in., a width of 1.7 in., and a height of 6 in. (Fig. 2.5).
- Cut each sample in half with an electric cutter machine, and label the direction in which the cores are cut. The cutting direction is be considered as the flow direction for the rest of the experiments.
- Prepare the core samples with a silicone-based sealant used for creating a perfect fit of the core sample into the cell. Fig. 2.5 shows core samples before and after the silicone cover and the mold structure used as well.

The detailed core sample preparation procedure is as follows:

1. Weigh rock sample.
2. Put tape in top and bottom surface, cut edges with razor cutter.
3. Apply two layers of the silicone primer (SS415501P). Allow 15 minutes waiting time in between layers.
4. Clean metal surface and bottom plastic part of mold with cloth and stoner spray. Fig. 2.5 presents the mold structure used. It is made of stainless steel, with a plastic bottom.

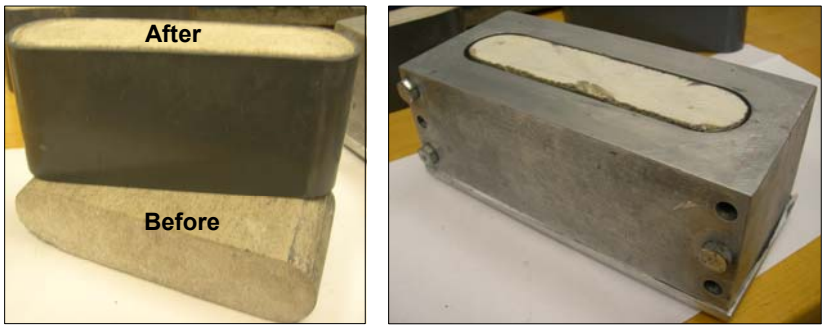

Fig. 2.5- Core samples and mold used to create the sealant

5. Assemble mold and screw the 4 bottom and the 3 side screws.
6. Place rock in mold and adjust to center position.
7. Mix 1 part of silicone potting compound with 1 part of silicon curing agent, weigh before mixing the second component to make sure the mixture is 50/50 of each component, either by volume or by weight percent.
8. Using a disposable injection system, pour mixture in mold carefully until filled to the top without spilling over the sides.
9. After filling the mold to the top, take off the top tape before putting in the oven and clean the outside of the mold to prevent from dripping any extra silicon mixture.
10. Place sample in an oven and set the temperature to 100°C, wait approximately 1 hour.
11. Disassemble the cell and extract core sample.
12. Cut extra silicon on the edges with a razor cutter.
13. Label and store the rock sample.

2.2.2. Surface Characterization

We used a profilometer[12, 13] apparatus to characterize the surface of the rock. A profilometer is a precise vertical distance measurement device that can measure small surface variations in vertical surface topography as a function of position on the surface.

Additionally, with the profilometer, we can quantify the amount of rock dissolved in each scan providing valuable information to given experimental conditions. The profilometer uses a laser displacement sensor which measurement is made using a laser displacement sensor while the sample is moved along its length on a moving table (Fig. 2.6). That measurement is repeated several times over the width of the sample to cover the entire surface area.

The scanning of the surface is performed before and after the acid etching procedure on the surface of the rock which is exposed to acid. This process also includes photographing the surfaces before and after acidizing.

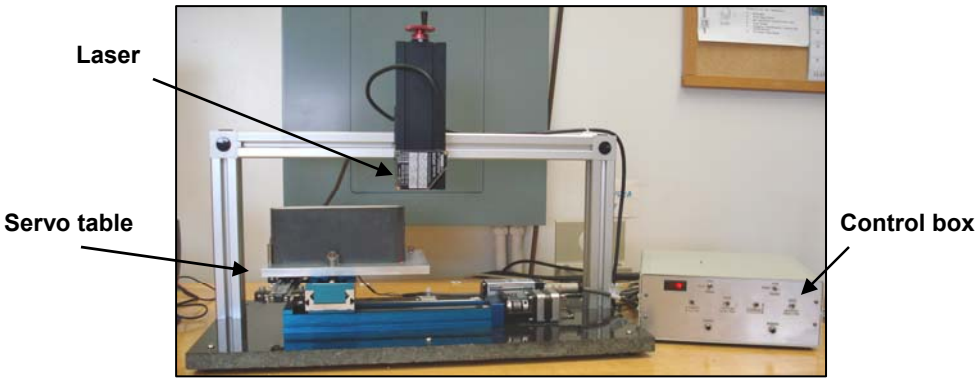

Fig. 2.6- The profilometer device used for surface characterization

2.2.3. Hardness Measurements

We used the rock embedment strength method described by Howard and Fast[15]. The method consists of indenting a steel ball a distance equal to half of its radius. We used a steel ball of 0.0625 in. in diameter, resulting in an indentation distance of 0.016 in. After the pressure is recorded, based on the applied load, and the projected area, the embedment pressure (S_{RE}) is calculated. The rock embedment strength equation (Equation 2.1) is shown below (from Howard and Fast):

$$S_{RE} = \frac{W(lbs)}{\frac{\pi d_i^2}{4}(in^2)} \tag{2.1}$$

In equation 2.1, W is the load applied and d_i the diameter of the projected area of the indentation. In our case we assumed the area of the indentation is equal to the cross sectional area of the steel ball. Fig. 2.7 shows the rock embedment strength measurement apparatus. The apparatus has 2 different gauges, the top gauge is for the pressure reading and the bottom gauge measures the indentation distance. We first calculated the pressure to indent the steel ball the required distance from which we calculate the load applied to the area of the piston of the machine. The piston has a diameter of 0.992 in., and a cross sectional area of 0.773 in^2.

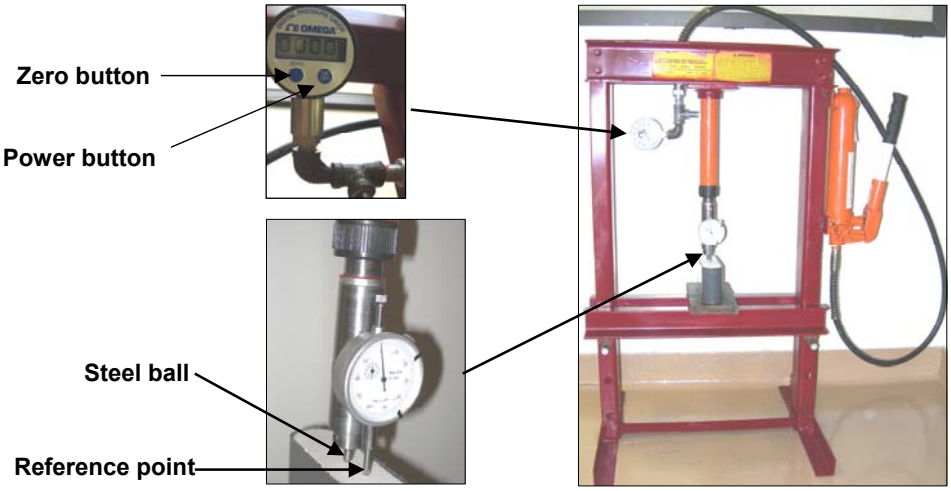

Fig. 2.7- Rock embedment strength machine operated with a hydraulic oil piston

On each fracture surface, we measured the rock embedment strength at 28 points before and after acidizing. The detailed hardness measurement procedure is as follows:

1. Use a guide to mark the points of measurements on the surface of the rock. Place the rock sample in the rock embedment strength base and bring down the steel ball until it is touching the rock surface.
2. Place the needles from the gauge device into the zero position. If the pressure gauge does not show a zero value in its screen, press the zero button to reset a zero value before starting the measurement.
3. Indent the steel ball to a fixed distance of 0.017 in., read the pressure required for the indentation, and record the reading in the control sheet.
4. Repeat Steps 1 to 3 for all the measurement points.

2.2.4. Acid Etching

- Saturate the core samples with brine with an available vacuum device. This process lasts until the vacuum screen pressure is 0.02 psi. Fig. 2.8 shows the glass vessel used for saturation, which is connected to the vacuum device.

Fig. 2.8- Saturation vessel connected to vacuum device

- Remove the cores from the vacuum device, weigh them, and record measurements on the control sheet.

- Assemble the test cell by placing the cores inside. Use vacuum grease on the sides of the cores to allow an ease in placing the cores inside the cell. Make sure the cores are placed in a vertical position inside the cell in such a way that the flow direction is set upwards.

- Place 0.012 in. shims through the middle division of the cell to maintain the fracture gap at the same distance. Push the cores inside until they touch the shims.

- Apply silicone sealant at the back side of the cores once placed in the cell. This sealant is applied through the edges of the core sample and the cell to prevent any leakage between the cell body and the core sample.

- Place the cell in the loading jack in vertical position. Position the side pistons and push them in using the hydraulic jack until they are touching the core samples.

- Remove the shims, connect all the lines, and lock the hydraulic jack device to prevent its movement during acid injection. Make sure the outlet of the line is placed in the disposal container for water.

- Set the pumping capacity to 70%, open the water line, and start the pump by flowing water through the set up. An average pressure of 250 psi is maintained in the cell pressure during the pre flush. The heater device is activated and set to an upper limit

depending upon the temperature of study. In our case we pumped acid at 175°F, so we set the upper limit of the heater to be 190°F. In this way the heater will shut down at temperatures higher than 190°F.

▪ Prepare the acid by gathering the necessary components: HCl, gelling agent, corrosion inhibitor, iron stabilizer, and water. Turn on the magnetic mixer, and measure the required quantities for the acid solution. First, mix the HCl and water. Add the corrosion inhibitor and iron stabilizer. Finally add the gelling agent slowly, and let the acid mix well.

▪ Open the brine line, turn on the pump, and increase the pumping capacity gradually until 100%. Monitor the temperature frequently until the desired temperature is achieved. For pumping acid at 175°F, a temperature of 155°F during water pumping is acceptable, since the temperature increases once the acid starts flowing.

▪ Increase the cell pressure to >1,000 psi. Make sure there are no leaks in any of the connections. Set the leakoff backpressure lower than the cell pressure to obtain a pressure differential of at most 0.5 psi. Record the volume of acid in the tank to the control sheet and experimental conditions during water pumping.

▪ Change the fluid from water to the acid and change the outlet line to the acid disposal container. Start monitoring the process and pump acid until the desired contact time. For our case we used 10 minutes, 20 minutes, and 30 minutes for contact time.

▪ Change the flow from acid to water once the testing time is completed. Turn off the heater and flush lines with water until the pH values from the outlet of leakoff and the main line are values between 7 and 7.5; this clean the lines of the acid.

▪ Lower the cell pressure and leakoff pressures gradually to zero, turn off the pump, and close the water flow.

▪ Disassemble the cell and using wooden blocks carefully push out the core samples with the hydraulic jack. Clean the cell; remove any residue from the rock or from the sealant.

▪ Neutralize the disposed acid with caustic soda. Stir and keep adding caustic soda until the pH of the solution is between 7 and 7.5. Place the neutralized acid in the required containers following the health and safety guidelines for proper disposal of toxic material.

▪ Dispose the water collected in the water container through the drains.

2.2.5. Conductivity Calculation

▪ Connect the power outlet of the flow controller and the pressure gauges. Open the flow controller to its maximum flow. You will hear a click sound when that point is achieved.

▪ Set up cores in the conductivity cell, the same way as for the acid etching procedure with the difference of pushing the cores inside until both faces of the core are in contact. Use the silicone sealant at the back of the cores to prevent any leakage between the cores and the body of the cell.

▪ Rest the cell with the pistons inside in the steel base used to prevent the movement of both ends of the cores once closure stress is applied by the load frame.

▪ Place the conductivity cell in a horizontal position in the conductivity load frame, making sure the flow direction is aligned with the corresponding inlet. The cell has to be placed in the middle of the contact area with the frame to ensure an even distribution of the force to the area.

▪ Connect all the lines and open the air line to move the loading frame until it is touching the top piston. At this point the pressure gauge should read a value of 0 psi closure stress, and the air pressure should be in a value between 0 and 5 psi.

▪ Open the backpressure regulator completely to atmosphere.

▪ Open the nitrogen tank to 80 psi. At this time nitrogen flow through the acidized fracture and the pressure gauges display a pressure drop along the fracture.

▪ Close the backpressure regulator until the pressure inside the cell reaches a value of 50 psi. If the pressure does not build up, the system probably has developed a leak, which requires disassembling the cell and repeating the procedure.

▪ Record the pressure drop across the fracture after 45 minutes for one closure stress value. Increase the flowrate and record its corresponding pressure drop. Repeat the readings for 4 different flowrates. When increasing the flowrate, an increase in the cell pressure will be observed. Adjust the backpressure regulator to lower the cell pressure to 50 psi for each reading.

▪ Increase the closure stress by 1,000 psi and let the pressure stabilize for 45 minutes. Repeat the recording of pressure drops for different flowrates as mentioned in the previous step, until the backpressure regulator can no longer control the cell pressure, or the pressure drop in the fracture is higher than the allowable range of the pressure transducer.

▪ Turn off the nitrogen flow and lower the loading frame pressure to allow the removal of the conductivity cell.

▪ Disconnect all the flow lines, disassemble the cell, and remove the cores with the hydraulic jack.

▪ Input the recorded pressure drops for each closure stress using spreadsheets previously formatted for conductivity calculation using the Forcheimer equation[11] (Equation 2.2).

$$\frac{\left(p_1^2 - p_2^2\right)Mh}{2ZRTL\mu\rho q} = \frac{1}{wk_f} + \frac{\beta\rho q}{w^2\mu h} \tag{2.2}$$

Equation 2.2 shows that the Forcheimer equation can be arranged as a straight line equation in which the "y" intercept is the inverse of the conductivity. The pressure squared difference (p_1^2-p_2^2) is what we measure in the lab at four different flowrates (q) under each closure stress. The values for all the other variables are presented in Table 2.1.

Table 2.1- Data used for conductivity calculations

M	Molecular mass of nitrogen, kg/kg mol	0.028
h	Height of fracture face, in	1.61
Z	Compressibility factor	1.00
R	Universal constant, J/mol K	8.32
L	Length of fracture over which pressure drop is measured, in	5.25
μ	Viscosity of nitrogen at standard conditions, Pa.s	1.747E-05
ρ	Density of nitrogen at standard conditions, kg/m^3	1.16085

2.2.6. Matrix Flow Calculation

To calculate the matrix flow, we first applied Darcy's law (Equation 2.3).

$$q_{sc} = \frac{kA}{2\mu p_{sc}} \frac{p_1^2 - p_2^2}{L} \tag{2.3}$$

In Equation 2.3 the pressure squared difference (p_1^2-p_2^2) is the unknown which is calculated for five different flowrates, using nitrogen as the flowing fluid. Flowrates of 5, 10, 15, and 20 lt /min were used. Standard conditions for pressure and temperature were assumed for calculation purposes (Table 2.2). Values for permeability (k) were 4 md for Indiana limestone, 10.7 md for San Andres dolomite and 7 md for the Cream chalk. Permeability measurements were made in a lab using a Probe Permeameter.

Table 2.2- Data used for matrix flow calculations

A	Cross section area in the flow direction, cm^2	6.45
p_{sc}	Absolute base pressure, atm	1
μ	Viscosity of nitrogen at standard conditions, cp	0.01747
L	Length of the rock, cm	13.335

Secondly, with the pressure drop as input data for each rock type, we applied Forcheimer's equation (Equation 2.2) to calculate the matrix flow conductivity. The values for matrix flow resulted in 41.5 md-ft for limestone, 111 md-ft for dolomite, and 72.7 md-ft for chalk.

2.3. Experimental Conditions

In this study the experimental variables were contact time and rock type. Contact times were 10 minutes, 20 minutes, and 30 minutes. We used three different rock types: Indiana limestone, San Andres dolomite, and Texas Cream chalk. The acid system selected for study was a gelled acid with 15% HCl, injected at an average temperature of 175°F.

To study the effect of acid on rock strength, we systematically measured two parameters in each experiment in addition to the conductivity, the rock embedment strength before and after acidizing, and the change in the vertical depth on the acidized surface by means of the profilometer.

In this study hardness measurements were done before the acid etching procedure at 28 different points of both sides of each core sample. The measurement points were selected on the face of the rock which was exposed to acid transport. The points were evenly spaced with 0.3 in. in the vertical direction and 1 in. in the horizontal direction, throughout the surface of the core to better evaluate the hardness variation within each formation type. In a similar manner, after the acid etching procedure, measurements were repeated at the same points as before acidizing to better evaluate the strength variation for each acid system and rock type of study. Fig. 2.9 shows an illustration of the measurement points on each core sample.

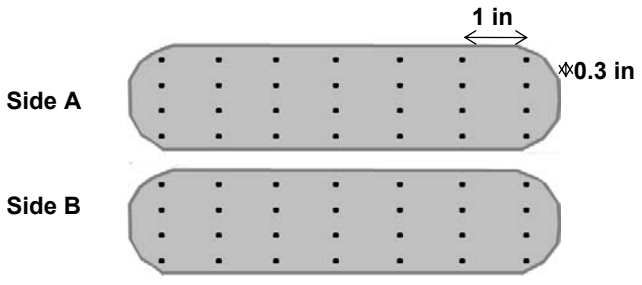

Fig. 2.9- Core faces with the points of strength measurements

2.4. Experimental Output

2.4.1. Hardness Measurements

The strength of the rock is presented in a table format for each set of samples. Table 2.3 presents an example of the strength values for Test 2.

Table 2.3 - Rock embedment strength measurements for Test 2

Test 2		Side A S_{RE}			Side B S_{RE}		
x	y	Before	After	Δz	Before	After	Δz
0.5	0.4	**29,700**	**34,300**	**0.0264**	**33,500**	**45,300**	**0.0292**
1.5	0.4	**42,800**	**35,000**	**0.0294**	22,200	60,500	0.0304
2.5	0.4	54,200	61,700	0.0324	42,600	31,000	0.0377
3.5	0.4	17,600	44,600	0.0347	35,300	37,000	0.0381
4.5	0.4	**38,500**	**37,800**	**0.0247**	**46,600**	**40,300**	**0.0295**
5.5	0.4	32,200	42,800	0.0378	40,800	35,300	**0.0275**
6.5	0.4	22,400	36,000	0.0334	**31,000**	**37,800**	**0.0210**
0.5	0.7	42,800	27,000	0.0495	30,700	27,500	0.0475
1.5	0.7	36,800	28,200	0.0476	38,300	34,000	0.0408
2.5	0.7	19,100	47,900	0.0423	45,800	33,500	0.0301
3.5	0.7	32,700	32,700	0.0337	39,800	39,300	0.0316
4.5	0.7	50,400	66,000	0.0449	24,700	23,400	0.0466
5.5	0.7	33,300	55,400	0.0415	23,700	28,200	0.0364
6.5	0.7	32,200	31,500	0.0394	32,200	51,100	0.0397
0.5	1	31,500	25,400	0.0354	27,700	36,800	0.0470
1.5	1	34,500	42,300	0.0431	33,800	44,300	0.0413
2.5	1	41,600	37,300	0.0424	37,800	35,800	0.0423
3.5	1	26,500	51,100	0.0351	39,300	27,700	0.0398
4.5	1	44,100	56,400	0.0343	49,100	44,100	0.0388
5.5	1	41,600	41,300	0.0320	30,200	26,700	0.0440
6.5	1	**28,200**	**25,200**	**0.0300**	**36,300**	**33,300**	**0.0233**
0.5	1.3	**28,200**	**40,300**	**0.0205**	33,500	43,800	0.0329
1.5	1.3	43,300	34,800	0.0304	49,900	53,700	**0.0256**
2.5	1.3	**55,400**	**38,500**	**0.0213**	**46,900**	**55,400**	**0.0230**
3.5	1.3	**45,300**	**42,800**	**0.0280**	**52,900**	**37,300**	**0.0218**
4.5	1.3	100,800	36,000	0.0336	**51,900**	**36,800**	**0.0275**
5.5	1.3	**28,200**	**50,400**	**0.0273**	35,800	36,000	0.0389
6.5	1.3	**33,500**	**32,700**	**0.0291**	**39,300**	**22,200**	**0.0221**

Bold: high points, Δz<0.030

There are 3 principal columns in each table. The first principal column represents the coordinates of the measurements. The second principal column all the values corresponding to one of the fracture faces, side A; including the rock embedment strength values before and after acidizing, along with the vertical distance change in its corresponding coordinate. The third principal column illustrates the same characteristics but on the other fracture surface, side B. The values in bold font represent the points of measurements identified as "high points", points in which the vertical distance change was lowest.

For each contact time and rock type tested we selected a cutoff value in the vertical distance variation for considering the high points. In Appendix B, a similar table is presented for each experiment performed with its corresponding cutoff value.

2.4.2. Surface Profile

3D images are generated by the profilometer from the scanned surfaces of the core samples. The images are represented with a color scale, which corresponds to depth of dissolution, with values ranging from 0 to 0.30 inches. The values increase from a red shade to a darker shade of blue. The detailed procedure of surface profile measurement was described by Malagon[13]. Examples of the images are presented in Fig. 2.10.

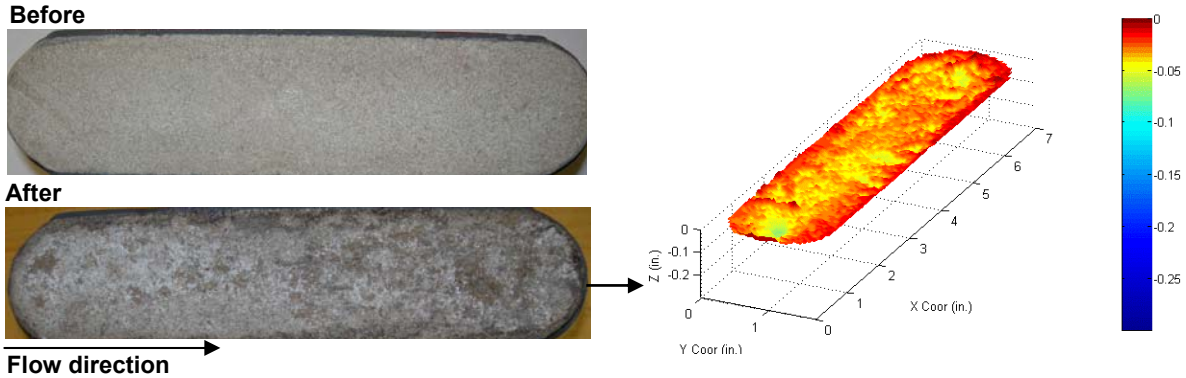

Fig. 2.10- Photographs before and after acidizing and 3D surface image after acidizing

Additionally, we can obtain the vertical distance change in any of the local points. Since the profilometer has a resolution of 5,000 points, we filtered the numerical values of vertical change for each of the 28 points in which we measured rock embedment strength, with the goal to match the hardness values with the vertical distance change. From this, we identified the high points in the surface of the rock, which are thought to influence the retained conductivity at high closure stresses. Furthermore, from the profilometer we can estimate the volume of rock dissolved by subtracting the volume of rock after acidizing from the volume before.

2.4.3. Conductivity Values

Conductivity values are obtained by applying the Forcheimer equation (Equation 2.2) for 5 different flow rates under each closure stress. The pressure drop across the fracture and the cell pressure are recorded for each flowrate. By applying Equation 2.2 the '*x*' and '*y*' components are estimated and plotted. The points resulting for each flow rate are connected and the resulting line is extrapolated to the '*y*' axis to estimate the intercept with the vertical axis. After all the values are graphed for each closure stress, the conductivity profile can be carefully analyzed to evaluate the rocks' response under different experimental conditions. Fig. 2.11 presents an example of conductivity profile for San Andres dolomite.

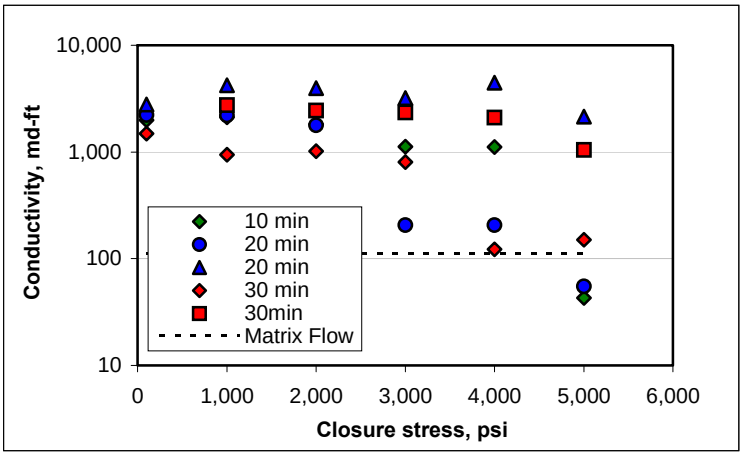

Fig. 2.11- Conductivity profile for San Andres dolomite

2.5. - Comparison of Laboratory Conditions

Laboratory conditions have evolved considerably. Fig. 2.12 shows the core samples used for different experimental studies. Describing from left to right, Fig. 2.12 a) shows the cylindrical cores used in the empirical study for the original acid fracturing conductivity correlation. The cores had approximately 3 inches in height. Later, Gong[6, 7] Fig. 2.12 b), used core samples with different size and shape, to investigate etched surface profile and to account for fluid leakoff which was not considered by Nierode and Kruk. Gong used a rectangular shaped sample with larger dimensions in length and width. More recently, after Zou[11] Fig. 2.12 c) we have used a rectangular shape core sample with a larger surface exposed to acid and larger in height. A larger surface allows us a better interpretation of etching pattern and an improved leakoff condition.

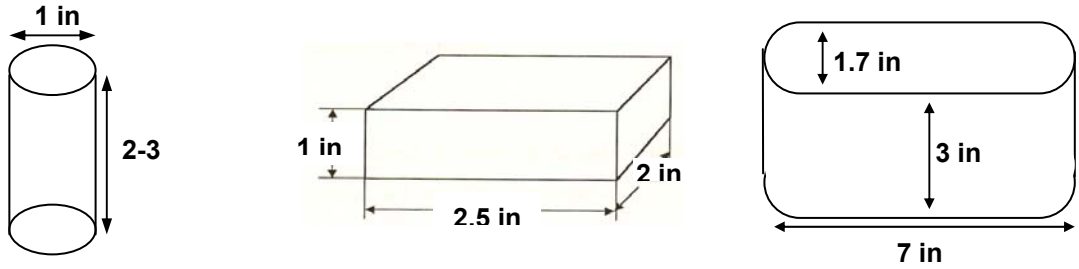

a) N-K, 1973 b) Gong, 1997 c) Zou, 2006

Fig. 2.12- Core sample size comparison

Concerning the acid system, since the experimental conditions are not specified in detail in the Nierode-Kruk publication, it is assumed that hydrochloric acid was used. Gong used hydrochloric acid as well. However, we are using a modern gelled acid system to evaluate what is currently used to represent the field conditions as much as possible.

Regarding injection rate, in the Nierode-Kruk correlation it is not specified, Gong used 0.01 lt min and we are using 1 lt/min. Fig. 2.13 shows the etching patterns for the same experimental conditions, at different flowrates. From left to right, a) is the surface

profile for Gong's experiments, and to the right b) is the surface obtained with the experimental set up we are using. Illustrations for the Nierode-Kruk experiments were not available for comparison. If we analyze the etching pattern we can see different asperities caused by the difference in injection rates, this is mainly due to the scaling of conditions of our laboratory as compared to Gong's. Etching pattern affects conductivity; hence it will affect the conductivity measured in the lab.

a) Gong, 1997 c) Zou, 2006

Fig. 2.13- Etched surface comparison

CHAPTER III

EXPERIMENTAL RESULTS AND DISCUSSION

We conducted fifteen experiments with three different rock types acidized with a gelled acid system, at an average temperature of 175°F. For each rock tested, three contact times were used: 10, 20, and 30 minutes. The experiments of 20, and 30 minutes were repeated to evaluate the consistency of our experimental procedure, and to investigate conductivity response variation based on the particular properties of the rock sample. Conductivity values are presented in a tabulated format in Appendix A for all the rocks tested. The experimental conditions along with the amount of rock dissolved are summarized in Table 3.1. From Table 3.1 we can identify the increase in etched volume with an increase in contact time for all rocks studied. This behavior is expected, since at longer acid contact time, a higher volume of rock is dissolved than at shorter contact times.

Table 3.1 – Summary of experimental conditions

Test No.	Rock Type	Contact Time (min)	Etched Volume (in^3)
1	Indiana Limestone	10	0.56
2		20	0.63
3		20	0.67
4		30	0.66
5		30	0.76
6	San Andres Dolomite	10	0.19
7		20	0.32
8		20	0.39
9		30	0.48
10		30	0.47
11	Cream chalk	10	0.41
12		20	0.54
13		20	0.62
14		30	1.03
15		30	0.71

For each rock type tested, the conductivity response related to contact time and rock embedment strength change is different, and they are discussed respectively. All the experimental data including photographs, 3D surface profiles, and rock embedment strength measurements are presented for each test in Appendices B-1 to B-15.

The hardness distributions for all rock types were fitted to the best statistical distribution available, with the goal to estimate a mean hardness value for each rock sample. It was shown that for all rock types, the hardness distribution before acidizing was normally or log-normally distributed (Appendix B-2 to B-15). For the hardness values after acidizing, most of the rocks did not show a clear distribution.

3.1. Indiana Limestone

For the five experiments with Indiana limestone, the mean values of rock embedment strength measurements ranged from 28,300 psi to 39,200 psi (Table 3.2). Table 3.2 presents a summary of the hardness measurements for each limestone test. The rock hardness values before and after acidizing are presented for average values considering all points of measurements, and for the average values of the high points as well. Red values represent increase in hardness after acid, caused by the exposure of harder surfaces after acid. Detailed hardness values for each test are presented for reference in Appendices B2- B5.

Table 3.2- Rock embedment strength values for Indiana limestone

Test No.	Contact Time (min)	Etched Volume (in^3)	Mean S_{RE} Before (psi)	Mean S_{RE} After (psi)	% Reduction S_{RE}	Mean S_{RE} Before (psi)	Mean S_{RE} After (psi)	Mean % Reduction S_{RE}
			All points			High Points		
1	10	0.56	29,700	28,400				
2	20	0.63	39,000	36,400	6.7%	40,800	38,300	2.3%
3	20	0.67	32,600	34,200	-4.9%	30,400	29,000	4.7%
4	30	0.66	28,300	28,700	-1.4%	27,400	31,500	-11.0%
5	30	0.76	39,200	38,400	2.0%	37,800	39,300	-3.0%

Notice (Table 3.2) that Test 1 does not present average hardness values for the high points category, this is because the hardness values before and after acidizing are only from nine measuring points, as opposed to the 28 done in all the other tests. For that, hardness values were not considered to explain the conductivity response when comparing the influence of contact time for Indiana limestone.

Fig. 3.1 presents the 3D surface profile of the etching pattern for Indiana limestone at different contact times, showing a trend of shallow, more randomly distributed etching with wormholes at short contact times to a deep, channel-like etching at longer contact times. Channel formation is favorable to retain the fracture conductivity after closure because channels are much harder to crush. Thus, we expect better conductivity behavior at longer contact times when channels are clearly developed than at shorter contact times. Appendix B-1 through B-5 presents the 3D surface profile of both faces for each test.

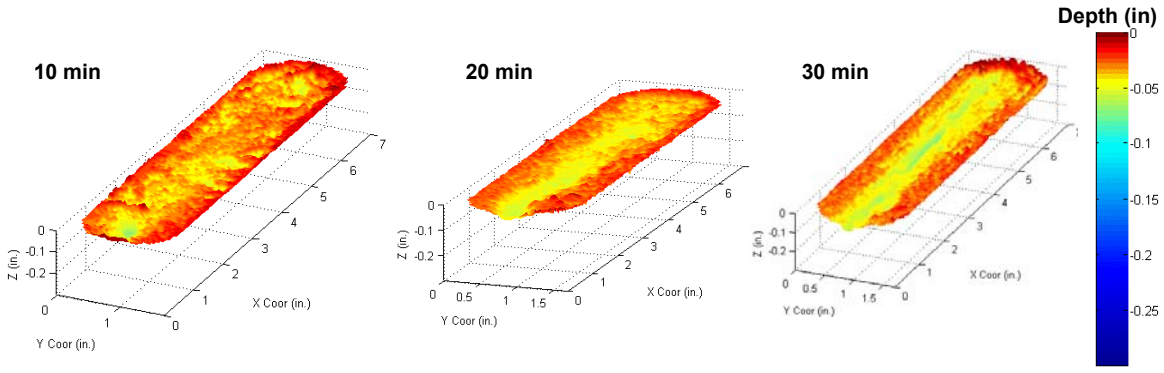

Fig. 3.1- 3D surface profile for Indiana limestone at different contact times

Fig. 3.2 shows the measured conductivity for all five experiments for Indiana limestone. The matrix flow is presented as a dashed line. The matrix flow is the conductivity value below which the fracture is completely closed.

Analyzing the graph (Fig. 3.2) we can see that one of the tests with the longest contact time (30 minutes) has higher values of conductivities than all the other tests, followed by the contact times of 20 minutes, and contact times of 10 minutes. The

results suggest that longer contact times can yield better conductivity even at high closure stress, however the rock has to be hard enough and channels clearly developed.

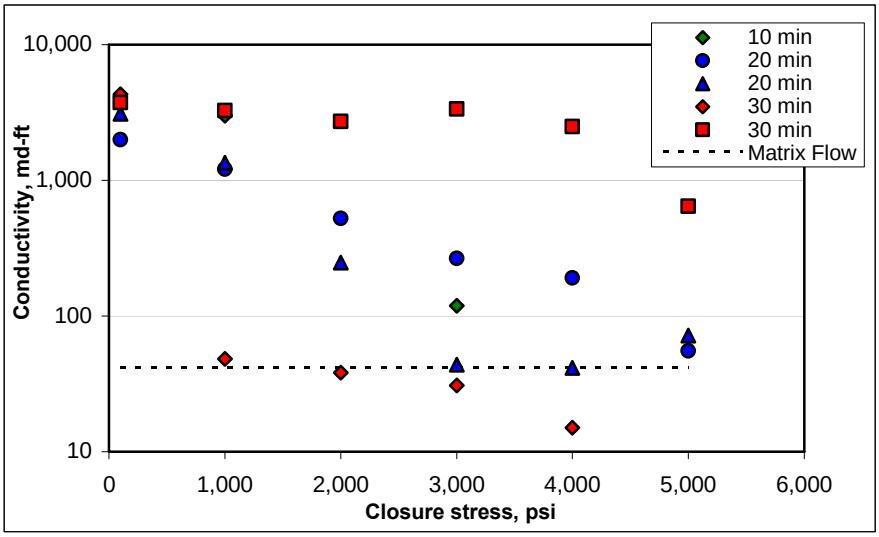

Fig. 3.2- Conductivity values for Indiana limestone

Fig. 3.3 shows the hardness values for all limestone tests considering all the points of measurements Fig. 3.3 a), and only the high points Fig. 3.3 b).

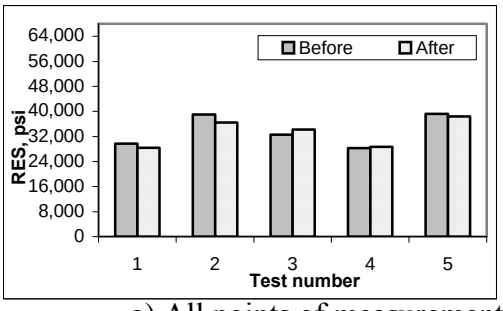

a) All points of measurements

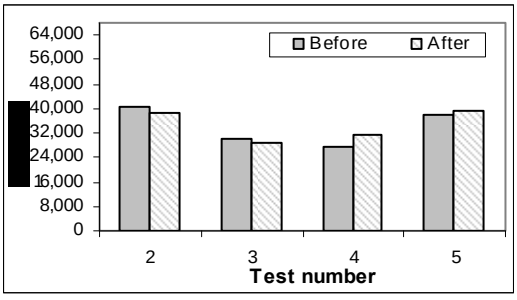

b) High points

Fig. 3.3- Rock embedment strength values for Indiana limestone

We can see (Fig. 3.3) that the tests with higher strength before acidizing also had higher strength after, considering all points of measurements and also considering only high points. We also recognized that the etching pattern is not the only factor for sustained conductivity. Rock strength plays an important role in the resulting conductivity. If there is no clear channel on the fracture surface, the conductivity is provided by the support of the high points on the surface created by uneven etching, and the hardness of these high points is the critical factor for retaining conductivity after closure.

Combining the rock embedment strength measurements with the conductivity results, we noticed that at twenty minutes contact time, Test 2 has higher rock embedment strength value before, and after acidizing compared with Test 3 (Fig. 3.4 a)). Test 2 also had a better sustained conductivity at higher closure stresses (Fig. 3.4 b)). Test 2 shows a clear channel pattern through the center of the fracture while Test 3 shows more surface dissolution lacking the presence of channels (Fig. 3.4 c)). The presence of channels and higher values of rock embedment strength is the reason for the better conductivity response for Test 2 compared with Test 3.

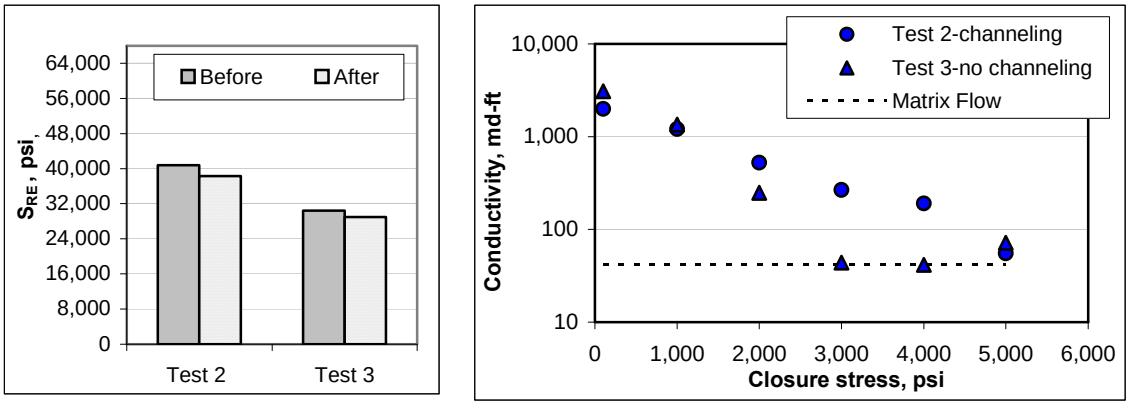

a) S_{RE} measurements b) conductivity profile

Fig. 3.4- Experimental results for 20 minutes tests, Indiana limestone

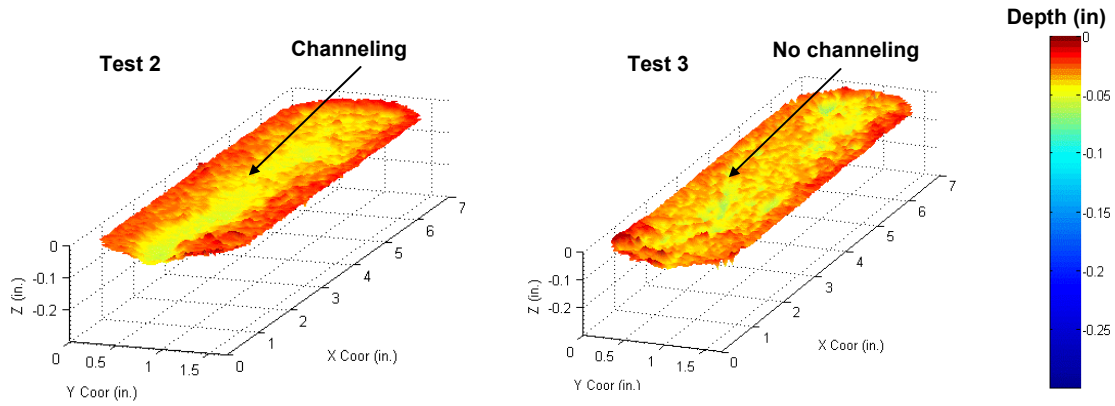

c) 3D surface profile

Fig. 3.4- Experimental results for 20 minutes tests, Indiana limestone

For the 30 minutes tests, Test 5 had higher S_{RE} values before and after acidizing than Test 5 (Fig.3.5 a)). One of the experiments (Test 4) crushed completely at low closure stresses, as opposed to Test 5 which sustained conductivities up to closure stresses of 4,000 psi (Fig. 3.2 b)). Although Test 4 and 5 clearly developed a channeling etching pattern (Fig. 3.5 c)), Test 5 developed a wider channel, and also had higher hardness values before and after acid than Test 4. In this case channeling governed conductivity for contact times of 30 minutes. As contact times increased, conductivity was influenced by the hardness values after acidizing as well as the etching pattern.

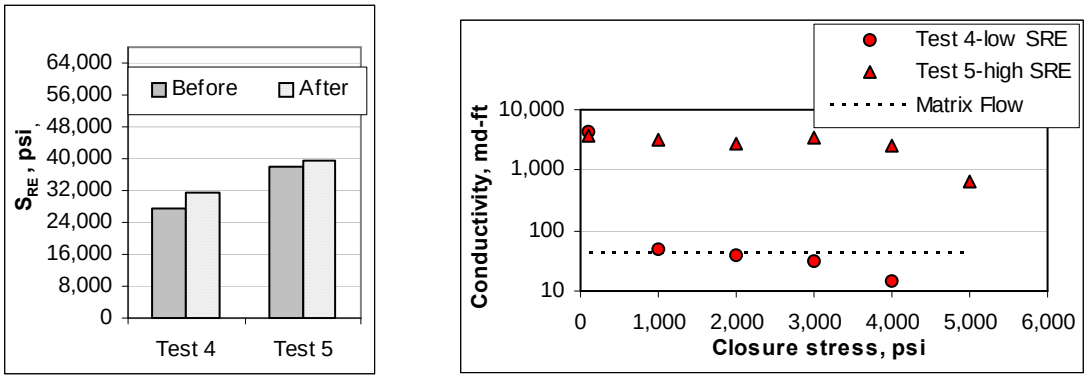

a) S_{RE} measurements b) Conductivity profile

Fig. 3.5- Experimental results for 30 minutes tests, Indiana limestone

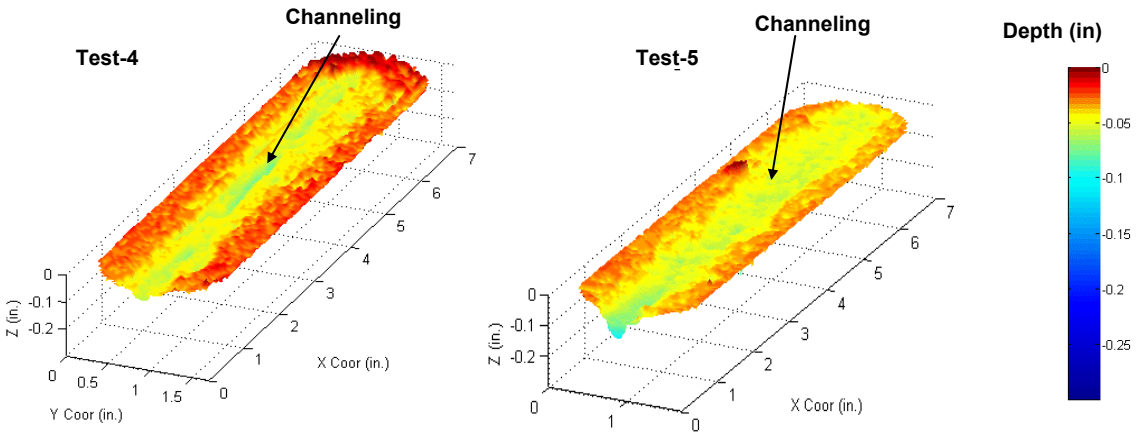

c) 3D surface profile

Fig. 3.5- Experimental results for 30 minutes tests, Indiana limestone

For limestone, channeling dominates the conductivity response when channels are formed, and rock strength influences the result after channeling formation. If there is lack of channeling, rock strength is the key factor for retaining conductivity.

3.2. San Andres Dolomite

The dolomite samples tested in this study had a distinctive feature compared to the limestone. Since channels are not easily developed for dolomite as for limestone because of the difference in reaction rates, the key parameter in acid fracture conductivity for dolomite is the rock strength which is represented by the rock embedment strength values in this study. In general, the rock embedment strength was higher for dolomite compared with limestone, and a higher conductivity was expected from the dolomite tests.

The values for rock strength measurements ranged from 50,000 psi to 67,500 psi (Table 3.3) before and after acidizing, a much higher range than the limestone hardness values.

Table 3.3- Rock embedment strength values for San Andres dolomite

Test No.	Contact Time (min)	Etched Volume (in^3)	Mean S_{RE} Before (psi)	Mean S_{RE} After (psi)	% Reduction S_{RE}	Mean S_{RE} Before (psi)	Mean S_{RE} After (psi	% Reduction S_{RE}
			All points			High points		
6	10	0.19	58,600	54,800	6.5%	59,100	54,100	11.5%
7	20	0.32	56,900	52,200	8.3%	54,500	45,100	15.0%
8	20	0.39	50,100	50,900	-1.6%	47,200	45,600	0.3%
9	30	0.48	67,400	59,600	11.6%	68,000	52,200	23.0%
10	30	0.47	57,400	58,800	-2.4%	54,400	53,800	2.0%

Fig. 3.6 displays the 3D surface profile of the etched surfaces at different contact times for dolomite. In some experiments, we observed that after the acid etching procedure the fracture faces revealed a grainy crystalline structure, while most of them had a more uniform etching pattern compared with the limestone. The dissolved rock volume was increased as the contact time increased (Table 3.3), and channeling was not observed in the experiments (Fig. 3.6). Detailed images of the fracture faces before and after acid injection are presented in the Appendices B-6 to B-10.

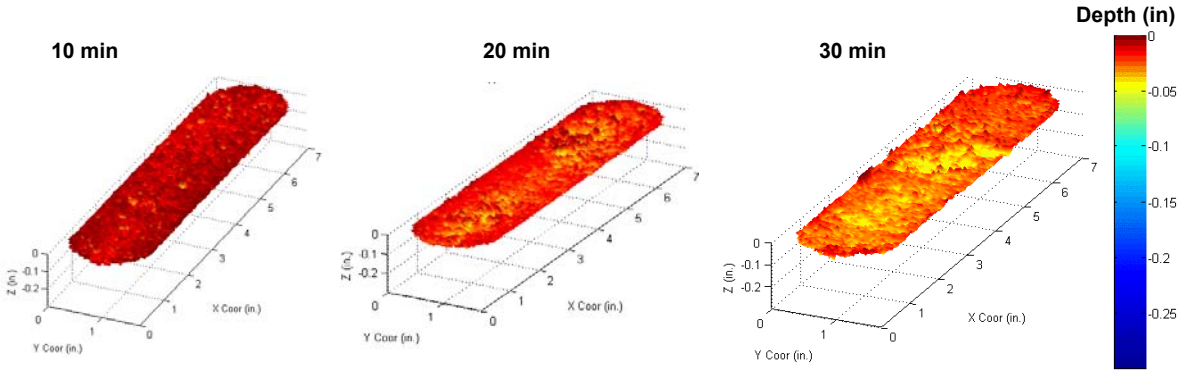

Fig. 3.6- 3D surface profile for San Andres dolomite at different contact times

Fig. 3.7 shows the conductivity profile for the San Andres dolomite experiments. Analyzing the results we can identify that conductivities are sustained for closure

stresses up to 5,000 psi, mainly caused by the hard nature of this rock as compared to limestone. Matrix flow is represented by a dashed line under which the fracture is considered closed. It is apparent from Fig. 3.7 that short contact time of 10 minutes sustained conductivity at high closure stresses as well as long contact times of 30 minutes.

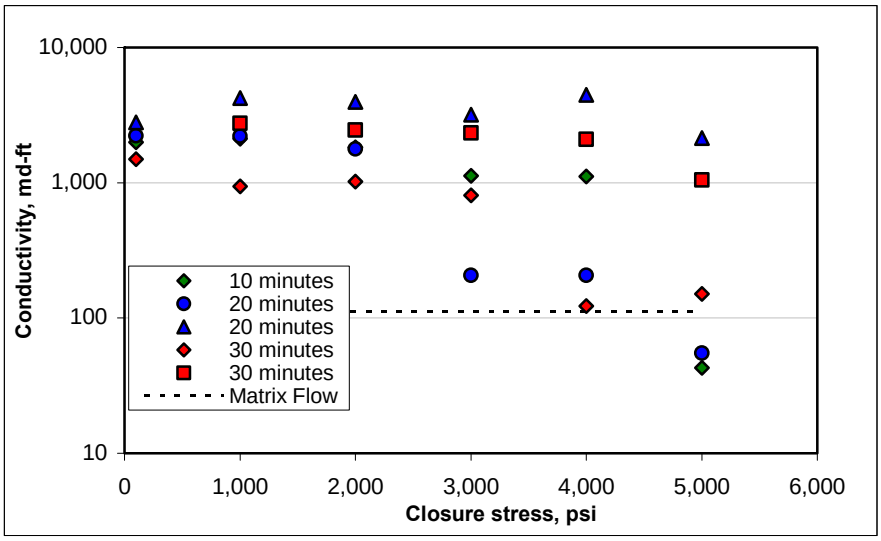

Fig. 3.7- Conductivity values for San Andres dolomite

We combined the rock embedment strength data from Table 3.3 with the conductivity results (Fig. 3.7) to explain the conductivity profile for dolomite. Figure 3.8 shows the relationship between hardness reduction and conductivity at high closure stresses of 4,000 psi (Fig. 3.8 a)) and 5,000 psi (Fig. 3.8 b)). From Figure 3.8, it is apparent that the higher the hardness reduction, the lower the conductivity values at closure high closure stress, independent of contact time.

The rock samples which had lower rock embedment strength reduction from mean values considering all points, demonstrated a better sustained conductivity under closure stresses, than rocks with higher rock strength reduction.

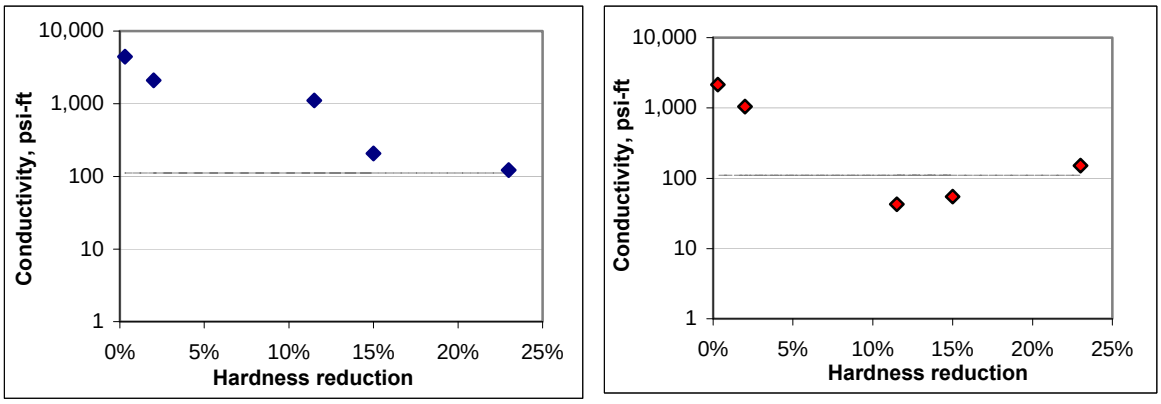

a) 4,000 psi closure stress b) 5,000 psi closure stress

Fig. 3.8- Conductivity vs hardness reduction for San Andres dolomite

Fig. 3.9 shows the relationship between conductivity response and hardness reduction at different closure stresses. In Fig.3.9, the *x* axis is the test number ordered in increasing value of hardness reduction, the right *y* axis shows the hardness reduction represented by points in the plot, and the left *y* axis the conductivity values represented by bars at different closure stresses.

From Fig. 3.9, a decreasing trend in conductivity is interpreted for all tests independent of contact time, as closure stress increases. Additionally, as the degree of weakening decreases, the conductivity increases. For the 20 minutes tests (Test 7 and Test 8), Test 8 had 0.3% reduction after acidizing, maintaining a very high conductivity to high closure stresses. Meanwhile Test 7 had a 15% reduction and its effect is observed on the conductivity decline at 3,000 psi closure stress. The resulting conductivity of Test 8 is higher than that of Test 7, especially and more importantly, at high closure stress, the difference in conductivity is attributed to the weakening of the rock surface caused by the acid.

Similarly, for the 30 minute tests (Test 9 and Test 10) the conductivity for Test 10 is higher than that of Test 9. The strength was reduced only 2% in Test 10, while Test 9 was reduced 29% (Fig. 3.9).

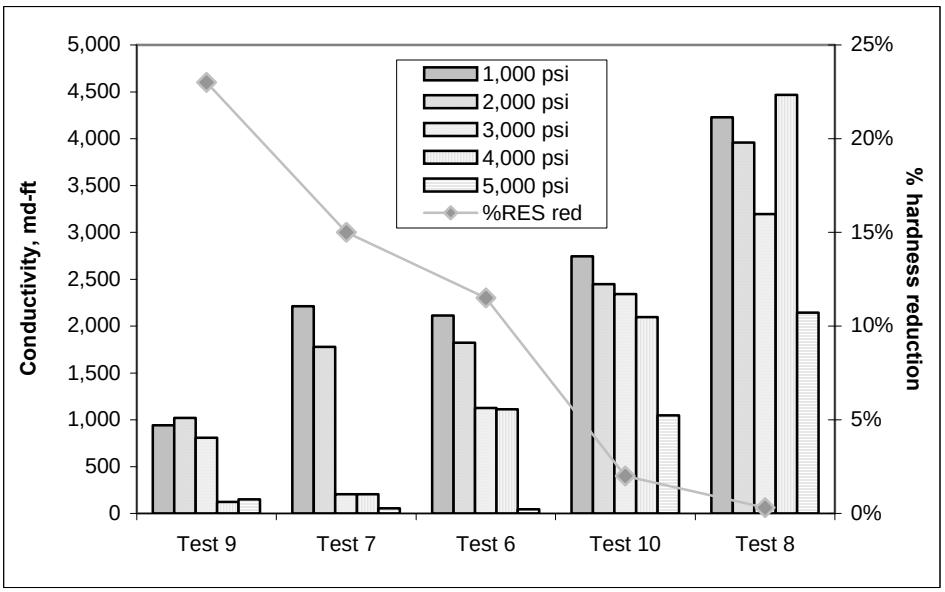

Fig. 3.9- Conductivity profile and hardness reduction for San Andres dolomite

For dolomite rocks, the rocks with lower hardness reduction in the high points demonstrated a better sustained conductivity. Even though the effect of contact time cannot be clearly correlated to conductivity from these experiments, it is apparent that longer contact times do not always provide higher conductivity after fracture closure (Fig. 3.9).

3.3. Texas Cream Chalk

The Texas Cream chalk is a softer rock compared with the Indiana limestone and San Andres dolomite. Table 3.4 shows that hardness values for the Cream chalk are between 20,000 psi to 28,000 psi, a lower range than the other rocks tested. Detailed values for hardness measurements are presented in Appendices B-11 to B-15, in addition to the etched surface profiles.

Table 3.4- Rock embedment strength values for Texas Cream chalk

Test No.	Contact Time (min)	Etched Volume (in^3)	Mean S_{RE} Before (psi)	Mean S_{RE} After (psi)	% Reduction S_{RE}	Mean S_{RE} Before (psi)	Mean S_{RE} After (psi)	Mean % Reduction S_{RE}
			All points			High Points		
11	10	0.41	26,800	19,600	26.0%	26,200	20,000	29.0%
12	20	0.54	26,100	27,500	-5.4%	26,500	25,700	3.7%
13	20	0.62	23,700	23,200	2.1%	23,000	21,800	4.2%
14	30	1.03	26,000	28,700	-10.4%	25,200	24,900	0.4%
15	30	0.71	28,000	22,500	19.6%	26,800	22,900	9.5%

The 3D surface profile for the different contact times of study are presented in Fig. 3.10. It can be seen that at short contact times the etching pattern is mostly surface dissolution, to a scattered channeling for longer contact times.

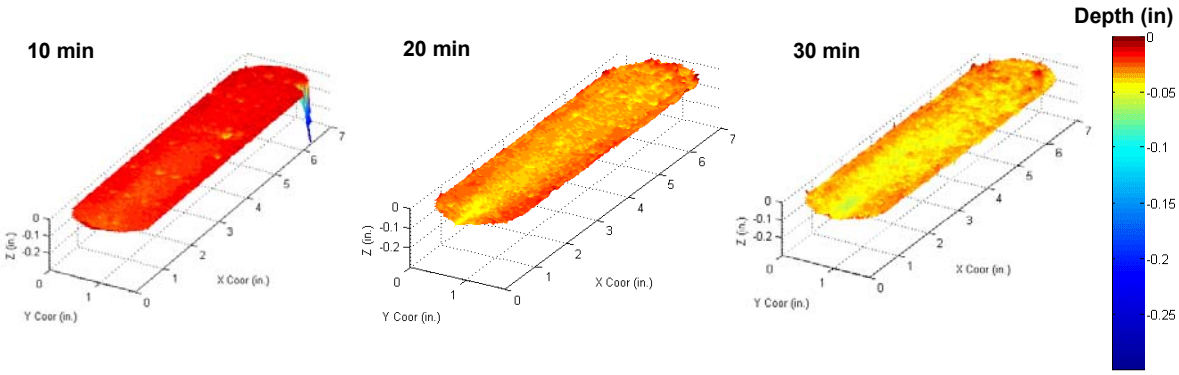

Fig. 3.10- 3D surface profile for Texas Cream chalk at different contact times

Fig. 3.11 displays the conductivity results, with a dashed line representing matrix flow below which the fracture is considered closed. First of all, we observed that in all 5 experiments (Tests 11-15) the fracture was completely closed at much lower closure stress compared with the limestone and the dolomite. Considering the softer nature of the chalk, this is expected. Secondly, the 20 minute tests support the findings from

limestone and dolomite, that is, in the lack of channeling, hardness values govern conductivity.

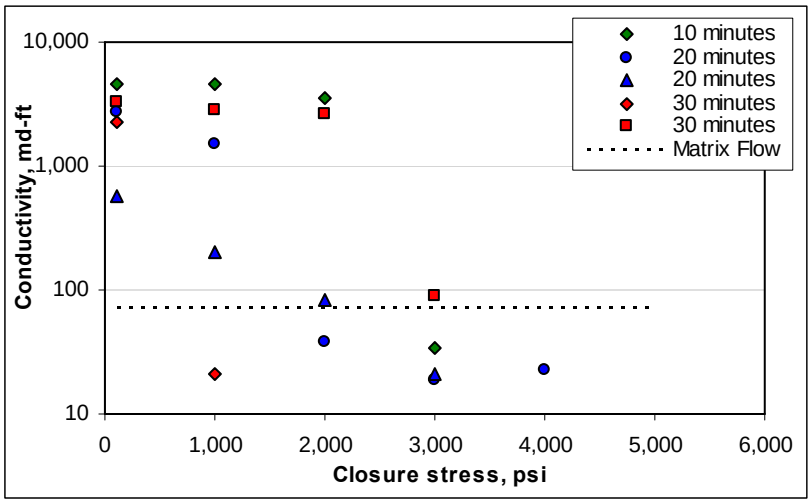

Fig. 3.11- Conductivity values for Texas Cream chalk

If we evaluate the hardness values for the 20 minutes tests (Test 12 and Test 13), from Fig. 3.12 a) we identified that the hardest rock before acidizing was also the hardest rock after acidizing. The conductivity profile (Fig.3.12 b)) illustrates that the rock with highest S_{RE} resulted in higher conductivity.

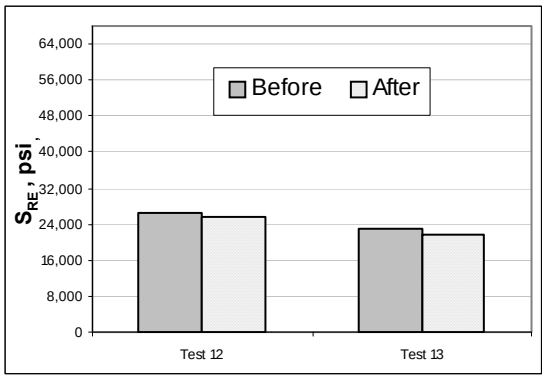

a) SRE measurements

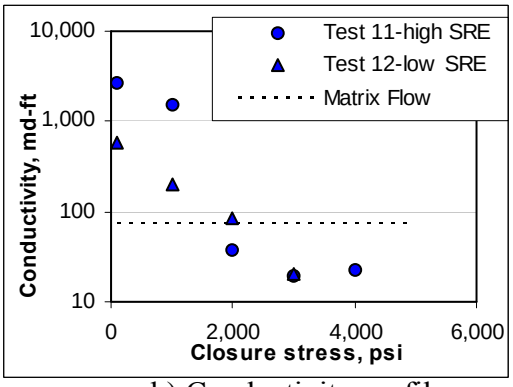

b) Conductivity profile

Fig. 3.12- Experimental results for Texas Cream chalk at 20 minutes

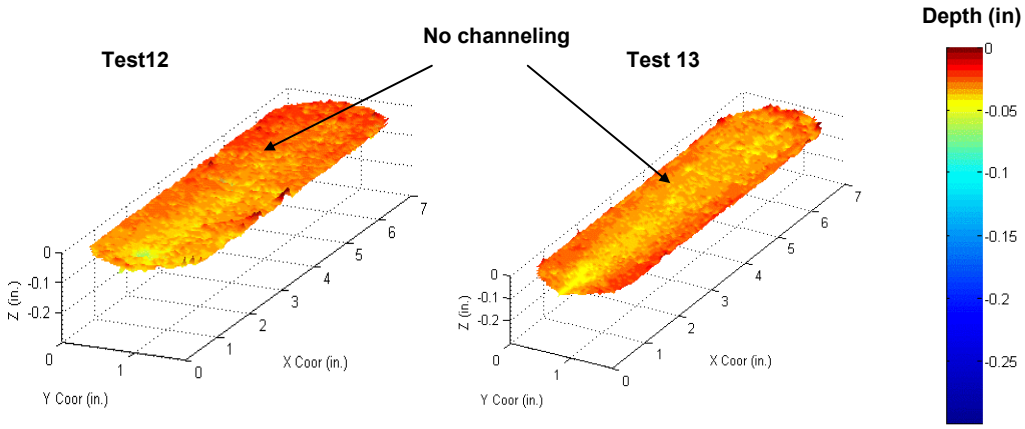

c) 3D surface profiles

Fig. 3.12- Experimental results for Texas Cream chalk at 20 minutes

The etching pattern of the 20 minutes tests (Fig. 3.12 c)) is mostly surface dissolution with no dominant channel formation. From our results, it is apparent in the lack of channeling, hardness governs conductivity for the chalk.

For the 30 minutes tests, Test 15 had higher hardness values than Test 14 (Fig. 3.13 a), but its conductivity response fell at lower closure stresses than that of Test 14 (Fig. 3.13 b)).

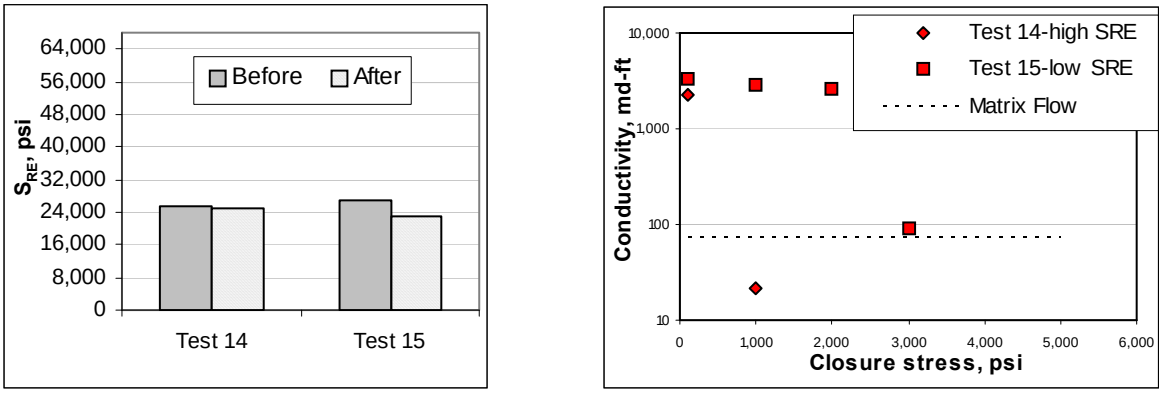

a) SRE measurements

b) Conductivity profile

Fig. 3.13- Experimental results for Texas Cream chalk at 30 minutes

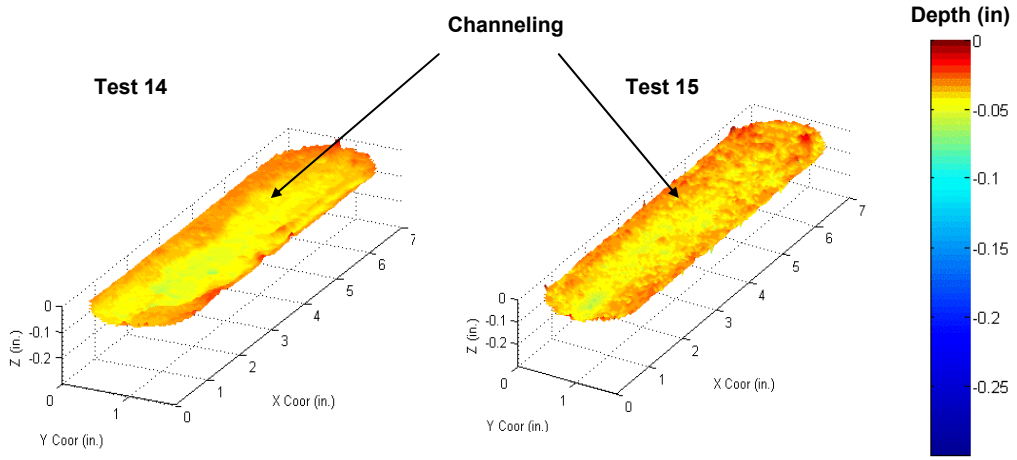

c) 3D surface profiles

Fig. 3.13- Experimental results for Texas Cream chalk at 30 minutes

Even though Test 14 had more dominant channel formation (Fig. 3.12 c)) and higher hardness values than Test 15, this is contradicting to the results obtained in all the other tests. We do not understand the conductivity profile for these testing conditions.

3.4. Important Parameters in Acid Fracturing Conductivity

3.4.1. Effect of Acid on Hardness Variation

As mentioned before, to study the effect of acid on rock strength, we measured two parameters in each experiment in addition to the conductivity, the rock embedment strength before and after acidizing, and the change in the vertical depth on the acidized surface. From these measurements we determined the coordinates of the high and low points of the etched surface to compare with the coordinates of the rock embedment strength measurements. The high-point hardness values for limestone at 10 minutes were not measured (Test 1).

By comparing the local rock embedment strength measured around the faces of the fractures with the surface elevation map after acidizing, we observed that the rock embedment strength values of the high points on the fracture surface apparently are more related to the fracture conductivity under stress than the overall average rock embedment

strength. From Table 3.5, we identified, if we considered the rock embedment strength values from all the points of measurements (high and low) the mean value obtained after acid was sometimes higher than the unacidized mean value, and sometimes lower. Whereas, if we only considered the high points which are likely responsible for retaining conductivity after closure, the mean values for those points were usually lower than the mean rock embedment strength values before acid injection for all contact times, as shown in Table 3.5, except for the case of limestone 30 minutes.

Table 3.5- Rock embedment strength values for all tests

Test	Rock Type	Contact Time (min)	Mean S_{RE} Before (psi)	Mean S_{RE} After (psi)	% Reduction S_{RE}	Mean S_{RE} Before (psi)	Mean S_{RE} After (psi)	Mean % Reduction S_{RE}
			All points			High Points		
1	Indiana Limestone	10	29,700	28,400				
2		20	39,000	36,400	6.7%	40,800	38,300	2.3%
3		20	32,600	34,200	-4.9%	30,400	29,000	4.7%
4		30	28,300	28,700	-1.4%	27,400	31,500	-11.0%
5		30	39,200	38,400	2.0%	37,800	39,300	-3.0%
6	San Andres Dolomite	10	58,600	54,800	6.5%	59,100	54,100	11.5%
7		20	56,900	52,200	8.3%	54,500	45,100	15.0%
8		20	50,100	50,900	-1.6%	47,200	45,600	0.3%
9		30	67,400	59,600	11.6%	68,000	52,200	23.0%
10		30	57,400	58,800	-2.4%	54,400	53,800	2.0%
11	Cream chalk	10	26,800	19,600	26.0%	26,200	20,000	29.0%
12		20	26,100	27,500	-5.4%	26,500	25,700	3.7%
13		20	23,700	23,200	2.1%	23,000	21,800	4.2%
14		30	26,000	28,700	-10.4%	25,200	24,900	0.4%
15		30	28,000	22,500	19.6%	26,800	22,900	9.5%

Lower hardness values after acid illustrate the weakening of the rock surface caused by the exposure to the acid. Higher values of hardness values after acid are produced as a result of the dissolution of soft areas of the rock surface exposing a new harder surface to sustain conductivity. It is clear that acid reduces the hardness of the rock, and from our results it is apparent that its effect on conductivity is higher for the dolomite than the limestone, and the chalk. For limestone the ranking of hardness

amongst the test samples was maintained after acidizing as well, and the conductivity profile is in agreement with the hardness profile, independent of contact time. For dolomite, the rocks which were weakened the most resulted in lower conductivity, and for chalk due to its soft nature conductivity fell at very low closure stresses and the effect of hardness reduction could not be thoroughly investigated.

3.4.2. Effect of Etching Pattern on Acid Fracture Conductivity

A different etching pattern was observed for each different kind of rock. Channeling was observed in limestone and chalk, especially for longer contact times of 30 minutes. As for the case of dolomite, since it has a much slower reaction rate with the acid as compared to chalk and limestone[1], the pattern observed was mostly surface dissolution, with an increasing amount of rock dissolved with increasing time (Fig. 3.14).

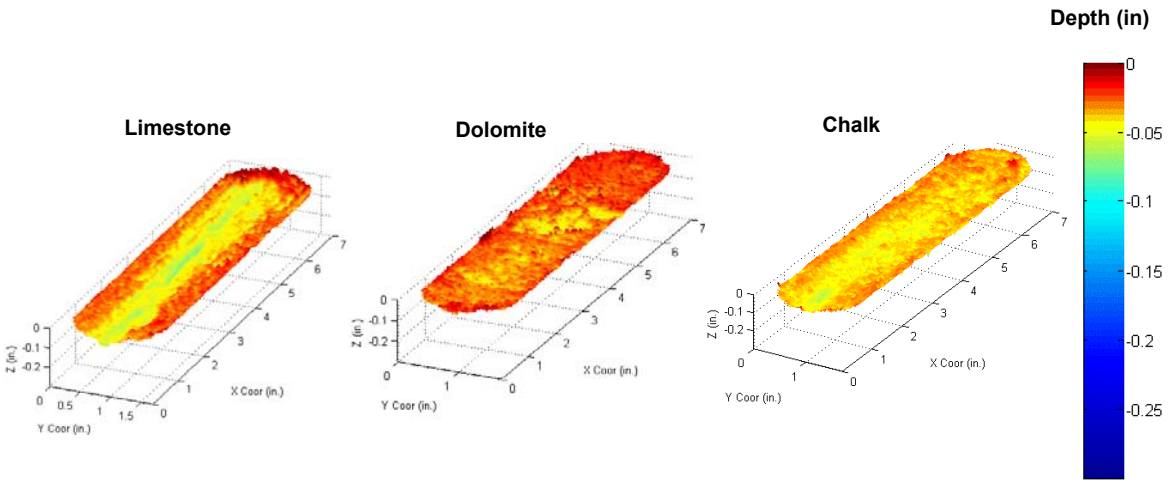

Fig. 3.14- 3D surface profiles for 30 minutes contact time

It is apparent that in the case of limestone and chalk, the formation of channeling favors conductivity. If channeling is not created, the hardness of the rock in the high points is thought to govern the sustainability of conductivity under closure stress.

3.4.3. Effect of Acid Contact Time on Acid Fracture Conductivity

From Fig. 3.15 we can see that for Indiana limestone, in most of the cases longer contact times resulted in higher conductivities, except for one of the tests of 30 minutes (Test 4) in which the initial low hardness values caused early failure.

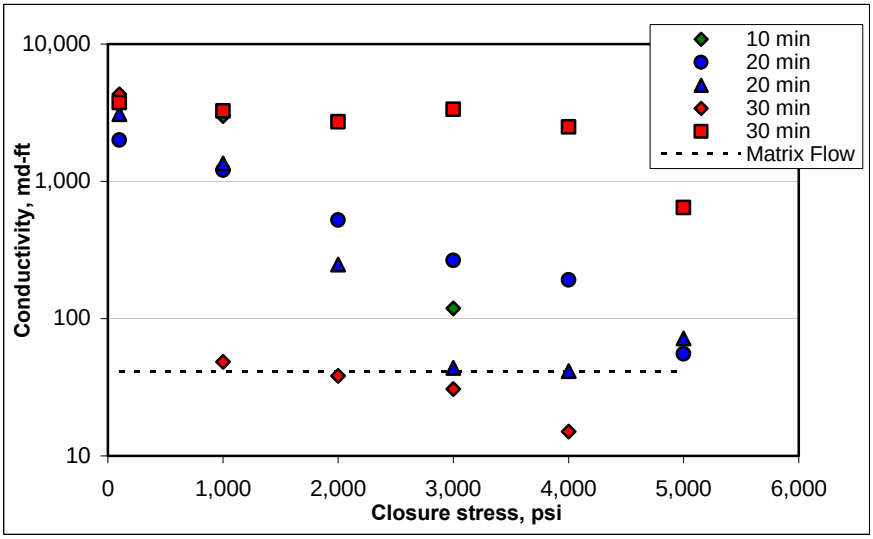

Fig. 3.15- Conductivity profile for Indiana limestone

The conductivity profile observed in the limestone experiments is in agreement with the suggested profile developed by Nierode-Kruk, which suggests that longer contact times should result in higher conductivities. However, our experimental results caution that rock strength should be considered in the analysis of acid fracture conductivity, since from our experiments it was shown that one of the tests at the longest contact time of 30 minutes exhibited a conductivity decline at low closures stresses of 1,000 psi, caused by the lower values of hardness as compared to the other limestone tests.

Dolomite samples exhibited sustainability of higher closure stress as compared to the limestone and the chalk, because of its harder nature. Conductivity response was

very similar for short contact times as well as longer contacts times. From Fig. 3.16 a) it is seen that the 10 minutes test maintains conductivity in values which are approximate for tests of 20 and 30 minutes. From our results in Fig.3.16 b), the conductivity response we identified is not only dependent on acid contact time; it is dependent on the hardness values before and after as well, and on the degree of hardness weakening after acid.

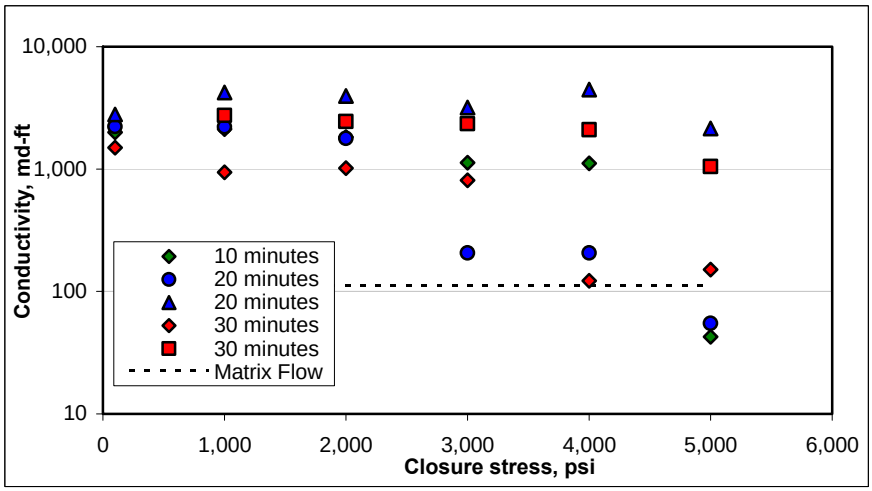

a) Conductivity profile at different contact times

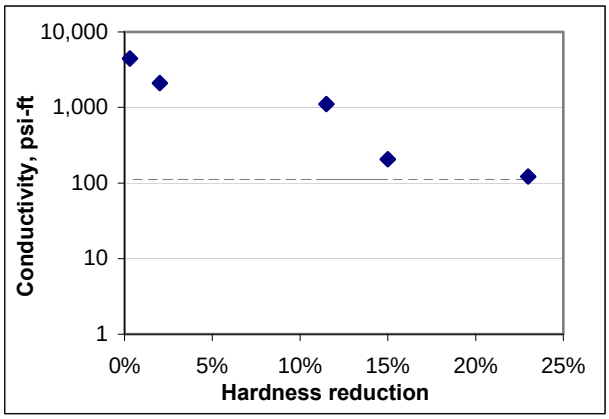

b) Conductivity vs hardness reduction at 4,000 psi closure stress

Fig. 3.16- Conductivity profile for San Andres dolomite

Analyzing the conductivity profile of the Cream chalk samples (Fig. 3.17) in respect to time, it also suggests that longer contact times not always results in higher conductivities as it is currently assumed.

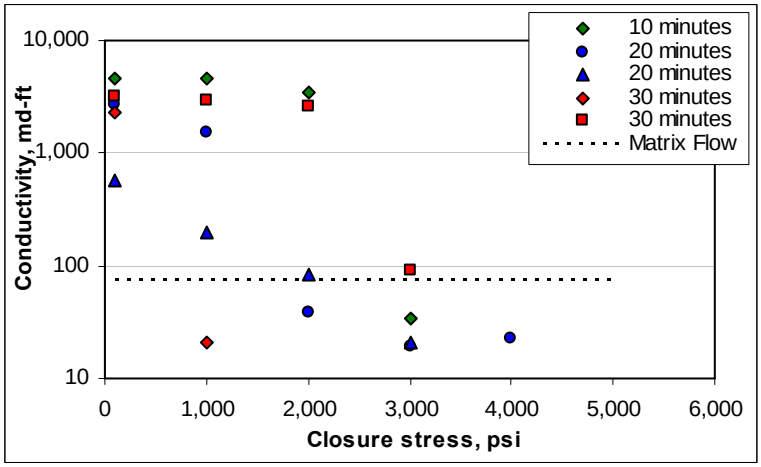

Fig. 3.17- Conductivity profile for Texas Cream chalk

Fig. 3.18 shows the conductivity profile at 20 minutes for the rocks tested, at different closure stress. Conductivity is plotted in the *x* axis and closure stress in the *y* axis. We noticed that dolomite retained conductivity up to higher closure stresses than all the other rocks tested, even without channeling in its etching pattern. This behavior is the results of the hard nature of the rock.

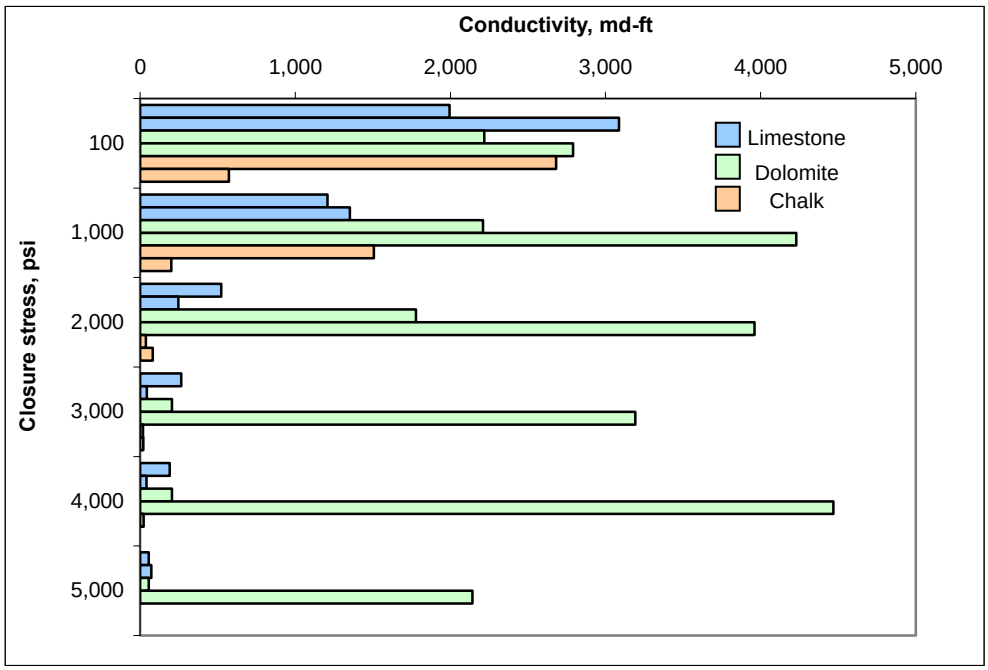

Fig. 3.18- Conductivity profile for rocks tested at 20 minutes contact time

3.5. Conductivity Comparison

The experimental conductivity values were compared with the conductivity values predicted by the available correlation (Nierode-Kruk). The values for rock embedment strength were to be 40,000 psi for Indiana limestone, 63,000 psi for San Andres dolomite, and 13,200 for the chalk.

Detailed conductivity calculations using the Nierode-Kruk correlation are presented in Appendices C-1 to C-3. As an example, this section only discusses the results for Indiana limestone. A similar result was observed for dolomite and chalk as well.

Fig. 3.19 to 3.21 shows the conductivity profile for Indiana limestone at 10, 20, and 30 minutes contact time respectively, for all the experimental tests. The correlation is represented by a straight line and the experimental data as points. Fig. 3.19 and Fig. 3.20 show the conductivity profile predicted by the available correlation illustrating that at short contact times of 10 and 20 minutes, conductivity values are overestimated by the

available correlation in all the tests, for low closure stresses and high closure stresses as well.

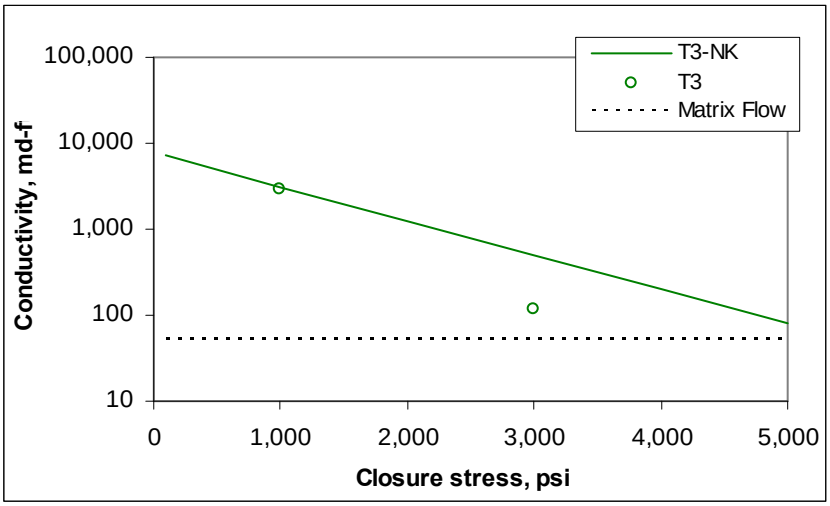

Fig. 3.19- Conductivity comparison, Indiana limestone 10 min

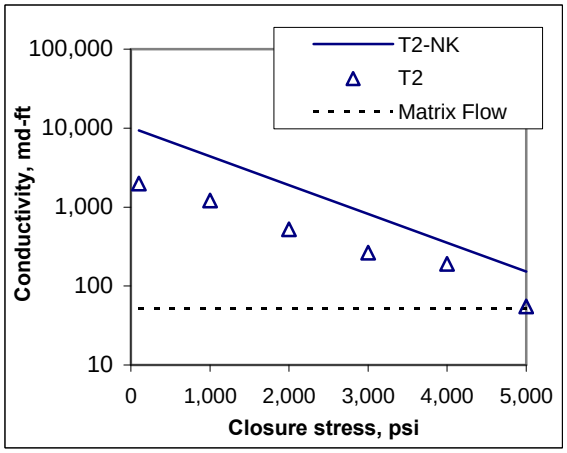

a) Test 2, S_{RE}=39,000 psi

Fig. 3.20- Conductivity comparison, Indiana limestone 20 min

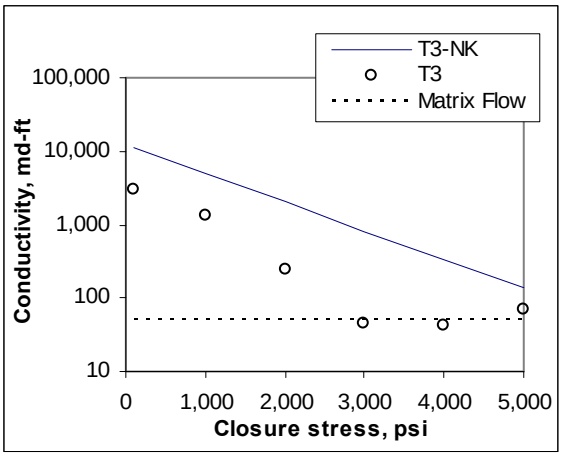

b) Test 3, S_{RE}=32,600 psi

Fig. 3.20- Conductivity comparison, Indiana limestone 20 min

For longer contact times of 30 minutes (Fig.3.20), conductivity values are similar when comparing the predicted value using the available correlation and the experimental data, values at low closure stress for the harder rock and very different at higher closure stress.

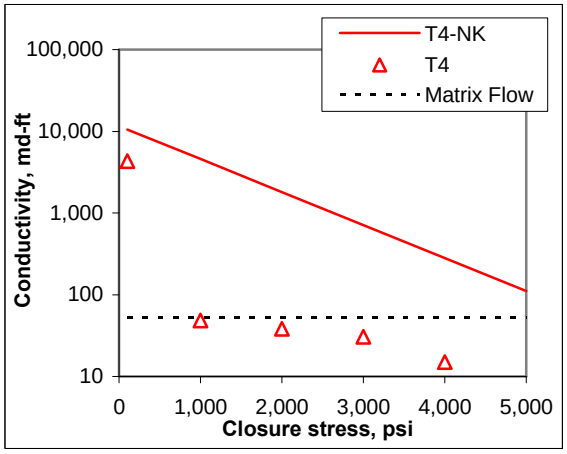

a) Test 4, S_{RE}=28,300 psi

Fig. 3.21- Conductivity comparison, Indiana limestone 30 min

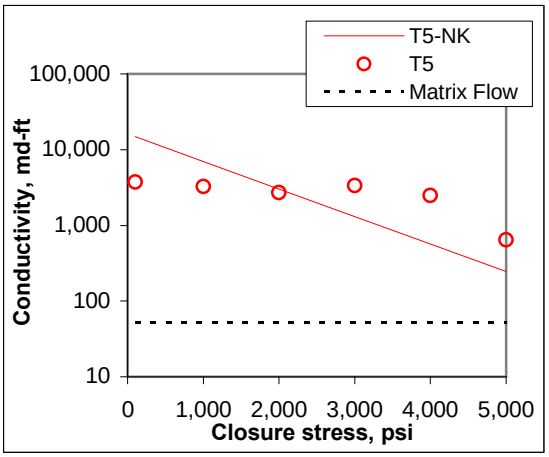

b) Test 5, S_{RE}=39,200 psi

Fig. 3.21- Conductivity comparison, Indiana limestone 30 min

The difference in conductivity profiles can be the result of different experimental conditions. The original correlation is based on limited empirical data where the acid system used was straight hydrochloric acid, while we are using a gelled acid system. Additionally, fluid leakoff was not accounted for in the original correlation. Finally, from Fig. 3.20 and 3.21, were the tests were repeated, the Nierode-Kruk correlation predicts very similar values, while our experimental results provide a wider range mainly governed by the etching pattern and hardness values as well.

CHAPTER IV

CONCLUSIONS AND RECOMMENDATIONS

4.1. Conclusions

From the experimental results, we conclude:

1. Acid etching patterns can aid in understanding conductivity response. When channels are developed in acid fracturing, they dominate the conductivity behavior after closure. Since channels are harder to crush compared with distributed etching, rock strength can not explain the conductivity response correctly. This is especially true for limestone and chalk at contact times of 20 minutes.

2. When channels are not present in acid fractures, rock strength becomes the critical parameter affecting the conductivity after closure. The rock embedment strength reductions of the high-points that support the fracture open are clearly related to the resulting conductivity. Higher reduction in rock strength at the high-points yields lower conductivity after closure. This applies to the dolomite samples for contact times of 20 and 30 minutes.

3. Among the three types of rock tested, Texas Cream chalk has the lowest rock strength values and the fractures closed at much lower stress compared with the limestone and dolomite which had higher hardness values. The dolomite has the highest rock embedment strength and best conductivity results compared with other rocks tested. Dolomite retains conductivity at high closure stress even without channels.

5. Additional extensive experiments are necessary to generate the correlations between contact time and rock strength to acid fracture conductivity.

6. The effects of hardness variation on acid fracture conductivity are higher in dolomite than limestone and chalk.

4.2. Recommendations

Acid fracturing conductivity experiments were performed in a laboratory facility which is more representative of field conditions than previous work. However, the dimensionless number used to scale down from field conditions still is not at the same value as in the field. The effect of injection rate on etching pattern should be studied to verify the appearance of asperities created at different rates, with the goal to quantify and illustrate if the injection rate actually makes a difference.

The analysis of hardness variation considering the high points and all points provided similar results. The ranking based on hardness values in both cases was frequently maintained among the different tests. It is recommended to estimate mean values considering as many points as possible, differentiating among high and low points provides limited information.

Additionally, general rock properties such as Young's modulus should also be evaluated besides the rock embedment strength to quantify the rock response to acid and its effect on conductivity. Hardness values only represent the local values in specific points, whereas Young's modulus would probably characterize hardness in a general way.

Finally, these fifteen experiments provide a basis for better understanding of acid fracture conductivity. We carefully quantified the hardness variation under different conditions which has not been done before. However, extensive additional experiments are recommended to properly relate contact time to acid fracture conductivity.

REFERENCES

1. *Reservoir Stimulation*, M.J. Economides, and N.K Nolte, (eds.), Prentice Hall, Englewood Cliffs, New Jersey (1988), 13-3, 13-12, 17-2.
2. Nierode, D.E., and Kruk, K.F.: "An Evaluation of Acid Fluid Loss Additives, Retarded Acids, and Acidized Fracture Conductivity," paper SPE 4549 presented at the 1973 Annual Fall Meeting, Las Vegas, Nevada, 30 September–3 October.
3. Economides, M.J., Hill, A.D., and Ehlig-Economides, C.: *Petroleum Production Systems*, Prentice Hall Petroleum Engineering Series., Upper Saddle River, New Jersey (1994) 412.
4. Kunak, A.O.: "Effect of Rock Embedment Strength and Formation Type on Conductivity of an Acidized Vertical Fracture," MS thesis, The U. of Texas at Austin, (1993).
5. Beg, M. S., Kunak, A. O., Gong, M., Zhu, D., and Hill, A. D.: "A Systematic Experimental Study of Acid Fracture Conductivity," paper SPE 31098 presented at the 1996 SPE International Symposium on Formation Damage Control, Lafayette, Louisiana, 14-15 February.
6. Gong, M., Lacote, S., and Hill, A.D.: "New Model of Acid-Fracture Conductivity Based on Deformation of Surface Asperities," paper SPE 39431 presented at the 1998 SPE International Formation Damage Symposium, Lafayette, Louisiana, 18-19 February.
7. Gong, M.: "Mechanical and Hydraulic Behavior of Acid Fractures – Experimental Studies and mathematical Modeling," PhD dissertation, The U. of Texas at Austin, (1997).
8. Navarrete, R.C., Miller, M.J., and Gordon, J.E.: "Laboratory and Theoretical Studies for Acid Fracture Stimulation Optimization," paper SPE 39776 presented at the 1998 SPE Permian Basin Oil and Gas Recovery Conference, Midland, Texas, 23-26 March.

9. Abass, H.H., Al-Mulhem, A.A., and Mirajuddin, K.R.: "Acid Fracturing or Proppant Fracturing in Carbonate Formation? A Rock Mechanic's View," paper SPE 102590 presented at the 2006 SPE Annual Technical Conference and Exhibition, San Antonio, Texas, 24-27 September.
10. Nasr-El-Din, H.A., Al-Driweesh, S. M., Metcalf, A. S., and Chesson, J.: "Fracture Acidizing: What Role Does Formation Softening Play in Production Response?" paper SPE 103344 presented at the 2006 SPE Annual Technical Conference and Exhibition, San Antonio, Texas, 24-27 September.
11. Zou, C.L.: "Development and Testing of an Advanced Acid Fracture Conductivity Apparatus," M.S. Thesis, Texas A&M U, College Station, Texas (2005).
12. Malagon, C., Pournik, M., and Hill, A.D.: "The Texture of Acidized Fracture Surfaces-Implications for Acid Fracture Conductivity," paper SPE 102167-MS presented at the 2006 SPE Annual Technical Conference and Exhibition, San Antonio, Texas, 24-27 September.
13. Malagon, C.: "The Texture of Acidized Fracture Surfaces-Implications for Acid Fracture Conductivity," M.S. Thesis, Texas A&M U., College Station, Texas (2006).
14. API RP-61, *API Recommended Practices for Evaluating Short Term Proppant Pack Conductivity*, eighth draft, API, Production Dept., Dallas (Feb1989).
15. Howard, G. C and Fast, C. R.: *Hydraulic Fracturing, SPE Monograph "Vol. 2"*, Henry L. Doherty Series, New York and Dallas: SPE of AIME, 1970.

APPENDIX A

DETAILED CONDUCTIVITY VALUES FOR EACH EXPERIMENT

Test No.	Rock Type	Contact Time	Closure Stress (psi)					
		min	100	1,000	2,000	3,000	4,000	5,000
1	Indiana limestone	10	-	2,987	-	119	6	4
2		20	1,994	1,208	523	266	191	55
3		20	3,088	1,352	248	44	42	72
4		30	4,314	48	38	31	15	-
5		30	3,736	3,264	2,709	3,348	2,484	644
6	San Andres dolomite	10	1,995	2,114	1,823	1,125	1,114	43
7		20	2,220	2,210	1,779	206	206	55
8		20	2,792	4,230	3,959	3,193	4,468	2,143
9		30	1,490	943	1,019	808	122	151
10		30		2,745	2,447	2,341	2,097	1,047
11	Cream chalk	10	4,650	4,600	3,470	34	-	-
12		20	2,682	1,506	38	19	22	-
13		20	572	201	83	21	-	-
14		30	2,252	21	-	-	-	-
15		30	3,243	2,878	2,615	90	-	-

APPENDIX B1
EXPERIMENTAL DATA FOR TEST 1-INDIANA LIMESTONE, 10 MINUTES

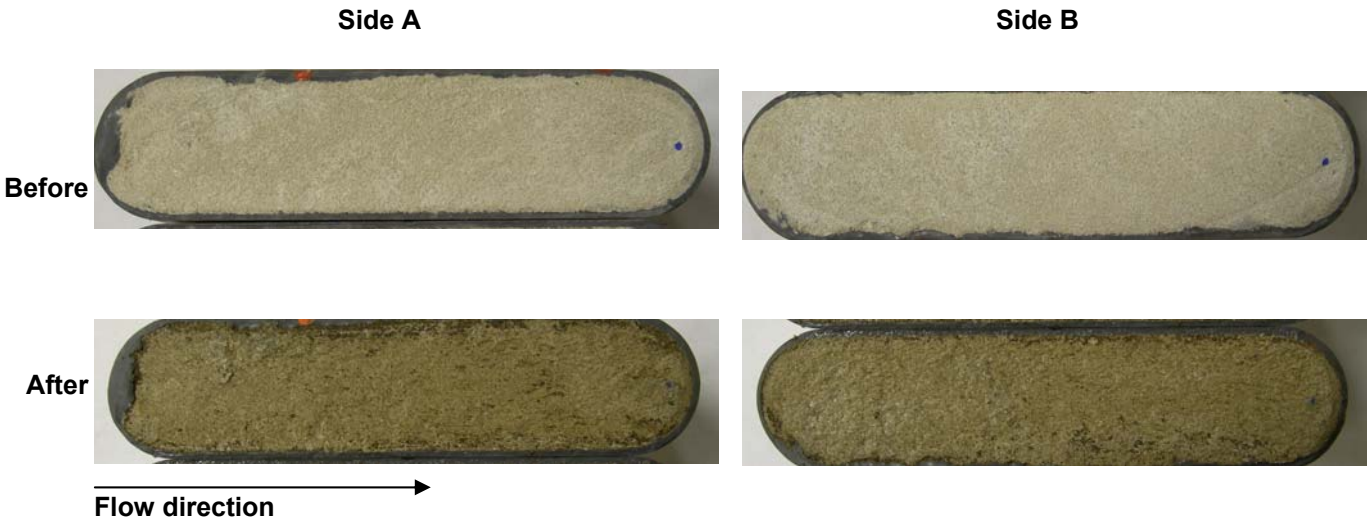

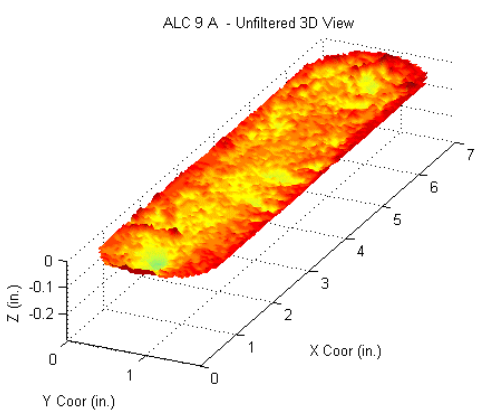

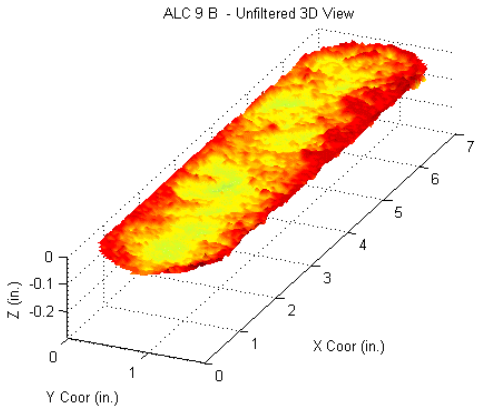

APPENDIX B2

EXPERIMENTAL DATA FOR TEST 2-INDIANA LIMESTONE, 20 MINUTES

Test 2		S_{RE} (A)			S_{RE} (B)		
x	y	Before	After	Δz	Before	After	Δz
0.5	0.4	**29,700**	**34,300**	**0.0264**	**33,500**	**45,300**	**0.0292**
1.5	0.4	**42,800**	**35,000**	**0.0294**	22,200	60,500	0.0304
2.5	0.4	54,200	61,700	0.0324	42,600	31,000	0.0377
3.5	0.4	17,600	44,600	0.0347	35,300	37,000	0.0381
4.5	0.4	**38,500**	**37,800**	**0.0247**	**46,600**	**40,300**	**0.0295**
5.5	0.4	32,200	42,800	0.0378	40,800	35,300	**0.0275**
6.5	0.4	22,400	36,000	0.0334	**31,000**	**37,800**	**0.0210**
0.5	0.7	42,800	27,000	0.0495	30,700	27,500	0.0475
1.5	0.7	36,800	28,200	0.0476	38,300	34,000	0.0408
2.5	0.7	19,100	47,900	0.0423	45,800	33,500	0.0301
3.5	0.7	32,700	32,700	0.0337	39,800	39,300	0.0316
4.5	0.7	50,400	66,000	0.0449	24,700	23,400	0.0466
5.5	0.7	33,300	55,400	0.0415	23,700	28,200	0.0364
6.5	0.7	32,200	31,500	0.0394	32,200	51,100	0.0397
0.5	1	31,500	25,400	0.0354	27,700	36,800	0.0470
1.5	1	34,500	42,300	0.0431	33,800	44,300	0.0413
2.5	1	41,600	37,300	0.0424	37,800	35,800	0.0423
3.5	1	26,500	51,100	0.0351	39,300	27,700	0.0398
4.5	1	44,100	56,400	0.0343	49,100	44,100	0.0388
5.5	1	41,600	41,300	0.0320	30,200	26,700	0.0440
6.5	1	**28,200**	**25,200**	**0.0300**	**36,300**	**33,300**	**0.0233**
0.5	1.3	**28,200**	**40,300**	**0.0205**	33,500	43,800	0.0329
1.5	1.3	43,300	34,800	0.0304	49,900	53,700	**0.0256**
2.5	1.3	**55,400**	**38,500**	**0.0213**	**46,900**	**55,400**	**0.0230**
3.5	1.3	**45,300**	**42,800**	**0.0280**	**52,900**	**37,300**	**0.0218**
4.5	1.3	100,800	36,000	0.0336	**51,900**	**36,800**	**0.0275**
5.5	1.3	**28,200**	**50,400**	**0.0273**	35,800	36,000	0.0389
6.5	1.3	**33,500**	**32,700**	**0.0291**	**39,300**	**22,200**	**0.0221**

Bold: high points, Δz<0.030

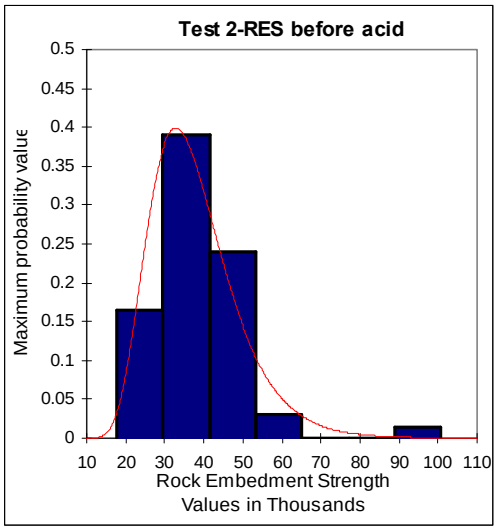
Test 2-RES before acid
Maximum probability value
0.5
0.45
0.4
0.35
0.3
0.25
0.2
0.15
0.1
0.05
0
10 20 30 40 50 60 70 80 90 100 110
Rock Embedment Strength
Values in Thousands


Side A
Side B
Before
After
Flow direction

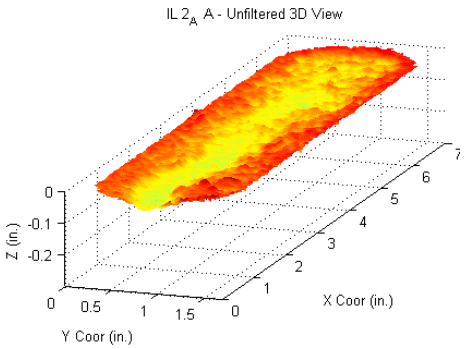
IL 2A A - Unfiltered 3D View
Z (in.)
0
-0.1
-0.2
0 0.5 1 1.5
Y Coor (in.)
0 1 2 3 4 5 6 7
X Coor (in.)

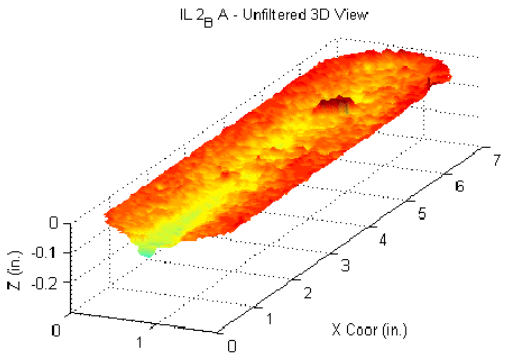
IL 2B A - Unfiltered 3D View
Z (in.)
0
-0.1
-0.2
0 1
0 1 2 3 4 5 6 7
X Coor (in.)

APPENDIX B3

EXPERIMENTAL DATA FOR TEST 3-INDIANA LIMESTONE, 20 MINUTES

Test 3		S_{RE} (A)			S_{RE} (B)		
x	y	Before	After	Δz	Before	After	Δz
0.5	0.4	26,200	32,200	0.0316	29,000	33,000	N/A
1.5	0.4	37,300	23,900	0.0359	38,500	39,000	N/A
2.5	0.4	33,000	33,800	0.0334	43,600	44,300	N/A
3.5	0.4	**34,800**	**37,300**	**0.0281**	34,000	59,200	N/A
4.5	0.4	24,700	16,900	0.0556	25,900	40,100	N/A
5.5	0.4	**39,800**	**31,200**	**0.0278**	37,800	32,200	N/A
6.5	0.4	**24,200**	**25,400**	**0.0324**	39,600	29,700	N/A
0.5	0.7	**20,200**	**43,600**	**0.0199**	31,500	58,200	N/A
1.5	0.7	32,000	41,100	0.0426	24,900	39,800	N/A
2.5	0.7	34,800	46,100	0.0446	27,700	32,200	N/A
3.5	0.7	**25,400**	**36,000**	**0.0278**	29,200	23,900	N/A
4.5	0.7	28,000	31,500	0.0340	27,200	43,100	N/A
5.5	0.7	28,500	23,900	0.0319	34,000	33,000	N/A
6.5	0.7	25,900	45,800	0.0466	45,300	36,000	N/A
0.5	1	**31,700**	**13,600**	**0.0279**	32,200	29,200	N/A
.5	1	32,500	22,400	0.0379	40,600	55,200	N/A
2.5	1	33,800	36,300	0.0371	39,000	21,900	N/A
3.5	1	29,700	44,800	0.0341	36,800	34,300	N/A
4.5	1	44,100	40,600	0.0319	29,200	65,500	N/A
5.5	1	30,700	38,000	0.0404	29,000	24,900	N/A
6.5	1	**28,700**	**29,200**	**0.0284**	23,900	49,100	N/A
0.5	1.3	**34,300**	**32,700**	**0.0286**	39,600	25,900	N/A
1.5	1.3	**22,700**	**16,100**	**0.0266**	23,200	37,000	N/A
2.5	1.3	36,500	35,000	0.0406	35,300	73,100	N/A
3.5	1.3	**28,200**	**29,700**	**0.0193**	33,800	35,300	N/A
4.5	1.3	**28,700**	**27,200**	**0.0279**	24,700	39,600	N/A
5.5	1.3	**40,300**	**21,900**	**0.0254**	30,500	55,200	N/A
6.5	1.3	29,700	27,200	0.0385	27,700	25,400	N/A

Bold: high points, Δz<0.030

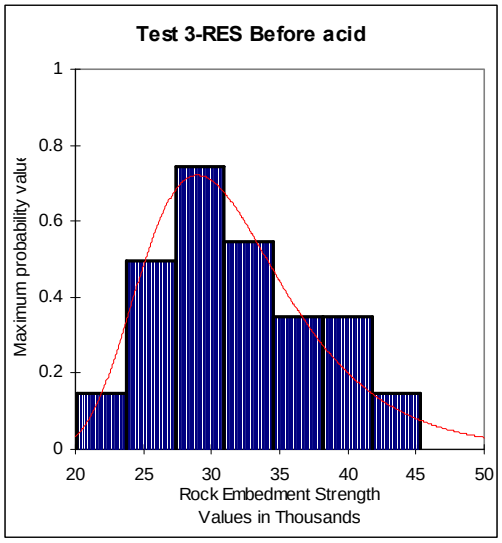
Test 3-RES Before acid
Maximum probability valu
1
0.8
0.6
0.4
0.2
0
20
25
30
35
40
45
50
Rock Embedment Strength
Values in Thousands


Side A
Side B
Before
After
Flow direction

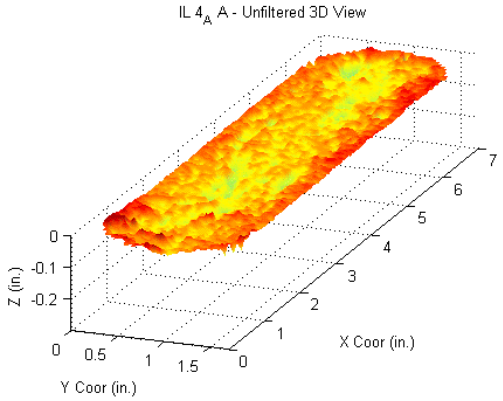
IL 4A A - Unfiltered 3D View
Z (in.)
0
-0.1
-0.2
0
0.5
1
1.5
Y Coor (in.)
0
1
2
3
4
5
6
7
X Coor (in.)

N/A

APPENDIX B4

EXPERIMENTAL DATA FOR TEST 4-INDIANA LIMESTONE, 30 MINUTES

Test 4		S_{RE} (A)			S_{RE} (B)		
x	**y**	**Before**	**After**	**Δz**	**Before**	**After**	**Δz**
0.5	0.4	**22,700**	**20,200**	**0.0300**	22,200	34,800	0.0317
1.5	0.4	**25,700**	**25,700**	**0.0249**	**32,700**	**30,200**	**0.0267**
2.5	0.4	21,900	21,400	0.0418	**27,500**	**25,200**	**0.0297**
3.5	0.4	19,400	25,200	0.0340	35,300	45,300	0.0331
4.5	0.4	20,900	25,900	0.0354	27,700	26,200	0.0313
5.5	0.4	28,200	18,100	0.0477	**31,000**	**22,700**	**0.0244**
6.5	0.4	**21,700**	**24,200**	**0.0013**	**27,200**	**26,500**	**0.0239**
0.5	0.7	25,400	24,700	0.0431	28,200	30,200	0.0364
1.5	0.7	26,700	26,200	0.0328	25,400	35,300	0.0449
2.5	0.7	26,500	26,200	0.0476	34,500	23,700	0.0386
3.5	0.7	17,600	49,100	0.0662	29,700	29,700	0.0511
4.5	0.7	21,200	37,800	0.0452	27,200	34,800	0.0493
5.5	0.7	23,700	32,500	0.0504	30,000	45,300	0.0362
6.5	0.7	21,700	42,800	0.0451	26,200	30,500	0.0436
0.5	1	20,900	35,300	0.0391	23,400	37,300	0.0332
1.5	1	33,300	40,100	0.0460	28,000	22,400	0.0433
2.5	1	30,200	34,500	0.0384	29,700	28,700	0.0621
3.5	1	30,500	30,200	0.0420	28,200	69,500	0.0596
4.5	1	30,200	22,200	0.0334	31,200	38,000	0.0370
5.5	1	32,000	26,200	0.0459	34,300	54,700	0.0471
6.5	1	**33,000**	**32,200**	**0.0276**	23,700	45,300	0.0379
0.5	1.3	22,400	20,200	0.0304	**24,200**	**35,300**	**0.0226**
1.5	1.3	**24,200**	**22,700**	**0.0274**	**304,800**	**40,300**	**0.0283**
2.5	1.3	**27,700**	**20,200**	**0.0247**	**35,300**	**29,700**	**0.0261**
3.5	1.3	31,500	50,400	0.0411	42,100	45,300	0.0347
4.5	1.3	**26,700**	**24,400**	**0.0237**	28,500	20,200	0.0368
5.5	1.3	**27,000**	**24,900**	**0.0260**	29,700	40,300	0.0358
6.5	1.3	**20,200**	**25,400**	**0.0251**	37,300	17,400	0.0358

Bold: high points, Δz<0.030

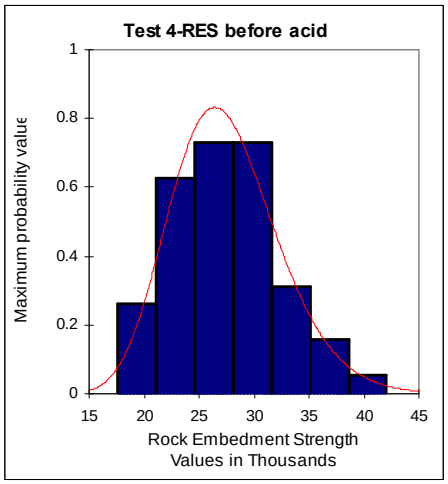
Test 4-RES before acid
Maximum probability value
1
0.8
0.6
0.4
0.2
0
15
20
25
30
35
40
45
Rock Embedment Strength
Values in Thousands


Side A
Side B
Before
After
Flow direction

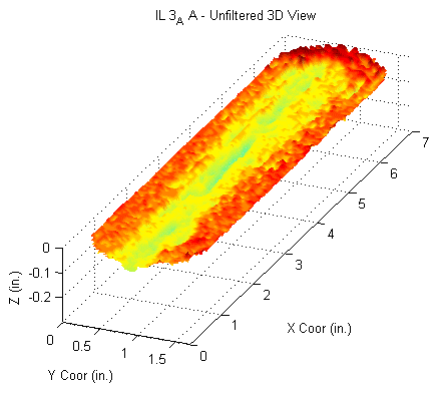
IL 3A A - Unfiltered 3D View
Z (in.)
0
-0.1
-0.2
Y Coor (in.)
0
0.5
1
1.5
X Coor (in.)
0
1
2
3
4
5
6
7

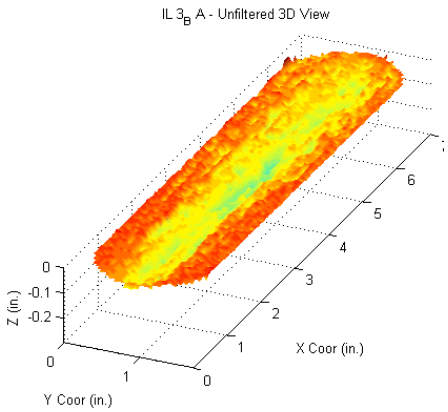
IL 3B A - Unfiltered 3D View
Z (in.)
0
-0.1
-0.2
Y Coor (in.)
0
1
X Coor (in.)
0
1
2
3
4
5
6

APPENDIX B5

EXPERIMENTAL DATA FOR TEST 5-INDIANA LIMESTONE, 30 MINUTES

Test 5		S_{RE} (A)			S_{RE} (B)		
x	y	Before	After	Δz	Before	After	Δz
0.5	0.4	31,700	23,700	**0.03285**	**34,500**	**30,200**	**0.0351**
1.5	0.4	**27,700**	**39,300**	**0.03136**	**40,300**	**50,400**	**0.0351**
2.5	0.4	42,800	25,900	0.03937	38,500	47,900	0.0442
3.5	0.4	30,700	34,300	0.03701	**42,800**	**48,900**	**0.0294**
4.5	0.4	**24,700**	**23,200**	**0.03171**	**47,400**	**52,400**	**0.0294**
5.5	0.4	**32,700**	**20,400**	**0.03015**	54,900	28,500	0.0406
6.5	0.4	35,300	23,900	0.03804	27,000	45,300	0.0379
0.5	0.7	37,800	42,300	0.05612	44,100	70,500	0.052
1.5	0.7	46,400	48,100	0.04346	**36,800**	**32,700**	**0.0383**
2.5	0.7	44,800	32,200	0.04501	**37,000**	**33,000**	**0.0394**
3.5	0.7	52,900	50,600	0.03587	39,300	45,300	0.0394
4.5	0.7	47,600	32,700	0.03983	44,600	49,600	0.0474
5.5	0.7	21,200	22,900	0.04326	38,800	51,400	0.0521
6.5	0.7	24,700	17,600	0.04993	**51,600**	**51,900**	**0.0362**
0.5	1	42,300	40,300	0.04562	68,000	20,200	0.0362
1.5	1	51,600	46,600	0.03749	28,700	32,700	0.043
2.5	1	**32,700**	**32,500**	**0.0316**	35,800	42,100	0.0511
3.5	1	45,800	45,300	0.04069	44,300	45,600	0.0446
4.5	1	35,800	32,500	0.04045	42,300	57,900	0.0503
5.5	1	53,400	63,000	0.04032	37,500	31,500	0.0489
6.5	1	35,300	50,600	0.03929	**41,300**	**42,300**	**0.0321**
0.5	1.3	**33,800**	**32,700**	**0.02906**	**37,800**	**28,500**	**0.0321**
1.5	1.3	**46,900**	**44,800**	**0.03354**	40,300	30,200	0.0454
2.5	1.3	**39,800**	**37,300**	**0.02628**	**42,300**	**39,800**	**0.0301**
3.5	1.3	41,100	35,500	0.03755	**33,800**	**44,100**	**0.0301**
4.5	1.3	38,500	67,500	0.04397	37,500	52,900	0.0424
5.5	1.3	47,100	65,500	0.04645	42,300	52,900	0.0389
6.5	1.3	31,500	57,200	0.05195	33,500	33,800	0.0352

Bold: high points, Δz<0.035

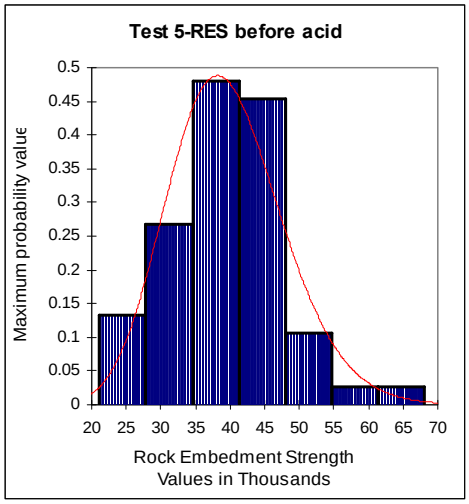
Test 5-RES before acid
Maximum probability value
0.5
0.45
0.4
0.35
0.3
0.25
0.2
0.15
0.1
0.05
0
20 25 30 35 40 45 50 55 60 65 70
Rock Embedment Strength
Values in Thousands


Side A
Side B
Before
After
Flow direction

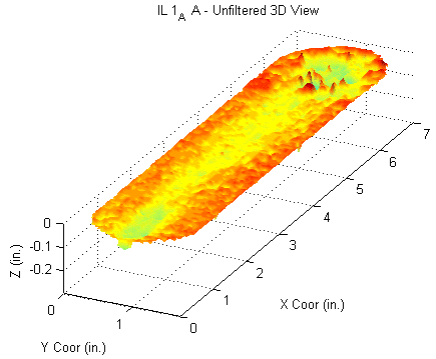
IL 1A A - Unfiltered 3D View
Z (in.)
0
-0.1
-0.2
Y Coor (in.)
0
1
X Coor (in.)
0
1
2
3
4
5
6
7

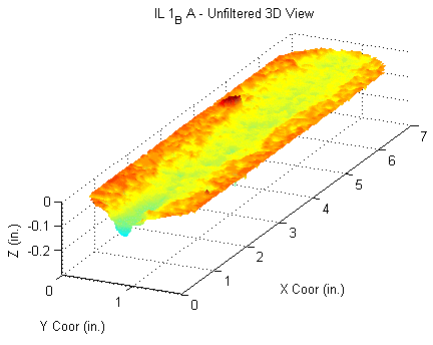
IL 1B A - Unfiltered 3D View
Z (in.)
0
-0.1
-0.2
Y Coor (in.)
0
1
X Coor (in.)
0
1
2
3
4
5
6
7

APPENDIX B6

EXPERIMENTAL DATA FOR TEST 6-SAN ANDRES DOLOMITE, 10 MINUTES

Test 6		S_{RE} (A)			S_{RE} (B)		
x	y	Before	After	Δz	Before	After	Δz
0.5	0.4	**52,900**	**13,100**	**0.0143**	57,900	100,800	0.0241
1.5	0.4	**90,400**	**39,300**	**0.0127**	42,800	43,100	0.0177
2.5	0.4	54,200	20,200	0.0392	52,900	33,500	0.0152
3.5	0.4	**37,300**	**24,900**	**0.0072**	**53,200**	**57,400**	**0.0125**
4.5	0.4	71,300	65,000	0.0217	**41,300**	**32,200**	**0.0065**
5.5	0.4	67,500	73,800	0.0266	**65,500**	**43,300**	**0.0025**
6.5	0.4	89,700	31,200	0.0176	**49,100**	**81,900**	**0.0007**
0.5	0.7	38,300	80,900	0.0218	79,400	58,400	0.0331
1.5	0.7	**45,800**	**33,500**	**-0.0001**	55,400	45,300	0.0217
2.5	0.7	**68,000**	**70,300**	**0.0064**	35,500	46,400	0.0178
3.5	0.7	75,100	76,100	0.0198	41,800	49,600	0.0176
4.5	0.7	78,300	90,200	0.0194	**48,400**	**27,000**	**0.0084**
5.5	0.7	83,400	25,700	0.0158	**42,300**	**42,100**	**0.0009**
6.5	0.7	45,300	104,500	0.0204	**49,900**	**72,300**	**-0.0026**
0.5	1	31,500	56,700	0.0167	85,700	86,700	0.0313
1.5	1	**96,500**	**61,700**	**0.0112**	53,200	22,200	0.0205
2.5	1	**30,200**	**86,900**	**0.0107**	41,600	27,700	0.0174
3.5	1	**88,200**	**47,900**	**0.0056**	**68,300**	**57,700**	**0.0132**
4.5	1	**55,400**	**44,100**	**0.0128**	50,400	25,900	0.0057
5.5	1	**73,800**	**47,400**	**0.0119**	**39,300**	**52,400**	**0.0040**
6.5	1	**54,700**	**37,000**	**0.0148**	**50,400**	**88,400**	**0.0026**
0.5	1.3	45,300	29,500	0.0219	65,000	85,700	0.0231
1.5	1.3	93,200	96,000	-0.0025	47,100	22,700	0.0172
2.5	1.3	**73,100**	**106,100**	**0.0106**	36,000	25,200	0.0154
3.5	1.3	**61,700**	**32,700**	**0.0144**	**88,200**	**63,000**	**0.0104**
4.5	1.3	**55,900**	**126,000**	**0.0099**	**49,100**	**37,800**	**0.0064**
5.5	1.3	47,600	67,000	0.0156	**41,300**	**30,000**	**0.0031**
6.5	1.3	**72,800**	**51,600**	**0.0044**	**68,800**	**61,500**	**-0.0063**

Bold: high points, Δz<0.015

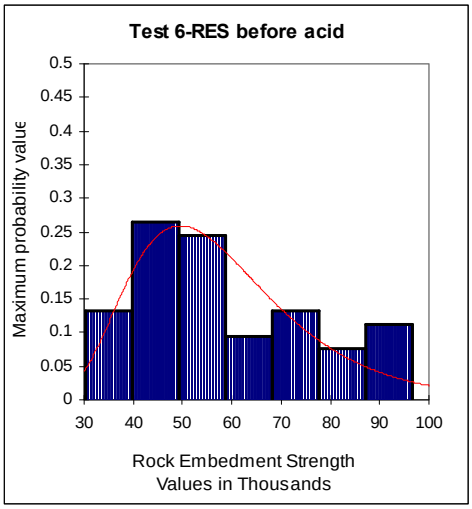
Test 6-RES before acid
Maximum probability value
0.5
0.45
0.4
0.35
0.3
0.25
0.2
0.15
0.1
0.05
0
30
40
50
60
70
80
90
100
Rock Embedment Strength
Values in Thousands

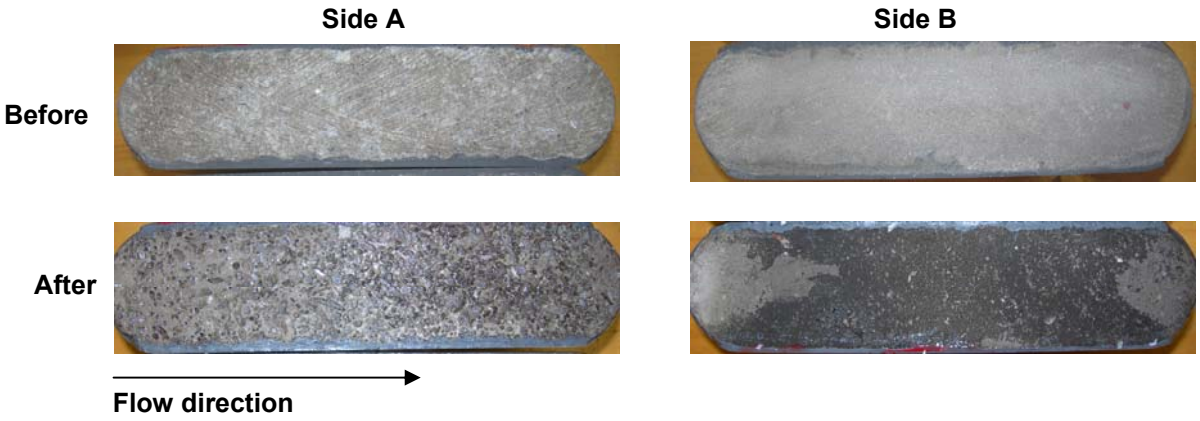
Side A
Side B
Before
After
Flow direction

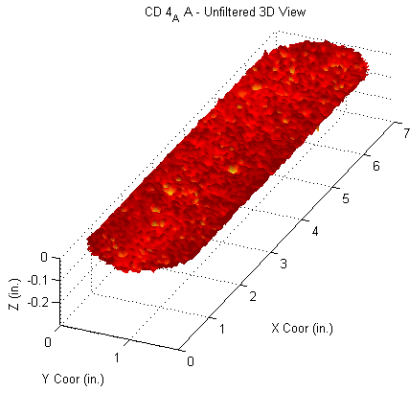
CD 4A A - Unfiltered 3D View
Z (in.)
0
-0.1
-0.2
Y Coor (in.)
0
1
X Coor (in.)
0
1
2
3
4
5
6
7

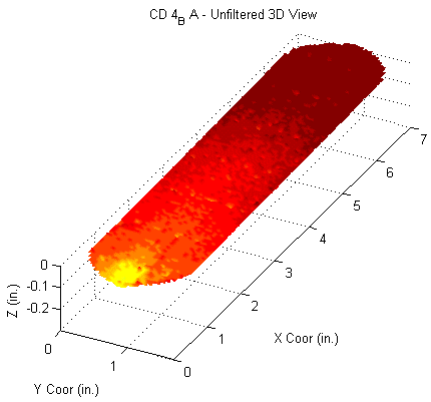
CD 4B A - Unfiltered 3D View
Z (in.)
0
-0.1
-0.2
Y Coor (in.)
0
1
X Coor (in.)
0
1
2
3
4
5
6
7

APPENDIX B7

EXPERIMENTAL DATA FOR TEST 7-SAN ANDRES DOLOMITE, 20 MINUTES

Test 7		S_{RE} (A)			S_{RE} (B)		
x	y	Before	After	Δz	Before	After	Δz
0.5	0.4	**56,400**	**24,700**	**-0.0007**	50,100	77,100	0.0379
1.5	0.4	70,800	24,200	0.0210	72,600	43,300	0.0300
2.5	0.4	**48,400**	**29,500**	**0.0112**	34,500	92,700	0.0205
3.5	0.4	**59,200**	**33,800**	**0.0155**	**42,300**	**21,700**	**0.0111**
4.5	0.4	**62,700**	**38,800**	**0.0188**	37,500	92,200	0.0248
5.5	0.4	60,500	26,500	0.0254	45,100	45,100	**0.0179**
6.5	0.4	68,000	27,200	0.0214	**72,600**	**62,200**	**0.0006**
0.5	0.7	**47,900**	**23,200**	**-0.0057**	75,600	72,600	0.0432
1.5	0.7	**48,400**	**45,800**	**0.0178**	53,200	57,200	0.0227
2.5	0.7	**68,300**	**21,900**	**0.0190**	66,000	52,700	0.0271
3.5	0.7	57,900	40,100	0.0212	55,200	43,600	0.0279
4.5	0.7	56,400	37,500	0.0216	66,300	93,700	0.0240
5.5	0.7	**49,400**	**41,100**	**0.0190**	61,000	104,800	0.0267
6.5	0.7	**60,500**	**23,700**	**0.0157**	**55,400**	**93,700**	**0.0102**
0.5	1	0	0	0.0262	75,600	70,000	0.0419
1.5	1	45,800	24,200	0.0215	69,500	89,700	0.0211
2.5	1	**47,600**	**40,800**	**0.0173**	74,600	77,300	0.0227
3.5	1	**45,100**	**41,100**	**0.0170**	**74,800**	**62,200**	**0.0075**
4.5	1	**34,800**	**34,500**	**0.0158**	77,600	64,200	0.0311
5.5	1	**34,000**	**30,700**	**0.0162**	**78,300**	**66,000**	**0.0109**
6.5	1	**57,700**	**43,100**	**0.0147**	**76,800**	**59,700**	**0.0097**
0.5	1.3	0	0	-0.0033	53,200	41,800	0.0225
1.5	1.3	**51,100**	**26,500**	**0.0174**	75,600	104,300	0.0251
2.5	1.3	**53,400**	**43,800**	**0.0188**	**46,900**	**59,500**	**0.0196**
3.5	1.3	50,100	50,100	-0.0024	**31,500**	**42,100**	**0.0031**
4.5	1.3	48,100	24,400	0.0240	**71,300**	**97,000**	**0.0197**
5.5	1.3	**50,100**	**39,000**	**0.0111**	**69,800**	**46,600**	**-0.0008**
6.5	1.3	**38,800**	**48,100**	**0.0124**	**48,100**	**66,300**	**0.0171**

Bold: high points, Δz<0.020

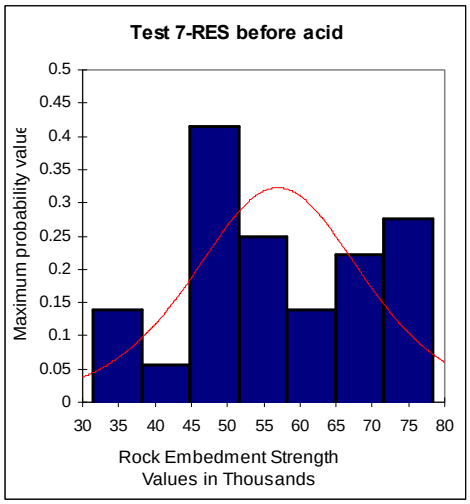
Test 7-RES before acid
Maximum probability value
0.5
0.45
0.4
0.35
0.3
0.25
0.2
0.15
0.1
0.05
0
30 35 40 45 50 55 60 65 70 75 80
Rock Embedment Strength
Values in Thousands

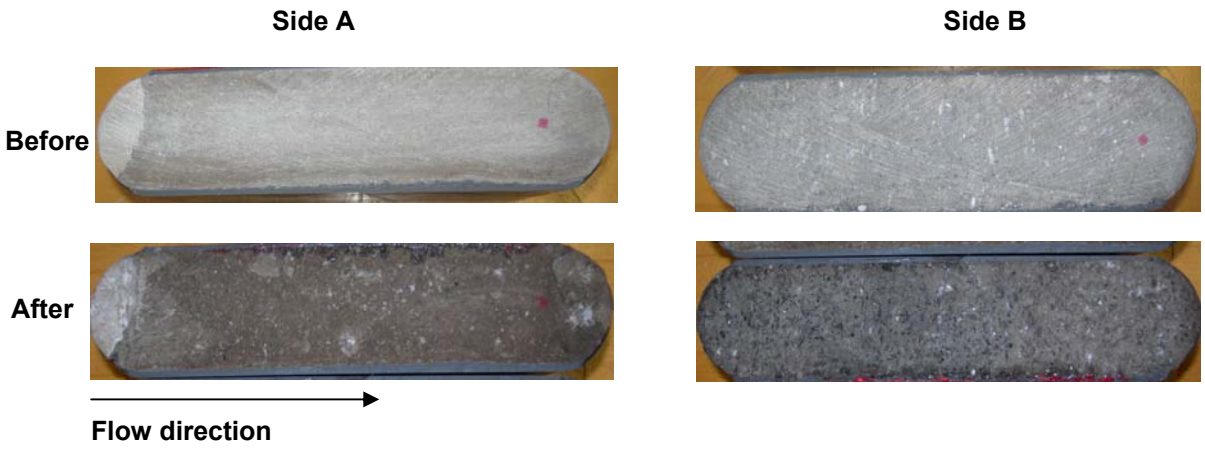
Side A
Side B
Before
After
Flow direction

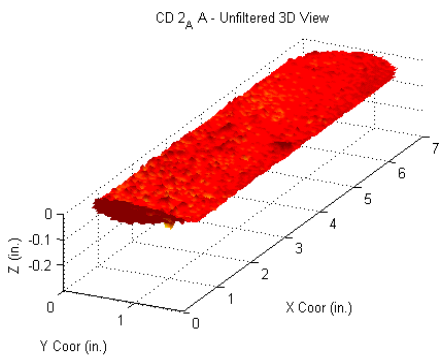
CD 2A A - Unfiltered 3D View
Z (in.)
0
-0.1
-0.2
X Coor (in.)
Y Coor (in.)

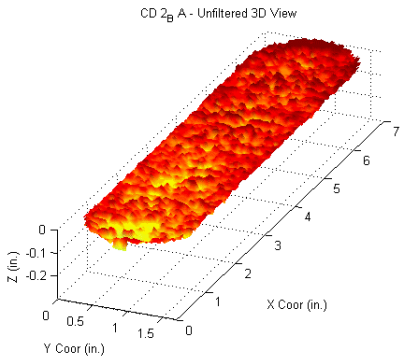
CD 2B A - Unfiltered 3D View
Z (in.)
0
-0.1
-0.2
X Coor (in.)
Y Coor (in.)

APPENDIX B8

EXPERIMENTAL DATA FOR TEST 8-SAN ANDRES DOLOMITE, 20 MINUTES

Test 8		S_{RE} (A)			S_{RE} (B)		
x	y	Before	After	Δz	Before	After	Δz
0.5	0.4	**30,200**	**35,500**	**0.0137**	**53,700**	**54,200**	**0.0203**
1.5	0.4	**29,500**	**43,300**	**0.0184**	43,300	42,300	0.0255
2.5	0.4	**45,300**	**26,200**	**0.0164**	60,000	57,400	0.0242
3.5	0.4	**36,500**	**52,100**	**0.0202**	52,700	34,500	0.0223
4.5	0.4	42,800	69,000	0.0282	42,300	46,100	0.0296
5.5	0.4	68,000	95,700	0.0283	63,700	37,800	0.0247
6.5	0.4	**42,300**	**75,800**	**0.0207**	51,400	37,800	0.0273
0.5	0.7	**37,800**	**47,100**	**0.0159**	33,000	45,600	0.0269
1.5	0.7	46,600	55,400	0.0224	58,400	28,500	0.0290
2.5	0.7	**29,700**	**33,300**	**0.0200**	**57,400**	**64,000**	**0.0185**
3.5	0.7	70,500	48,100	0.0297	64,200	50,900	0.0219
4.5	0.7	53,200	59,500	0.0285	78,900	40,600	0.0384
5.5	0.7	28,000	19,900	0.0386	56,400	67,000	0.0291
6.5	0.7	29,000	35,300	0.0252	49,600	37,000	0.0306
0.5	1	24,700	53,900	0.0401	44,800	53,200	0.0291
1.5	1	50,900	51,900	0.0237	**73,600**	**79,400**	**0.0172**
2.5	1	52,400	30,700	0.0260	59,200	85,100	0.0291
3.5	1	55,400	67,300	0.0214	43,800	41,100	0.0249
4.5	1	76,100	94,500	0.0237	51,400	39,600	0.0334
5.5	1	35,300	76,800	0.0393	60,500	25,700	0.0259
6.5	1	58,200	59,500	0.0219	49,100	40,100	0.0238
0.5	1.3	**69,800**	**48,400**	**0.0104**	**35,300**	**30,700**	**0.0104**
1.5	1.3	**46,400**	**24,700**	**0.0169**	**42,300**	**37,000**	**0.0210**
2.5	1.3	**37,300**	**14,900**	**0.0200**	**49,100**	**34,800**	**0.0191**
3.5	1.3	56,900	49,600	0.0230	48,400	39,600	0.0247
4.5	1.3	**55,900**	**53,900**	**0.0176**	**64,000**	**53,400**	**0.0187**
5.5	1.3	**58,700**	**70,300**	**0.0207**	48,900	44,800	0.0222
6.5	1.3	63,500	47,900	0.0214	39,800	31,000	0.0272

Bold: high points, Δz<0.021

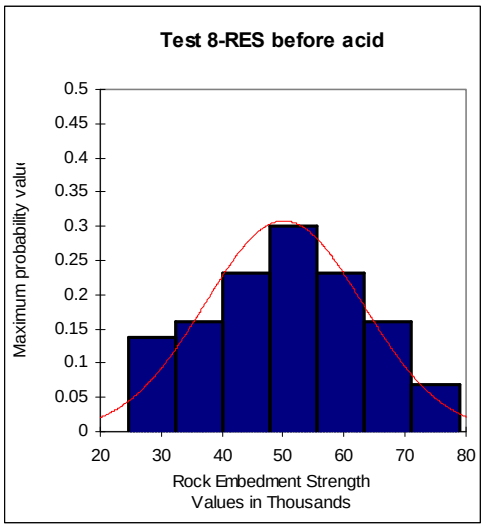
Test 8-RES before acid
Maximum probability valu
0.5
0.45
0.4
0.35
0.3
0.25
0.2
0.15
0.1
0.05
0
20
30
40
50
60
70
80
Rock Embedment Strength
Values in Thousands


Side A
Side B
Before
After
Flow direction

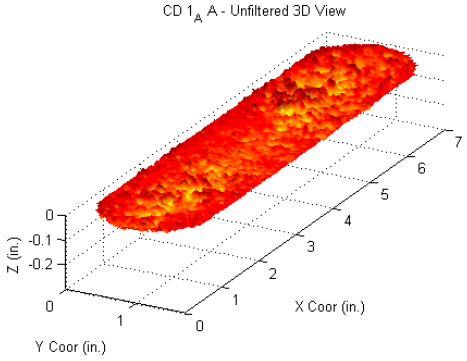
CD 1A A - Unfiltered 3D View
Z (in.)
0
-0.1
-0.2
Y Coor (in.)
0
1
X Coor (in.)
0
1
2
3
4
5
6
7

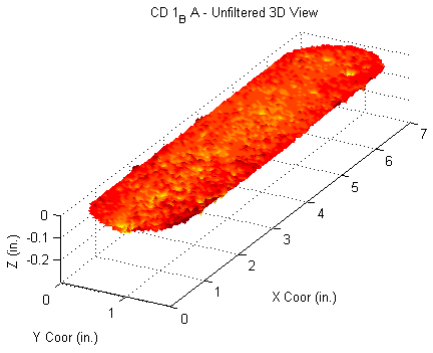
CD 1B A - Unfiltered 3D View
Z (in.)
0
-0.1
-0.2
Y Coor (in.)
0
1
X Coor (in.)
0
1
2
3
4
5
6
7

APPENDIX B9

EXPERIMENTAL DATA FOR TEST 9-SAN ANDRES DOLOMITE, 30 MINUTES

Test 9		S_{RE} (A)			S_{RE} (B)		
x	y	Before	After	Δz	Before	After	Δz
0.5	0.4	**53,400**	**31,700**	**0.0240**	52,900	56,700	0.0340
1.5	0.4	82,600	46,100	0.0310	46,900	58,900	0.0342
2.5	0.4	**92,700**	**62,700**	**0.0245**	82,100	62,700	0.0402
3.5	0.4	**89,900**	**40,800**	**0.0245**	**71,800**	**92,700**	**0.0220**
4.5	0.4	**81,100**	**41,800**	**0.0217**	**75,800**	**82,900**	**0.0263**
5.5	0.4	62,500	38,500	0.0274	71,500	76,100	0.0371
6.5	0.4	**57,400**	**28,000**	**0.0221**	**58,900**	**43,800**	**0.0294**
0.5	0.7	**65,000**	**35,500**	**0.0238**	80,600	67,800	0.0490
1.5	0.7	0	0	0.0372	43,800	73,600	0.0329
2.5	0.7	78,600	56,400	0.0236	73,600	56,700	0.0401
3.5	0.7	**66,500**	**69,000**	**0.0242**	84,100	90,700	0.0348
4.5	0.7	**71,500**	**63,200**	**0.0245**	103,300	69,500	0.0463
5.5	0.7	63,500	41,800	0.0254	54,700	115,400	0.0338
6.5	0.7	58,700	31,700	0.0257	53,400	126,000	0.0411
0.5	1	52,700	74,600	0.0300	**95,700**	**67,500**	**0.0292**
1.5	1	**86,400**	**36,500**	**0.0227**	70,000	44,100	0.0389
2.5	1	**80,600**	**70,300**	**0.0228**	65,000	85,700	0.0512
3.5	1	**68,000**	**43,600**	**0.0200**	28,700	31,200	0.0330
4.5	1	79,400	48,100	0.0324	100,800	126,000	0.0301
5.5	1	**47,900**	**17,600**	**0.0240**	55,700	80,600	0.0324
6.5	1	48,600	18,600	0.0132	**67,300**	**28,200**	**0.0262**
0.5	1.3	**54,400**	**40,600**	**0.0242**	58,400	95,000	0.0370
1.5	1.3	**57,700**	**54,900**	**0.0195**	**74,800**	**36,800**	**0.0110**
2.5	1.3	**65,200**	**81,600**	**0.0194**	**63,500**	**67,500**	**0.0281**
3.5	1.3	**75,300**	**59,500**	**0.0200**	56,400	94,000	0.0377
4.5	1.3	**66,000**	**58,900**	**0.0181**	93,700	112,100	0.0380
5.5	1.3	**58,700**	**65,200**	**0.0176**	**52,100**	**69,800**	**0.0235**
6.5	1.3	**42,300**	**23,900**	**0.0098**	**68,300**	**45,300**	**0.0241**

Bold: high points, Δz<0.025 **Bold: high points, Δz<0.030**

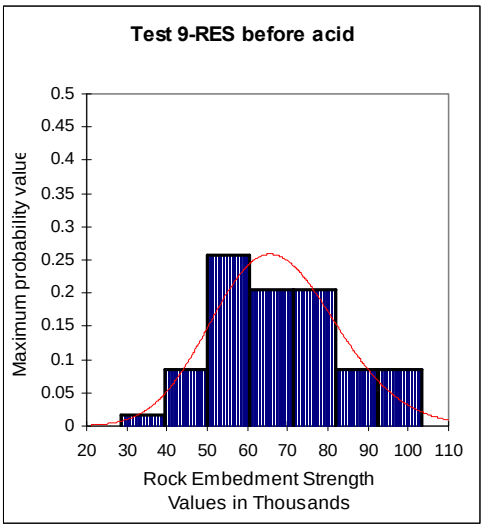
Test 9-RES before acid
Maximum probability value
0.5
0.45
0.4
0.35
0.3
0.25
0.2
0.15
0.1
0.05
0
20 30 40 50 60 70 80 90 100 110
Rock Embedment Strength
Values in Thousands


Side A
Side B
Before
After
Flow direction

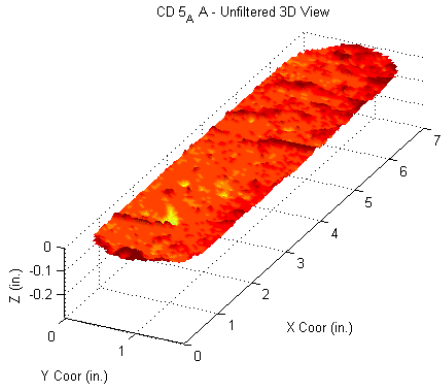
CD 5A A - Unfiltered 3D View
Z (in.)
0
-0.1
-0.2
Y Coor (in.)
0
1
X Coor (in.)
0
1
2
3
4
5
6
7

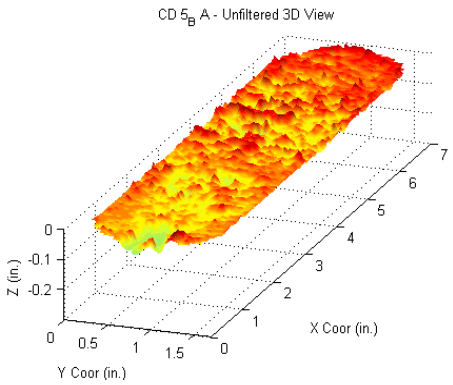
CD 5B A - Unfiltered 3D View
Z (in.)
0
-0.1
-0.2
Y Coor (in.)
0
0.5
1
1.5
X Coor (in.)
0
1
2
3
4
5
6
7

APPENDIX B10

EXPERIMENTAL DATA FOR TEST 10-SAN ANDRES DOLOMITE, 30 MINUTES

Test 10		S_{RE} (A)			S_{RE} (B)		
x	y	Before	After	Δz	Before	After	Δz
0.5	0.4	52,900	33,500	0.0268	**46,400**	**50,400**	**0.0230**
1.5	0.4	88,900	52,900	0.0293	41,100	61,000	0.0330
2.5	0.4	**29,500**	**20,400**	**0.0242**	**56,900**	**62,200**	**0.0245**
3.5	0.4	74,800	41,800	0.0513	51,400	68,300	0.0377
4.5	0.4	66,000	75,600	0.0329	70,000	73,300	0.0322
5.5	0.4	**79,100**	**33,000**	**0.0217**	62,200	89,400	0.0444
6.5	0.4	47,900	57,200	0.0279	**70,300**	**77,600**	**0.0121**
0.5	0.7	53,700	35,800	0.0263	56,900	78,100	0.0258
1.5	0.7	78,900	58,400	0.0338	39,600	104,800	0.0404
2.5	0.7	36,800	49,400	0.0313	71,800	77,300	0.0453
3.5	0.7	42,800	51,400	0.0277	33,500	37,000	0.0336
4.5	0.7	71,300	64,200	0.0294	62,200	88,700	0.0397
5.5	0.7	**89,700**	**32,000**	**0.0226**	64,700	72,800	0.0375
6.5	0.7	58,900	94,700	0.0267	70,000	60,000	0.0398
0.5	1	23,200	70,300	0.0265	55,900	40,600	0.0357
1.5	1	59,700	52,400	0.0278	58,200	84,100	0.0439
2.5	1	65,000	25,900	0.0310	**53,900**	**59,700**	**0.0198**
3.5	1	53,900	46,100	0.0291	**60,000**	**32,500**	**0.0093**
4.5	1	99,500	67,800	0.0289	65,500	35,800	0.0490
5.5	1	51,600	61,500	0.0251	**38,300**	**87,200**	**0.0228**
6.5	1	**27,500**	**34,300**	**0.0235**	**51,400**	**28,700**	**0.0130**
0.5	1.3	**55,200**	**54,900**	**0.0245**	**47,600**	**32,000**	**0.0231**
1.5	1.3	29,200	36,800	0.0253	37,300	63,000	0.0430
2.5	1.3	42,300	46,100	0.0250	68,500	63,500	0.0455
3.5	1.3	86,900	27,700	0.0290	62,700	73,800	0.0330
4.5	1.3	74,100	83,100	0.0464	**71,800**	**62,200**	**0.0186**
5.5	1.3	**31,200**	**63,000**	**0.0233**	**78,100**	**86,700**	**0.0170**
6.5	1.3	**51,600**	**65,000**	**0.0208**	**49,600**	**69,300**	**0.0157**

Bold: high points, Δz<0.025

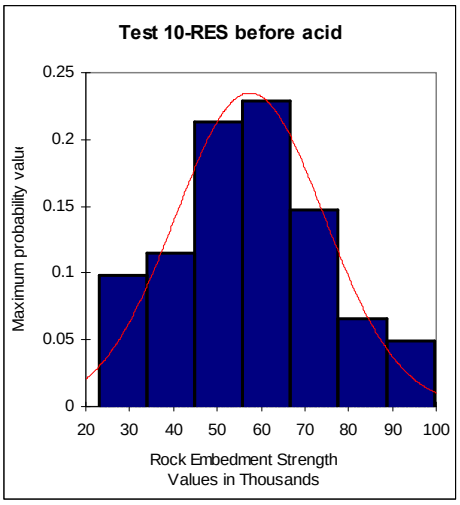
Test 10-RES before acid
Maximum probability valu
0.25
0.2
0.15
0.1
0.05
0
20
30
40
50
60
70
80
90
100
Rock Embedment Strength
Values in Thousands


Side A
Side B
Before
After
Flow direction

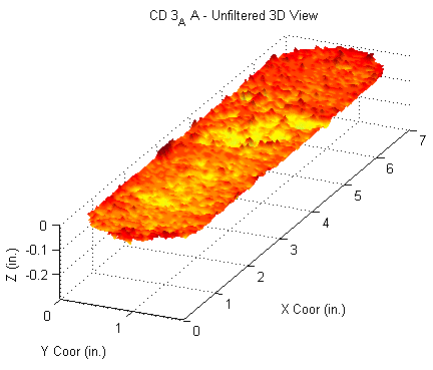
CD 3A A - Unfiltered 3D View
Z (in.)
0
-0.1
-0.2
Y Coor (in.)
0
1
X Coor (in.)
0
1
2
3
4
5
6
7

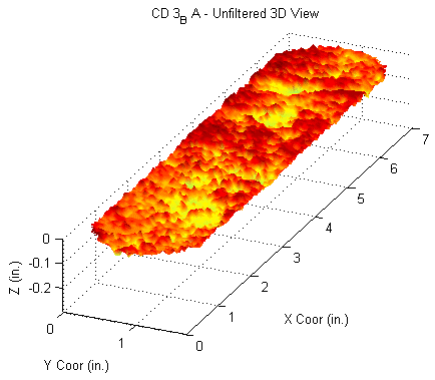
CD 3B A - Unfiltered 3D View
Z (in.)
0
-0.1
-0.2
Y Coor (in.)
0
1
X Coor (in.)
0
1
2
3
4
5
6
7

APPENDIX B11

EXPERIMENTAL DATA FOR TEST 11-TEXAS CREAM CHALK, 10 MINUTES

Test 11		S_{RE} (A)			S_{RE} (B)		
x	y	Before	After	Δz	Before	After	Δz
0.5	0.4	19,600	20,700	0.0225	25,400	15,100	0.0124
1.5	0.4	27,500	31,000	0.0308	**28,000**	**24,400**	**0.0165**
2.5	0.4	**27,000**	**22,700**	**0.0178**	33,300	23,200	0.0111
3.5	0.4	**27,200**	**17,100**	**0.0147**	**24,400**	**21,400**	**0.0171**
4.5	0.4	**23,700**	**19,400**	**0.0164**	**20,700**	**17,100**	**0.0209**
5.5	0.4	**20,900**	**18,600**	**0.0139**	24,400	16,400	0.0250
6.5	0.4	**27,000**	**23,200**	**0.0167**	21,900	16,600	0.0157
0.5	0.7	33,000	47,400	0.0243	44,300	20,700	0.0166
1.5	0.7	26,700	19,600	0.0257	36,500	23,700	0.0211
2.5	0.7	31,200	19,600	0.0235	22,700	23,700	0.0151
3.5	0.7	27,000	23,400	0.0210	20,700	19,600	0.0151
4.5	0.7	**24,200**	**13,900**	**0.0188**	**25,700**	**21,900**	**0.0244**
5.5	0.7	27,200	12,600	0.0240	22,400	17,100	0.0196
6.5	0.7	26,700	27,700	0.0209	27,000	10,100	0.0270
0.5	1	29,200	13,600	0.0266	25,400	19,400	0.0212
1.5	1	30,000	20,900	0.0315	20,900	19,900	0.0229
2.5	1	26,200	12,600	0.0235	24,900	16,100	0.0126
3.5	1	**28,700**	**14,600**	**0.0193**	26,200	26,200	0.0229
4.5	1	24,700	16,900	0.0276	36,000	20,900	0.0244
5.5	1	**29,700**	**20,400**	**0.0143**	35,000	14,100	0.0209
6.5	1	**29,200**	**18,100**	**0.0153**	31,500	21,700	0.0171
0.5	1.3	26,500	19,900	0.0210	**23,900**	**21,400**	**0.0166**
1.5	1.3	30,200	18,600	0.0282	21,900	13,900	0.0131
2.5	1.3	23,700	14,400	0.0205	19,600	25,700	0.0182
3.5	1.3	19,600	14,600	0.0193	26,700	19,400	0.0221
4.5	1.3	30,200	12,600	0.0252	30,700	21,900	0.0177
5.5	1.3	**29,700**	**21,700**	**0.0163**	40,100	12,100	0.0266
6.5	1.3	28,700	-	0.0434	-	-	0.0307

Bold: high points, Δz<0.020

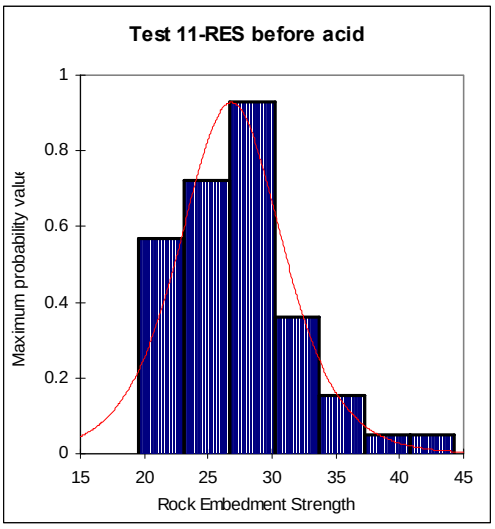
Test 11-RES before acid
Maximum probability value
1
0.8
0.6
0.4
0.2
0
15
20
25
30
35
40
45
Rock Embedment Strength

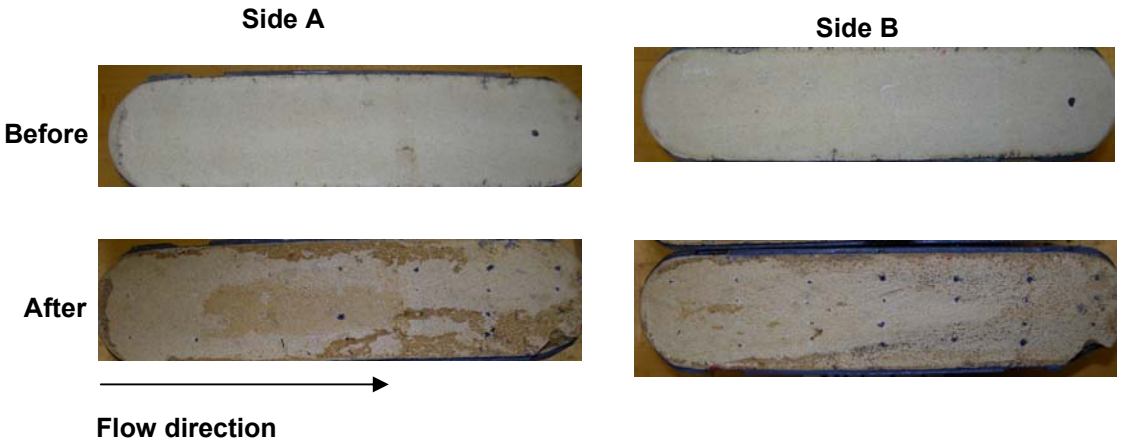
Side A
Side B
Before
After
Flow direction

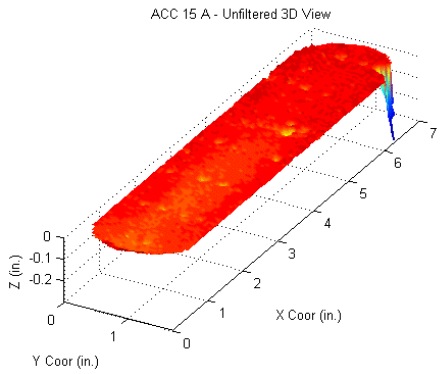
ACC 15 A - Unfiltered 3D View
Z (in.)
0
-0.1
-0.2
Y Coor (in.)
0
1
X Coor (in.)
0
1
2
3
4
5
6
7

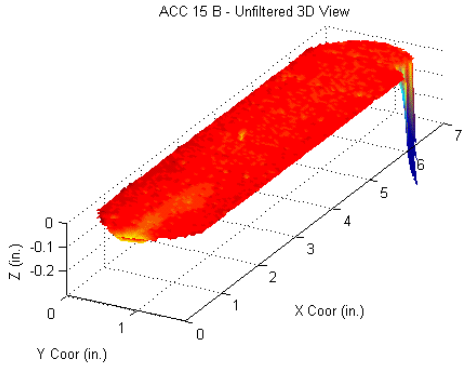
ACC 15 B - Unfiltered 3D View
Z (in.)
0
-0.1
-0.2
Y Coor (in.)
0
1
X Coor (in.)
0
1
2
3
4
5
6
7

APPENDIX B12

EXPERIMENTAL DATA FOR TEST 12-TEXAS CREAM CHALK, 20 MINUTES

Test 12		S_{RE} (A)			S_{RE} (B)		
x	y	Before	After	Δz	Before	After	Δz
0.5	0.4	**24,200**	**21,700**	**0.0224**	21,200	12,600	0.0319
1.5	0.4	**27,200**	**24,900**	**0.0240**	26,700	14,100	0.0318
2.5	0.4	**22,700**	**28,200**	**0.0245**	22,400	18,100	0.0307
3.5	0.4	**30,700**	**34,000**	**0.0196**	33,300	12,600	0.0302
4.5	0.4	**20,900**	**34,300**	**0.0185**	18,900	20,900	0.0358
5.5	0.4	**34,300**	**32,000**	**0.0143**	22,200	16,400	0.0325
6.5	0.4	**29,700**	**28,700**	**0.0139**	**26,200**	**22,900**	**0.0229**
0.5	0.7	17,600	18,400	0.0279	22,200	16,600	0.0386
1.5	0.7	26,700	25,200	0.0264	19,900	25,700	0.0401
2.5	0.7	27,200	25,900	0.0255	26,500	21,400	0.0347
3.5	0.7	19,400	30,500	0.0264	19,600	18,600	0.0340
4.5	0.7	**21,700**	**24,200**	**0.0247**	18,900	24,700	0.0270
5.5	0.7	53,400	39,300	0.0259	23,900	27,700	0.0312
6.5	0.7	25,900	31,700	0.0252	34,300	28,200	0.0255
0.5	1	21,400	32,200	0.0319	19,600	14,100	0.0395
1.5	1	27,200	21,900	0.0289	27,500	23,700	0.0338
2.5	1	42,100	19,100	0.0285	22,400	17,900	0.0307
3.5	1	**35,300**	**24,400**	**0.0243**	19,400	26,500	0.0273
4.5	1	**40,800**	**31,500**	**0.0243**	19,600	21,400	0.0376
5.5	1	**26,200**	**54,700**	**0.0217**	29,700	29,000	0.0267
6.5	1	**24,400**	**20,900**	**0.0183**	**27,500**	**17,400**	**0.0184**
0.5	1.3	18,100	25,700	0.0262	25,400	23,900	0.0421
1.5	1.3	18,600	17,100	0.0310	24,700	21,700	0.0286
2.5	1.3	**24,700**	**13,900**	**0.0224**	26,500	21,400	0.0267
3.5	1.3	13,600	9,800	0.0253	**24,700**	**23,700**	**0.0240**
4.5	1.3	**24,400**	**21,700**	**0.0221**	27,200	27,700	0.0288
5.5	1.3	**25,400**	**23,400**	**0.0199**	**21,400**	**21,200**	**0.0202**
6.5	1.3	**18,100**	**7,600**	**0.0162**	22,400	25,200	0.0273

Bold: high points, Δz<0.025

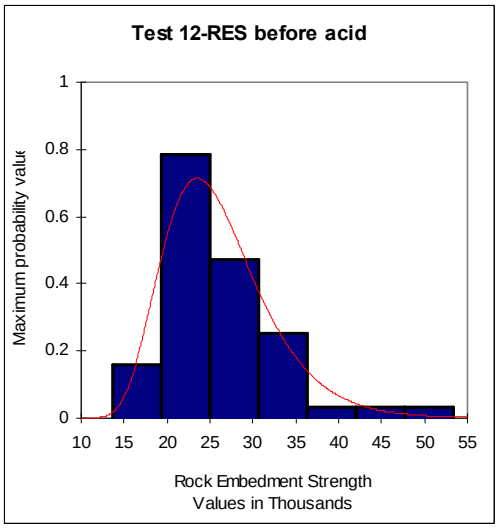
Test 12-RES before acid
Maximum probability value
1
0.8
0.6
0.4
0.2
0
10
15
20
25
30
35
40
45
50
55
Rock Embedment Strength
Values in Thousands

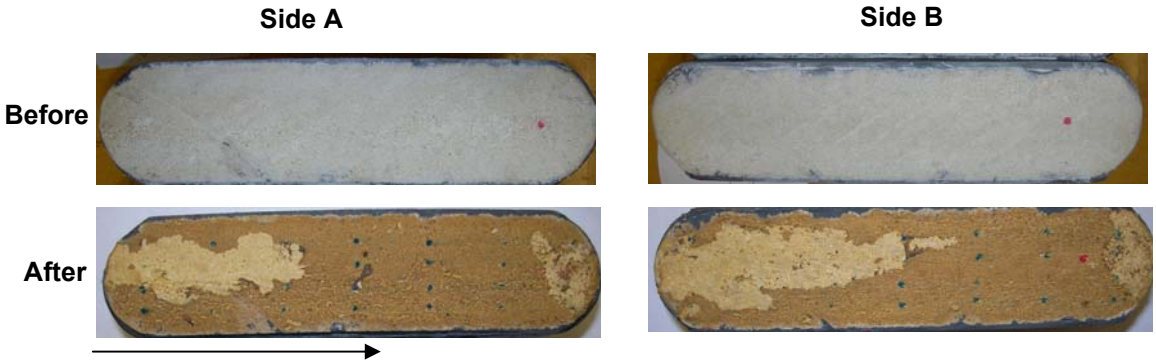
Side A
Side B
Before
After
Flow direction

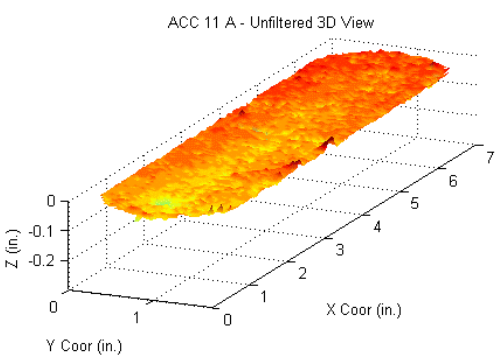
ACC 11 A - Unfiltered 3D View
Z (in.)
0
-0.1
-0.2
0
1
Y Coor (in.)
0
1
2
3
4
5
6
7
X Coor (in.)

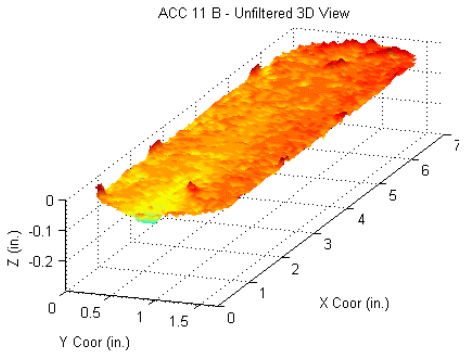
ACC 11 B - Unfiltered 3D View
Z (in.)
0
-0.1
-0.2
0
0.5
1
1.5
Y Coor (in.)
0
1
2
3
4
5
6
7
X Coor (in.)

APPENDIX B13

EXPERIMENTAL DATA FOR TEST 13-TEXAS CREAM CHALK, 20 MINUTES

Test 13		S_{RE} (A)			S_{RE} (B)		
x	y	Before	After	Δz	Before	After	Δz
0.5	0.4	**20,400**	**23,900**	**0.0277**	**21,200**	**12,600**	**0.0228**
1.5	0.4	**23,200**	**22,700**	**0.0234**	**26,700**	**14,100**	**0.0269**
2.5	0.4	**18,900**	**23,200**	**0.0281**	**22,400**	**18,100**	**0.0304**
3.5	0.4	**17,100**	**18,400**	**0.0340**	**33,300**	**12,600**	**0.0305**
4.5	0.4	**18,600**	**20,900**	**0.0321**	18,900	20,900	0.0358
5.5	0.4	**25,400**	**33,300**	**0.0305**	22,200	16,400	0.0395
6.5	0.4	**18,900**	**22,900**	**0.0330**	26,200	22,900	0.0423
0.5	0.7	26,200	19,600	0.0367	22,200	16,600	0.0368
1.5	0.7	22,200	18,600	0.0329	19,900	25,700	0.0364
2.5	0.7	23,700	16,100	0.0382	**26,500**	**21,400**	**0.0340**
3.5	0.7	18,600	20,200	0.0434	19,600	18,600	0.0388
4.5	0.7	**17,600**	**28,200**	**0.0314**	18,900	24,700	0.0370
5.5	0.7	**24,700**	**17,100**	**0.0348**	23,900	27,700	0.0404
6.5	0.7	**25,400**	**23,200**	**0.0349**	**34,300**	**28,200**	**0.0296**
0.5	1	**28,200**	**19,900**	**0.0296**	19,600	14,100	0.0367
1.5	1	**22,200**	**22,200**	**0.0311**	27,500	23,700	0.0396
2.5	1	**27,700**	**15,600**	**0.0348**	22,400	17,900	0.0311
3.5	1	**22,700**	**19,100**	**0.0309**	19,400	26,500	0.0362
4.5	1	**18,900**	**23,900**	**0.0326**	19,600	21,400	0.0383
5.5	1	22,400	20,200	0.0390	29,700	29,000	0.0385
6.5	1	27,700	30,200	0.0404	27,500	17,400	0.0380
0.5	1.3	**28,000**	**22,200**	**0.0247**	**25,400**	**23,900**	**0.0224**
1.5	1.3	17,600	37,800	0.0366	24,700	21,700	0.0305
2.5	1.3	**26,200**	**36,800**	**0.0324**	26,500	21,400	0.0370
3.5	1.3	**18,900**	**23,400**	**0.0316**	24,700	23,700	0.0355
4.5	1.3	**20,900**	**20,400**	**0.0320**	27,200	27,700	0.0417
5.5	1.3	46,100	50,600	0.0407	21,400	21,200	0.0365
6.5	1.3	31,200	20,700	0.0379	22,400	25,200	0.0372

Bold: high points, Δz<0.035

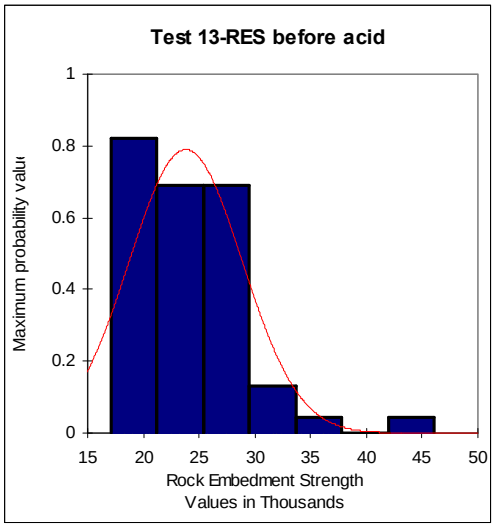
Test 13-RES before acid
Maximum probability valu
1
0.8
0.6
0.4
0.2
0
15
20
25
30
35
40
45
50
Rock Embedment Strength
Values in Thousands

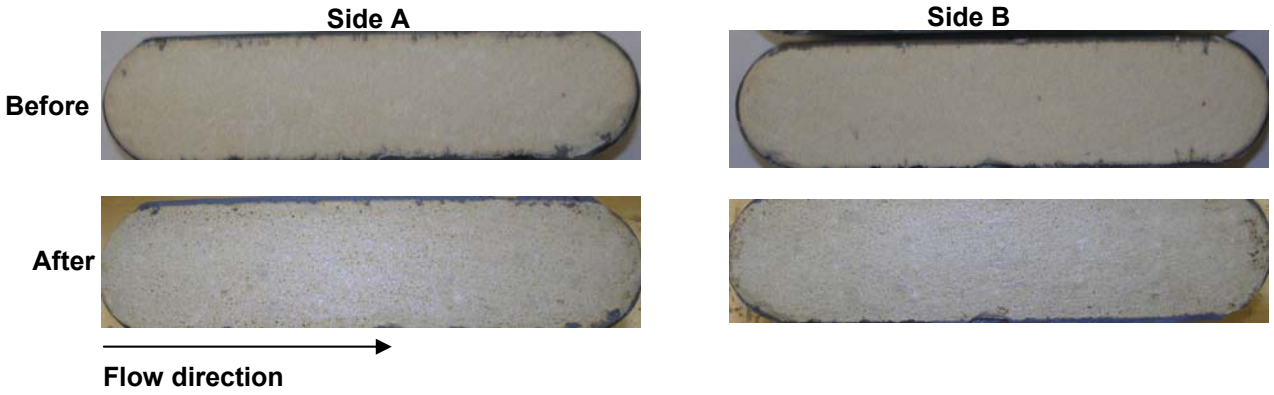
Side A
Side B
Before
After
Flow direction

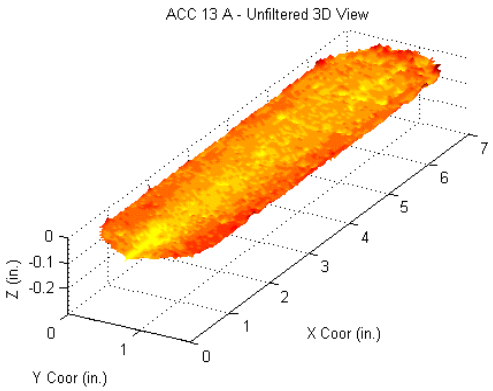
ACC 13 A - Unfiltered 3D View
Z (in.)
0
-0.1
-0.2
0
1
Y Coor (in.)
0
1
2
3
4
5
6
7
X Coor (in.)

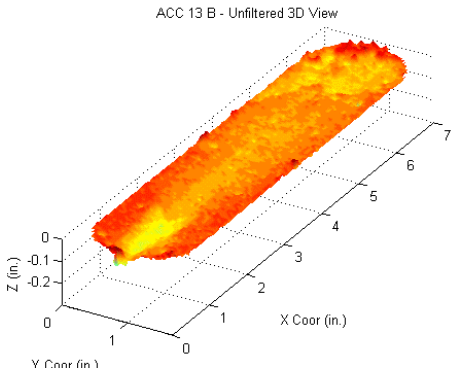
ACC 13 B - Unfiltered 3D View
Z (in.)
0
-0.1
-0.2
0
1
0
1
2
3
4
5
6
7
X Coor (in.)

APPENDIX B14

EXPERIMENTAL DATA FOR TEST 14-TEXAS CREAM CHALK, 30 MINUTES

Test 14		S_{RE} (A)			S_{RE} (B)		
x	y	Before	After	Δz	Before	After	Δz
0.5	0.4	34,300	17,900	0.0569	**22,700**	**17,600**	**0.0303**
1.5	0.4	39,600	21,700	0.0546	20,200	35,300	0.0520
2.5	0.4	**26,500**	**20,900**	**0.0453**	**24,200**	**29,200**	**0.0472**
3.5	0.4	**32,700**	**24,700**	**0.0476**	**25,400**	**20,400**	**0.0499**
4.5	0.4	**28,200**	**19,600**	**0.0450**	**24,700**	**21,400**	**0.0470**
5.5	0.4	**27,700**	**25,400**	**0.0421**	24,700	41,100	0.0558
6.5	0.4	**37,800**	**28,000**	**0.0453**	37,800	31,700	0.0672
0.5	0.7	40,300	36,500	0.0625	**34,000**	**25,200**	**0.0499**
1.5	0.7	27,000	23,200	0.0664	18,100	46,100	0.0549
2.5	0.7	30,200	23,700	0.0598	35,800	31,500	0.0581
3.5	0.7	28,500	29,200	0.0570	28,500	20,400	0.0594
4.5	0.7	**32,700**	**26,500**	**0.0550**	27,000	36,000	0.0787
5.5	0.7	24,900	27,000	0.0536	42,800	32,700	0.0716
6.5	0.7	32,700	20,700	0.0561	18,600	23,900	0.0603
0.5	1	**32,200**	**20,200**	**0.0446**	42,800	20,400	0.0666
1.5	1	26,500	27,200	0.0617	28,500	55,200	0.0656
2.5	1	17,600	38,500	0.0726	21,900	28,200	0.0564
3.5	1	40,300	23,400	0.0559	22,900	32,500	0.0568
4.5	1	21,700	24,700	0.0563	18,600	49,400	0.0543
5.5	1	**22,700**	**16,400**	**0.0489**	40,300	52,900	0.0635
6.5	1	**22,400**	**25,700**	**0.0456**	21,900	17,400	0.0570
0.5	1.3	**17,600**	**23,700**	**0.0462**	**17,900**	**14,900**	**0.0444**
1.5	1.3	25,700	43,300	0.0534	**20,700**	**30,000**	**0.0408**
2.5	1.3	27,200	29,200	0.0573	**21,900**	**32,000**	**0.0444**
3.5	1.3	20,700	31,500	0.0516	**17,100**	**40,300**	**0.0493**
4.5	1.3	**19,900**	**33,000**	**0.0464**	**21,900**	**32,200**	**0.0471**
5.5	1.3	**20,900**	**28,000**	**0.0444**	15,600	36,300	0.0565
6.5	1.3	**30,000**	**22,700**	**0.0424**	21,200	19,400	0.0617

Bold: high points, Δz<0.05

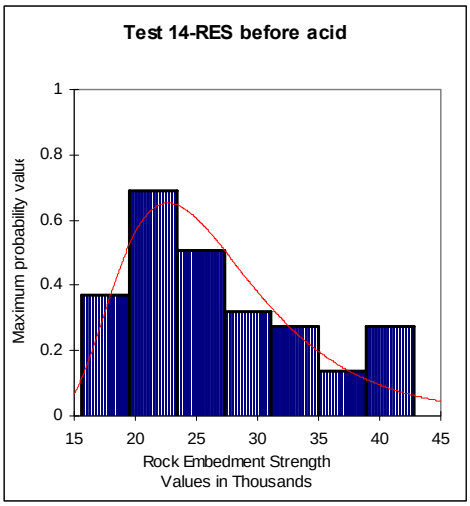

Side A **Side B**

Before

After

Flow direction

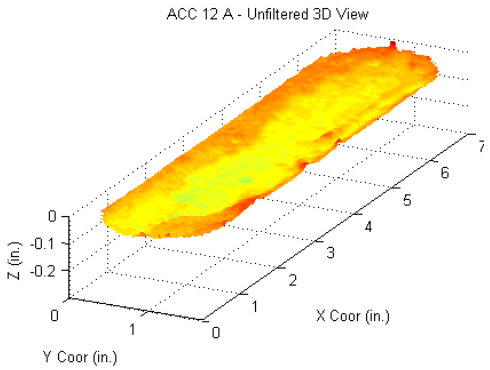

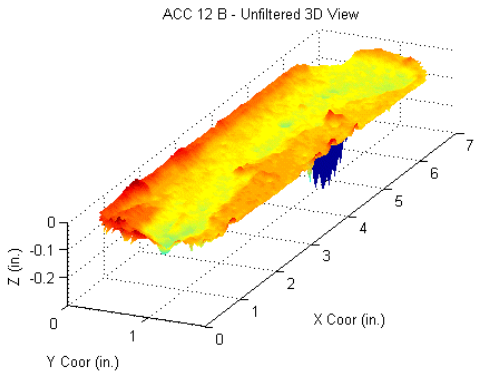

APPENDIX B15

EXPERIMENTAL DATA FOR TEST 15-TEXAS CREAM CHALK, 30 MINUTES

Test 15		S_{RE} (A)			S_{RE} (B)		
x	y	Before	After	Δz	Before	After	Δz
0.5	0.4	32,700	11,100	0.0420	**30,200**	**15,600**	**0.0281**
1.5	0.4	35,300	9,600	0.0357	**33,000**	**10,600**	**0.0331**
2.5	0.4	19,400	14,100	0.0418	21,400	23,900	0.0389
3.5	0.4	**38,000**	**23,400**	**0.0332**	32,700	25,400	0.0422
4.5	0.4	**25,400**	**23,900**	**0.0322**	**24,700**	**39,800**	**0.0297**
5.5	0.4	26,500	12,800	0.0396	34,000	39,800	0.0395
6.5	0.4	**32,500**	**23,700**	**0.0286**	20,200	16,900	0.0408
0.5	0.7	23,200	15,100	0.0385	32,700	16,400	0.0454
1.5	0.7	28,500	26,700	0.0372	**16,400**	**17,600**	**0.0328**
2.5	0.7	25,900	13,100	0.0515	**44,600**	**19,400**	**0.0330**
3.5	0.7	**29,700**	**10,600**	**0.0349**	**26,500**	**26,700**	**0.0346**
4.5	0.7	36,500	52,700	0.0378	**15,100**	**28,000**	**0.0339**
5.5	0.7	**31,200**	**29,000**	**0.0301**	33,000	43,600	0.0353
6.5	0.7	**27,700**	**26,700**	**0.0319**	**22,700**	**16,400**	**0.0291**
0.5	1	17,100	18,600	0.0406	32,200	27,000	0.0593
1.5	1	28,000	20,900	0.0403	26,500	7,600	0.0378
2.5	1	37,000	29,500	0.0366	18,900	27,000	0.0558
3.5	1	31,500	17,400	0.0366	35,800	50,400	0.0384
4.5	1	30,000	13,100	0.0366	43,300	14,600	0.0376
5.5	1	41,800	27,000	0.0356	**20,700**	**18,400**	**0.0348**
6.5	1	27,000	7,600	0.0349	**21,400**	**23,400**	**0.0300**
0.5	1.3	**19,400**	**14,600**	**0.0307**	22,200	23,200	**0.0349**
1.5	1.3	**27,000**	**31,200**	**0.0310**	19,600	21,400	0.0365
2.5	1.3	24,700	9,300	0.0349	**23,900**	**32,200**	**0.0331**
3.5	1.3	26,700	12,800	0.0367	20,700	42,100	0.0356
4.5	1.3	**29,200**	**25,900**	**0.0292**	26,700	10,100	0.0310
5.5	1.3	**34,500**	**15,900**	**0.0404**	**18,900**	**30,500**	**0.0337**
6.5	1.3	39,300	10,600	0.0242	23,400	38,800	0.0404

Bold: high points, Δz<0.035

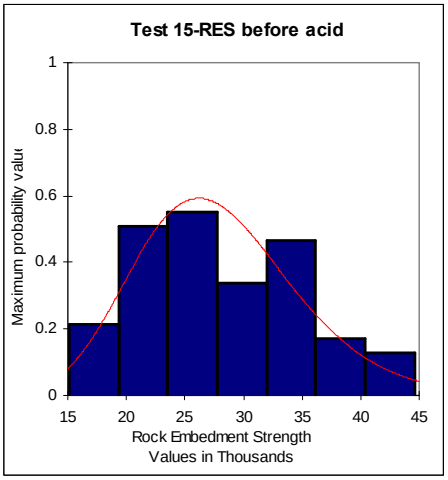
Test 15-RES before acid
Maximum probability valu
1
0.8
0.6
0.4
0.2
0
15
20
25
30
35
40
45
Rock Embedment Strength
Values in Thousands

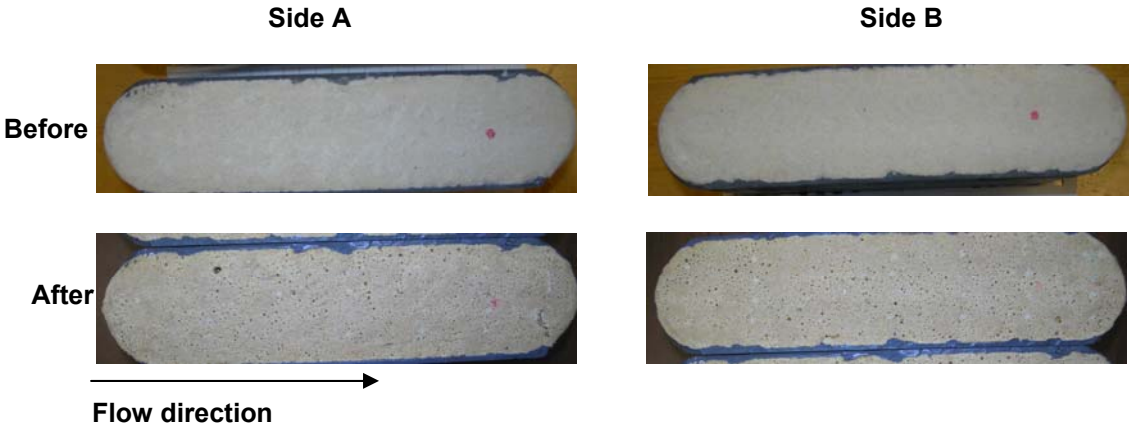
Side A
Side B
Before
After
Flow direction

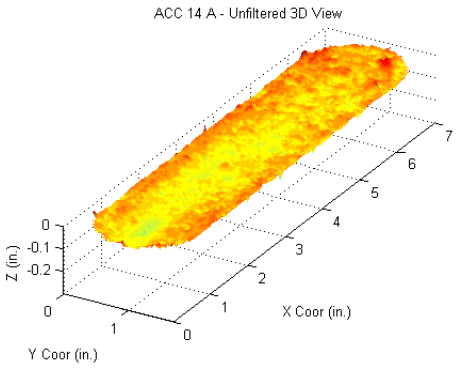
ACC 14 A - Unfiltered 3D View
Z (in.)
0
-0.1
-0.2
0
1
Y Coor (in.)
0
1
2
3
4
5
6
7
X Coor (in.)

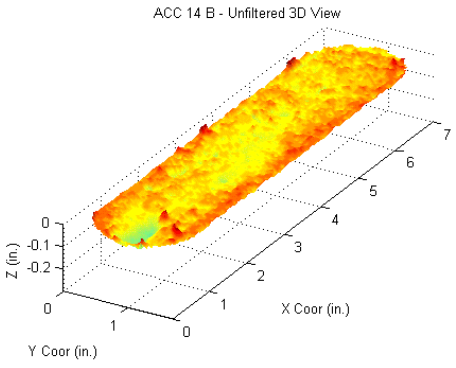
ACC 14 B - Unfiltered 3D View
Z (in.)
0
-0.1
-0.2
0
1
Y Coor (in.)
0
1
2
3
4
5
6
7
X Coor (in.)

APPENDIX C1
CONDUCTIVITY COMPARISON, SAN ANDRES DOLOMITE.
10-30 MINUTES

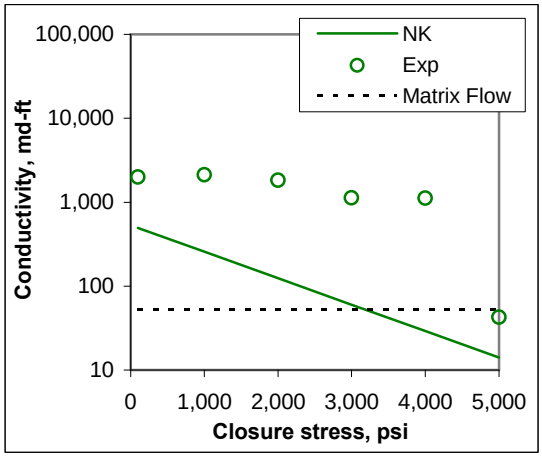

a) Test 6, 10 minutes

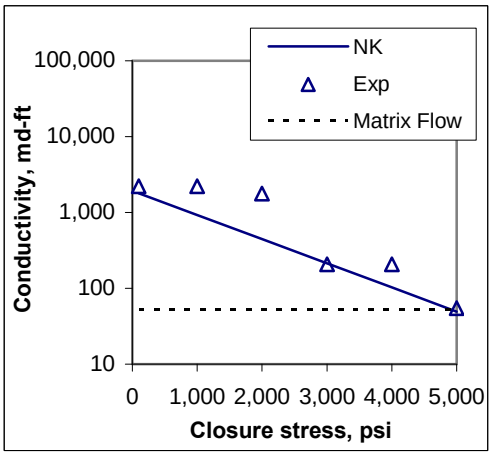

b) Test 7, 20 minutes, S_{RE}=56,900 psi

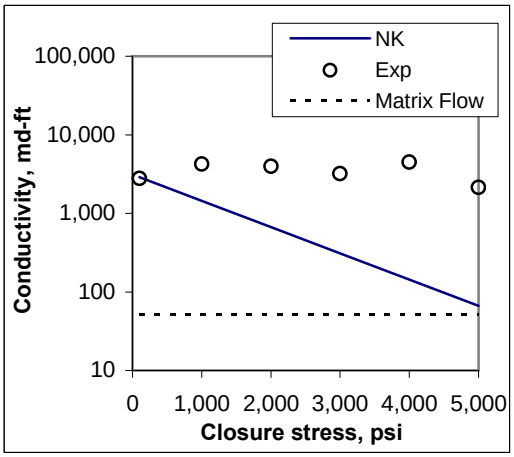

c) Test 8, 20 minutes, S_{RE}=50,100 psi

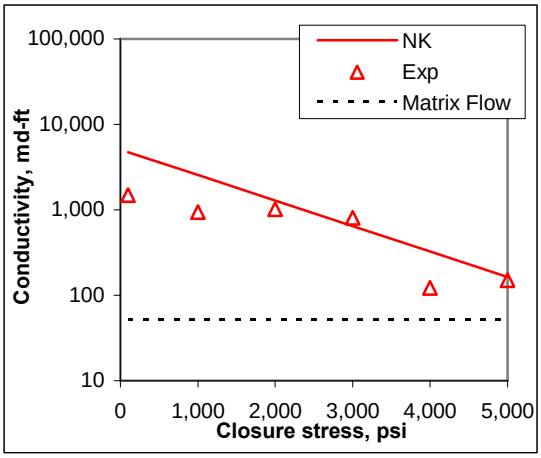

d) Test 9, 30 minutes, S_{RE}=67,400 psi

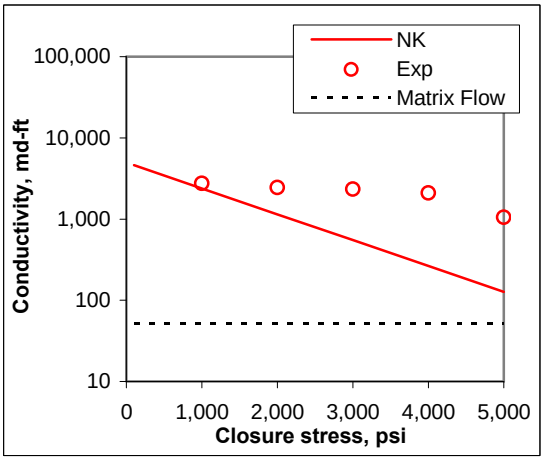

e) Test 10, 30 minutes, S_{RE}=57,400 psi

APPENDIX C2

CONDUCTIVITY COMPARISON, TEXAS CREAM CHALK. 10-30 MINUTES

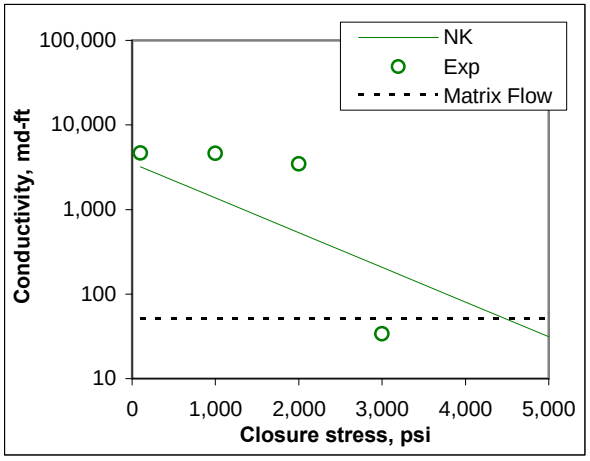

a) Test 11, 10 minutes

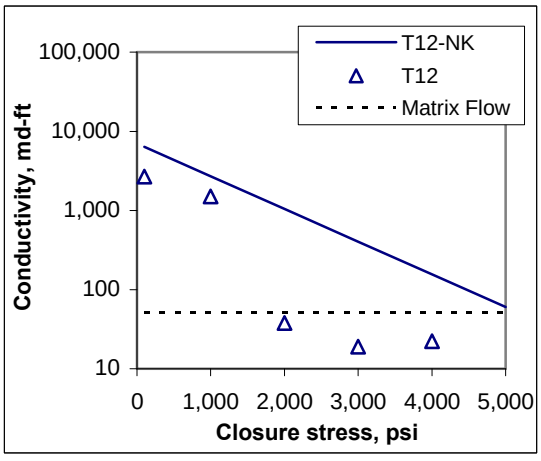

b) Test 12, 20 minutes, S_{RE}=26,100 psi

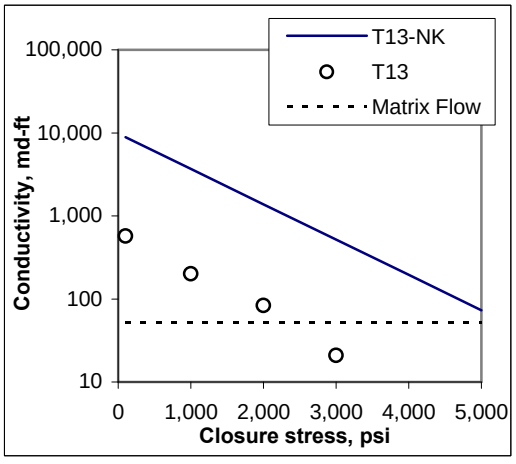

c) Test 13, 20 minutes, S_{RE}=23,700 psi

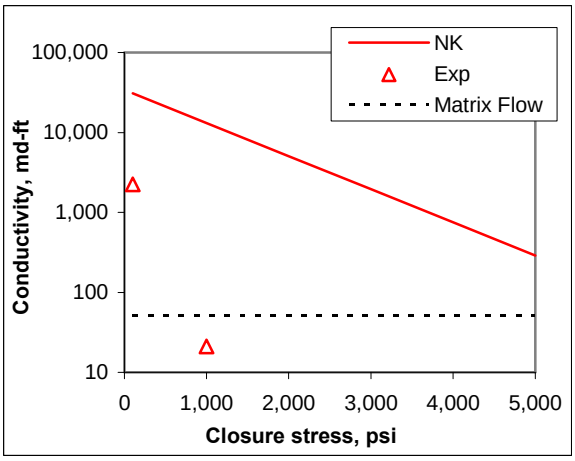

d) Test 14, 30 minutes, S_{RE}=26,000 psi

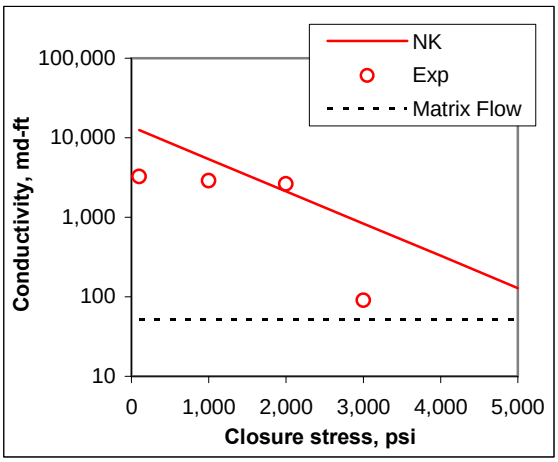

e) Test 15, 30 minutes, S_{RE}=28,000 psi

APPENDIX C3

CONDUCTIVITY CALCULATIONS USING NIERODE-KRUK CORRELATION

Test no.	Rock type	Contact time	Rock dissolved, in^3	w_i (cm)	DREC (md-in)	C_1	S_{RE}	C_2	Closure stress, psi					
									100	1,000	2,000	3,000	4,000	5,000
									Conductivity, md-ft					
1	Indiana Limestone	10	0.56	0.1189	5,596,830	93,337	29,700	0.00092	7,097	3,111	1,244	498	199	80
2		20	0.63	0.1326	7,779,315	122,349	39,000	0.00084	9,374	4,401	1,900	820	354	153
3		20	0.67	0.1410	9,342,917	142,227	32,600	0.00089	10,843	4,866	1,998	820	337	138
4		30	0.66	0.1397	9,081,834	138,952	28,300	0.00093	10,551	4,569	1,803	712	281	111
5		30	0.76	0.1599	13,636,373	194,074	39,200	0.00084	14,872	6,992	3,023	1,307	565	244
6	San Andres Dolomite	10	0.19	0.0400	213,405	6,366	58,600	0.00073	493	257	124	60	29	14
7		20	0.32	0.0676	1,029,401	23,205	56,900	0.00073	1,797	928	445	214	103	49
8		20	0.39	0.0821	1,842,688	37,450	50,100	0.00077	2,890	1,445	669	310	143	66
9		30	0.48	0.1000	3,331,296	60,930	67,400	0.00069	4,740	2,555	1,285	647	325	164
10		30	0.47	0.0989	3,225,163	59,330	57,400	0.00073	4,595	2,378	1,144	550	265	127
11	Cream chalk	10	0.41	0.0863	2,140,965	42,365	26,800	0.00095	3,212	1,372	533	207	81	31
12		20	0.54	0.1141	4,946,021	84,319	26,100	0.00095	6,388	2,711	1,046	403	156	60
13		20	0.62	0.1305	7,403,433	117,468	23,700	0.00098	8,876	3,676	1,380	518	195	73
14		30	1.03	0.2163	33,747,175	408,749	26,000	0.00095	30,964	13,127	5,059	1,949	751	289
15		30	0.71	0.1494	11,118,165	164,091	28,000	0.00093	12,456	5,380	2,117	833	328	129

VITA

Name:	Maria Georgina Melendez Castillo
Address:	3116 TAMU 407 Department of Petroleum Engineering College Station, Texas, 77843 Phone: 1-979-204-8731
Email Address:	mgmelendez@neo.tamu.edu
Education:	B.S., Industrial Engineering, La Universidad del Zulia, 2004 Maracaibo, Venezuela

This thesis was typed by the author.